Rapport BIPM-82/12
Rapport BIPM-83/5
(revised versions)

Calculated frequency differences of the hyperfine structure lines of some transitions ($\Delta F = \pm 1$, $\Delta F = 0$) and of cross-over lines of $^{127}I_2$ and $^{129}I_2$

Michael Gläser

August 1983
Bureau International des Poids et Mesures
Pavillon de Breteuil
F-92310 Sèvres, France

Table of Contents

Rapport BIPM-83/5

Calculated frequency differences of the hyperfine structure lines of some transitions ($\Delta F = \pm 1$, $\Delta F = 0$) and of cross-over lines of $^{129}I_2$ and $^{127}I_2$.

Part II :

Transitions at 633 nm : P(33)6-3 and R(80)1-0 of $^{127}I_2$ and P(54)8-4, P(69)12-6, P(33)6-3, R(60)8-4 of $^{129}I_2$; transitions at 612 nm : P(48)11-3, R(48)15-5 and R(34)17-6 of $^{127}I_2$

Michael Gläser

---

1. Introduction.

This work continues part I [1] of this report. For a more general introduction, part I should be consulted. Here, the remaining iodine transitions at the He-Ne laser emission wavelengths of 633 nm and of 612 nm, found by experiment, are discussed. Two further predicted transitions, which have not yet been found by experiment, have been calculated as well : the vibration-rotational transitions R(80)1-0 at 633 nm and R(34)17-6 at 612 nm, both of $^{127}I_2$.

The aim of these calculations is to show not only the observed but also the not-yet-observed positions of hyperfine structure (HFS) components of iodine in limited parts of the spectrum, accessible by laser radiations, in order to allow the metrologist to select HFS components which are well separated from neighboured lines and so are well suited as reference lines for a wavelength standard of high reproducibility.

The frequency shift of the middle zero-crossing point of the third derivative of a Lorentz profile due to overlapping by a second one has been calculated. This represents a rough estimation of the corresponding frequency shift of a laser stabilized to a saturated absorption line of a molecule at low saturation level by using the third harmonic locking technique.

Rotation-vibrational transitions having large enough probabilities to be detected or to disturb neighboured lines have been determined systematically in the particular wavelength domains.

2. Overlap-induced frequency shifts

The overlapping of the profiles of saturated absorption lines causes a frequency shift of the maxima of these lines and also a shift of the middle zero-crossing points of their third harmonics [2, 3]. These points usually are used as references for laser stabilization. To estimate this shift, it was supposed that only two lines are overlapping and that the observed line shapes closely approximate the third derivatives of Lorentzian profiles. This in turn, is realized only for small modulation amplitudes. Modulation, dispersion, pressure, saturation and background effects are not discussed here. If the observed lines deviate from Lorentzian shape due to such effects [2, 4, 5], the calculated shifts should be corrected correspondingly. If an overlapping of more than two profiles occurs, the results given below can be easily extended to that problem.

The Lorentz profiles

$$y_1 = \frac{1}{1 + x^2}$$

$$y_2 = \frac{b}{1 + a^2(x - x_2)^2}$$

have half widths at half maximum (HWHM) of 1 for y_1 and of $1/a$ for y_2. The maxima positions are : $x = 0$ and $x = x_2$ for y_1 and y_2, respectively. The maximum amplitudes are : 1 and b for y_1 and y_2, respectively.

The third derivatives are

$$y_1''' = \frac{24 \cdot x(1 - x^2)}{(1 + x^2)^4} \qquad \text{with } x_0 = (0, \pm 1) \text{ for } y_1''' = 0$$

$$y_2''' = \frac{24 \cdot ba^4(x - x_2)(1 - a^2(x - x_2)^2)}{(1 + a^2(x - x_2)^2)^4} \qquad \text{with } x_0 = (x_2, x_2 \pm 1/a) \text{ for } y_2''' = 0$$

Assuming equal HWHM for both profiles, i.e., $a = 1$, for the sum profile

$$y''' = y_1''' + y_2'''$$

the zero-crossing points x_0 satisfy the equation :

$$0 = \frac{x_0(1 - x_0^2)}{(1 + x_0^2)^4} + \frac{b(x_0 - x_2)(1 - (x_0 - x_2)^2)}{(1 + (x_0 - x_2)^2)^4}$$

The frequency shift Δx of the middle zero-crossing point x_m of profile y_1''' will be

$$\Delta x = x_m(y''' = 0) - x_m(y_1''' = 0)$$

$$= x_m(y''' = 0)$$

The values of the zero-crossing points of the sum profiles have been approximated by a computer function, which indicates consecutive elements of a data array having opposite signs. Figure 1 shows the line profiles y''' for b = 1 at different profile distances x_2. It should be remarked that the zero-crossing shift of y_1''' has the same sign as x_2 at distances x_2 smaller than the distance between two zero-crossing points, becomes zero at this zero-crossing distance and has a sign opposite to x_2 for distances larger than the zero-crossing distance (pushing effect). Figure 2 shows the absolute values of the zero-crossing shift of y_1''' as a function of the distance x_2 of the profile y_2''', for various constant values of the amplitude b. Figure 3 shows the absolute frequency shifts of y_1''' as a function of the amplitude b of y_2''', the distance x_2 being the fixed parameter. As an example, the superposition of the component a_{13} (i) by the cross-over line c_{22a} of the transition R(127)11-5 of $^{127}I_2$ will be considered : their frequency difference has been calculated to be 0.65 MHz [1] ; the amplitude of c_{22a} relative to a_{13} can be estimated to be 6×10^{-3}. Supposing a linewidth of 3 MHz (HWHM), the relative distance becomes $x_2 = 0.22$ and the zero-crossing shift of the third derivative becomes 1×10^{-3} relative to the linewidth (Fig.2), or 3 kHz in absolute value.

The procedure for estimating the zero-crossing shift, described above, leads to similar results as a more rigorous calculation taking modulation effects into account analytically [2,3]. Here, the calculation is simpler and starts from the observed lineshapes. The deviation, due to the neglect of the modulation distortion can be estimated to be about 20 % for a modulation amplitude equal to half the Lorentzian linewidth.

3. Rotation-vibrational transitions of iodine at the wavelengths $\lambda = 633$ nm and $\lambda = 612$ nm

The energies of the rotation-vibrational transitions of iodine for vibrational quantum numbers $0 \leq v'' \leq 9$ of the electronic ground state $X\ {}^1\Sigma_g^+$ and for $0 \leq v' \leq 62$ of the electronic excited state $B\ {}^3\Pi_{ou}^+$ can be calculated by using the constants given in reference [6] and by introducing appropriate isotope factors [7] for $^{129}I_2$ and ^{127}I-^{129}I. Table 1 shows the results of such calculations at the wavelengths $\lambda = 633$ nm and $\lambda = 612$ nm, slightly corrected by different constant amounts depending on the molecule. The error for the thus-corrected transition frequencies, estimated from 12 measured ones, is $\sigma = 30$ MHz.

The intensity I of the transitions [8, 9] is determined by

(1) the population of the initial energy level, that is, in the case of absorption, the population of the vibrational level in the ground state $N_{v''}$,
(2) the rotational intensity factor, $S(J', J'')$,
(3) the electronic transition probability, $(R_e)^2$, which can be assumed to be constant, and
(4) the Franck-Condon factor, FCF :

$$I = N_{v''} \cdot S(J', J'') \cdot (R_e)^2 \cdot FCF$$

with :
$$N_{v''} = e^{-G_{v''} \cdot (hc/kT)}$$

$$S(J', J'') = (C\nu/Q_r)(J' + J'' + 1)\ e^{-B''J''(J''+1)(hc/kT)}$$

$$FCF = \left[\int_{-\infty}^{+\infty} \phi'(x) \cdot \phi''(x)\ dx \right]^2$$

$G_{v''}$ represents the vibrational energy of the ground state, which depends on the vibrational quantum number v'' ; B'' represents the lowest order of rotational energy constants of the ground state, weakly dependent on v'' ; h, c, k, and T represent the Planck's constant, the speed of light, the Boltzmann constant and the temperature, respectively ; J'' and J'

represent the rotational quantum number of the ground state and the excited state, respectively ; ν is the transition frequency ; Q_r is the rotational state sum and C a constant factor, equal to $8\pi^3 I_0 N/(3hc)$, I_0 and N being the incident intensity and the total number of molecules, respectively.

To obtain a rough estimate of the Franck-Condon factors of the transitions concerned here, the wavefunctions ϕ' and ϕ'' have been approximated by simple Gauss functions, which are spaced by the estimated distance Δx between the maximum of the wavefunction near the higher limit of the potential curve of the ground state and the maximum at the lower limit of the potential curve of the excited state :

$$\phi'' = e^{-(x^2/2\alpha^2)}$$

$$\phi' = e^{-((x+\Delta x)^2/2\alpha^2)}$$

These functions may be good approximations of the wavefunctions if $\Delta x \geq 0$; that means, if only the external wings of the wavefunctions overlap. The turning points of the potential curves for the ground state given in ref.[10] and for the excited state given in ref.[11], as well as the energies of the vibrational levels, given in ref.[6], have been used to calculate this approximation. The FCFs have been normalized to $\Delta x = 0$. The influence of the rotational levels on the FCFs [9] has not been taken into account. The population factor of the vibrational levels and the rotational intensity factor have been calculated at T = 300 K by using the constants $G_{v''}$ and B" from ref.[6]. S(J', J") and $N_{v''}$ have been normalized to the maximum value of J, by taking ν as constant, and to v" = 0, respectively. The results are shown in Table 1. The stated relative intensities, having uncertainties mainly arising from the estimation of Franck-Condon factors, are uncertain by a factor of 2.

4. Hyperfine structure components

The procedure for calculating the frequency differences of the HFS components, based on a computer fitting program of H.J. Foth, has already been described [1]. Table 2 shows an overview of the total number of HFS components occurring at different iodine transitions [12]. Table 3 shows the molecular interaction constants resulting from the fit to measured frequency differences of the HFS components, with two exceptions : the constants of the transitions R(80)1-0 and R(34)17-6.

Those constants have been used for the calculation of the not-yet-measured HFS splittings and do not result from a fit, but from an extrapolation of other well-known constants. Tables 4 to 12 show the measured and calculated frequency differences of the HFS components. The nomenclature used corresponds to the recommendations in ref.[13, 14] and to the one most frequently used.

The values of the measured frequency differences given in Tables 4 to 12 are, for the most part, means of different published values : ref.[15] for P(33)6-3 of $^{127}I_2$, ref.[7, 16-21] for P(54)8-4, ref.[18, 20] for P(69)12-6, ref.[18, 22] for P(33)-6-3, ref.[18] for R(60)8-4 of $^{129}I_2$, ref.[23, 24] for P(48)11-3 and R(48)15-5 of $^{127}I_2$. For a summary, see ref.[25]. The computer fits have been carried out by applying a weight to each HFS component, depending on the uncertainty of its measured value. The uncertainties of the calculated frequency differences have been estimated from the deviations of the calculated values from the measured ones. Even though the fit has only been made for the $\Delta F = \pm 1$ transitions, the uncertainties of the $\Delta F = 0$ and cross-over frequencies should be the same order of magnitude.

Figures 3 to 50 give the positions of the calculated HFS components as vertical lines above ($\Delta F = \pm 1$), across (cross-over) and below ($\Delta F = 0$) the frequency axis. Diagonal lines each connect the top of a $\Delta F = \pm 1$ line with the bottom of a $\Delta F = 0$ line in cases where the two lines originate from transitions to or from a single common level. The corresponding cross-over lines appear at the cross-points of the diagonal lines and the frequency axis. Each transition is shown on several figures, the first of them showing the total HFS splitting frequency range, the following ones showing parts of this range using expanded frequency axes. Figures 51 to 57 present simultaneous views of all calculated transitions of the same frequency domains. The not-calculated transition P(33)6-3 of ^{127}I-^{129}I was added to the spectrum at $\lambda = 633$ nm ; the HFS components of this have been reported in ref.[18, 20, 21].

May 1983, revised : July 1983

References

1. Rapport BIPM-82/12.

2. HELMCKE, J., BAYER-HELMS, F., PTB-Bericht, Me-17, 1977, p. 111-131.

3. CÉREZ, P. and BRILLET, A., Metrologia, 13, 1977, p. 29-33.

4. GHOSH ROY, D.N., BERTINETTO, F., REBAGLIA, B.I. and CRESTO, P.C., J. Appl. Phys., 54, 1983, 531-534.

5. CÉREZ, P. and FELDER, R., to be published.

6. LUC, P., J. Mol. Spectr., 80, 1980, p. 41-55.

7. TESIC, M. and YOH-HAN PAO, J. Mol. Spectr., 57, 1975, p. 75-96.

8. HERZBERG, G., "Molecular Spectra and Molecular Structure : I. Spectra of Diatomic Molecules", van Nostrand Reinhold, New York, 1950.

9. BROWN, J.D., BURNS, G., LE ROY, R.J., Can. J. Phys., 51, 1973, p. 1664-1677.

10. LE ROY, R.J., J. Chem. Phys., 52, 1970, p. 2683-2689.

11. BARROW, R.F., YEE, K.K., J. Chem. Soc. Faraday II, 69, 1973, p. 684-700.

12. SPIEWECK, F., PTB-Bericht, Me-17, 1977, p. 33-41.

13. GLÄSER, M., DSCHAO Kegung and FOTH, H.J., Opt. Commun., 38, 1981, p. 119-123.

14. GLÄSER, M., Document CCDM/82-32.

15. MORINAGA, A. and TANAKA, K., Appl. Phys. Lett., 32, 1978, p. 114-116.

16. ROWLEY, W.R.C., Document CCDM/82-2.

17. CHARTIER, J.-M., Rapport BIPM-82/10.

18. GERLACH, R.W., Thesis, University Cleveland, Ohio, 1975.

19. KNOX, J.D. and YOH-HAN PAO, Appl. Phys. Lett., 18, 1971, p. 360-362.

20. MAGYAR, J.A. and BROWN, N., Metrologia, 16, 1980, p. 63-68.

21. Procès-Verbaux CIPM, 46, 1978, p. 33.

22. HELMCKE, J., BAYER-HELMS, F., IEEE Trans. Instrum. Meas., IM-23, 1974, p. 529-531.

23. CÉREZ, P., BRILLET, A., MAN-PICHOT, C. and FELDER, R., IEEE Trans. Instrum. Meas., IM-29, 1980, p. 352-354.

24. Determination of the frequency differences by using the original chart-recordings of ref.[23], made available by the authors.

25. Appendix M 5 of the Practical Realization of the proposed new definition of the metre, to be published in Procès-Verbaux CIPM 1983.

Table 1 :

Rotation-vibrational transitions for $v'' < 10$ and $J'' < 200$ of the iodine molecules $^{127}I_2$, $^{129}I_2$ and $^{127}I^{129}I$ at the wavelengths λ = 633 nm and λ = 612 nm. The transition frequencies ν are calculated by using the constants of ref.[6]. $N_{v''rel}$ represents the relative population of the vibrational ground level ; FCF_{rel}, the estimated relative Franck-Condon factor ; $S(J'J'')_{rel}$, the relative rotational intensity factor ; I_{rel}, the estimated relative intensity of this transition ; and I'_{rel}, represents the estimated intensity, relative to the best known transition of the corresponding molecule at the corresponding wavelength.

λ[nm]	Molecule	Transition	ν[MHz]	$N_{v''rel}$	FCF_{rel}	$S(J'J'')_{rel}$	I_{rel}	I'_{rel}
633	127	P(55)18-9	473 610.40	$1.24 \cdot 10^{-4}$		0.99	$< 1 \cdot 10^{-4}$	< 0.07
		R(111)19-9	610.73	$1.24 \cdot 10^{-4}$		0.38	$< 5 \cdot 10^{-5}$	< 0.04
		P(33)6-3	611.42	$4.72 \cdot 10^{-2}$	0.32	0.84	$1.3 \cdot 10^{-2}$	9.3
		R(80)1-0	611.79	1	$6.8 \cdot 10^{-6}$	0.8	$5.4 \cdot 10^{-6}$	$3.8 \cdot 10^{-3}$
		R(127)11-5	612.08	$6.36 \cdot 10^{-3}$	1	0.22	$1.4 \cdot 10^{-3}$	1
		R(182)17-7	612.25	$8.76 \cdot 10^{-4}$	0.39	0.015	$5.1 \cdot 10^{-6}$	$3.6 \cdot 10^{-3}$
	129	R(60)8-4	611.61	$1.73 \cdot 10^{-2}$	0.79	0.99	$1.4 \cdot 10^{-2}$	1
		P(54)8-4	612.06	$1.73 \cdot 10^{-2}$	0.79	0.99	$1.4 \cdot 10^{-2}$	1
		P(69)12-6	612.79	$2.35 \cdot 10^{-3}$	0.86	0.91	$1.8 \cdot 10^{-3}$	$1.3 \cdot 10^{-1}$
		P(184)5-1	613.00	$3.59 \cdot 10^{-1}$	0.027	0.013	$1.3 \cdot 10^{-4}$	$9.3 \cdot 10^{-3}$
		R(190)5-1	613.38	$3.59 \cdot 10^{-1}$	0.027	0.0093	$9.0 \cdot 10^{-5}$	$6.4 \cdot 10^{-3}$
		P(33)6-3	613.54	$4.72 \cdot 10^{-2}$	0.32	0.84	$1.3 \cdot 10^{-2}$	$9.3 \cdot 10^{-1}$
		R(153)4-1	613.62	$3.59 \cdot 10^{-1}$	0.017	0.073	$4.5 \cdot 10^{-4}$	$3.2 \cdot 10^{-2}$
	127/129	R(196)20-8	610.07	$3.28 \cdot 10^{-4}$		0.0064	$< 2 \cdot 10^{-6}$	$< 2 \cdot 10^{-4}$
		R(176)19-8	610.08	$3.28 \cdot 10^{-4}$		0.022	$< 7 \cdot 10^{-6}$	$< 5 \cdot 10^{-4}$
		P(33)6-3	612.49	$4.72 \cdot 10^{-2}$	0.32	0.84	$1.3 \cdot 10^{-2}$	1
		R(164)10-4	613.74	$1.73 \cdot 10^{-2}$	0.91	0.042	$6.6 \cdot 10^{-4}$	$5.1 \cdot 10^{-2}$
612	127	P(43)15-5	489 878.69	$6.36 \cdot 10^{-3}$	0.84	0.96	$5.1 \cdot 10^{-3}$	10^{-1}
		P(48)11-3	879.82	$4.72 \cdot 10^{-2}$	0.79	0.99	$3.7 \cdot 10^{-2}$	$7.6 \cdot 10^{-1}$
		R(123)26-9	880.00	$1.24 \cdot 10^{-4}$		0.26	$< 3 \cdot 10^{-5}$	$< 6 \cdot 10^{-4}$
		R(48)15-5	880.31	$6.36 \cdot 10^{-3}$	0.84	1	$5.3 \cdot 10^{-3}$	$1.1 \cdot 10^{-1}$
		R(47)9-2	880.53	$1.3 \cdot 10^{-1}$	0.38	1	$4.9 \cdot 10^{-2}$	1
		R(34)17-6	881.02	$2.35 \cdot 10^{-3}$	0.66	0.88	$1.4 \cdot 10^{-3}$	$3 \cdot 10^{-2}$
		R(188)24-7	881.09	$8.76 \cdot 10^{-4}$		0.01	$< 9 \cdot 10^{-6}$	$< 2 \cdot 10^{-4}$

Table 1 cont.

λ[nm]	Molecule	Transition	ν[MHz]	$N_{v"rel}$	FCF_{rel}	$S(J'J")_{rel}$	I_{rel}	I'_{rel}
612	129	R(20)7-1	489 878.23	$3.59 \cdot 10^{-1}$	0.09	0.61	$2.0 \cdot 10^{-2}$	$8 \cdot 10^{-1}$
		R(107)6-0	878.34	1	0.0036	0.43	$1.5 \cdot 10^{-3}$	$6 \cdot 10^{-2}$
		R(45)15-5	878.40	$6.36 \cdot 10^{-3}$	0.84	0.99	$5.3 \cdot 10^{-3}$	$2.1 \cdot 10^{-1}$
		R(72)22-8	878.41	$3.28 \cdot 10^{-4}$		0.93	$\leq 3 \cdot 10^{-4}$	$\leq 10^{-2}$
		P(103)16-5	878.74	$6.36 \cdot 10^{-3}$	0.79	0.47	$2.4 \cdot 10^{-3}$	$9.6 \cdot 10^{-2}$
		P(14)7-1	878.90	$3.59 \cdot 10^{-1}$	0.09	0.42	$1.4 \cdot 10^{-2}$	$5.6 \cdot 10^{-1}$
		P(156)25-8	879.15	$3.28 \cdot 10^{-4}$		0.076	$\leq 3 \cdot 10^{-5}$	$\leq 1 \cdot 10^{-3}$
		R(125)21-7	879.45	$8.76 \cdot 10^{-4}$		0.27	$\leq 2 \cdot 10^{-4}$	$\leq 8 \cdot 10^{-3}$
		R(113)14-4	879.90	$1.73 \cdot 10^{-2}$	0.99	0.36	$6.2 \cdot 10^{-3}$	$2.5 \cdot 10^{-1}$
		P(197)31-9	879.90	$1.24 \cdot 10^{-4}$		0.0081	$\leq 1 \cdot 10^{-6}$	$\leq 4 \cdot 10^{-5}$
		P(110)10-2	880.36	$1.3 \cdot 10^{-1}$	0.5	0.39	$2.5 \cdot 10^{-2}$	1
		P(120)26-9	881.89	$1.24 \cdot 10^{-4}$		0.32	$\leq 4 \cdot 10^{-5}$	$\leq 2 \cdot 10^{-3}$
		P(101)6-0	882.18	1	0.0036	0.5	$1.8 \cdot 10^{-3}$	$7.2 \cdot 10^{-2}$
		R(30)17-6	882.29	$2.35 \cdot 10^{-3}$	0.66	0.82	$1.3 \cdot 10^{-3}$	$5.2 \cdot 10^{-2}$
	127/129	P(39)9-2	879.30	$1.3 \cdot 10^{-1}$	0.38	0.92	$4.5 \cdot 10^{-2}$	
		P(148)7-0	879.71	1	0.0072	0.091	$6.6 \cdot 10^{-4}$	
		R(46)24-9	880.80	$1.24 \cdot 10^{-4}$		1	$\leq 1 \cdot 10^{-4}$	
		R(116)12-3	881.32	$4.72 \cdot 10^{-2}$	0.87	0.33	$1.4 \cdot 10^{-2}$	
		P(150)9-1	881.51	$3.59 \cdot 10^{-1}$	0.18	0.083	$5.4 \cdot 10^{-3}$	
		R(25)7-1	881.54	$3.59 \cdot 10^{-1}$	0.09	0.72	$2.3 \cdot 10^{-2}$	
		R(32)17-6	881.80	$2.35 \cdot 10^{-3}$	0.66	0.86	$1.3 \cdot 10^{-3}$	
		R(52)13-4	882.26	$1.73 \cdot 10^{-2}$	1	1	$1.7 \cdot 10^{-2}$	
		P(19)7-1	882.49	$3.59 \cdot 10^{-1}$	0.09	0.56	$1.8 \cdot 10^{-2}$	

Table 2 : Number of HFS-components of two Iodine molecules for different types of transition and for cross-over lines (c.o.).

		J" even			J" odd		
Molec.	2I	$\Delta F = \pm 1$	$\Delta F = 0$	C.O.	$\Delta F = \pm 1$	$\Delta F = 0$	C.O.
$^{127}I_2$	5	15	12	24	21	18	36
$^{129}I_2$	7	28	24	48	36	32	64

Table 3 : Molecular constants of the hyperfine splitting of the indicated iodine transitions. Most constants are fitted from measured frequency differences between HFS components. Only the constants of R(80)1-0 and of R(34)17-6 are interpolated by using other well-known constants. All values are given in MHz.

Transition Molecule	ΔeQq	eQq'	eQq"	ΔC	ΔD	ΔA
P(33)6-3 $^{127}I_2$	1952.7 ± 0.6	-509.7 ± 107.0	-2462.4 ± 107.0	0.0226 ± 0.0010	-0.024 ± 0.030	- 0.0078 ± 0.0080
R(80)1-0 $^{127}I_2$	1953 ± 5	-530	-2483	0.019 ± 0.003	0	0
P(54)8-4 $^{129}I_2$	1368.23 ± 0.23	-449.79 ± 21.00	-1818.02 ± 21.00	0.0157 ± 0.0001	-0.016 ± 0.011	- 0.0069 ± 0.0014
P(69)12-6 $^{129}I_2$	1360.80 ± 0.15	-440 ± 15	-1800.8 ± 15.0	0.0188 ± 0.0001	0 ± 0.008	0 ± 0.0009
R(60)8-4 $^{129}I_2$	1370.0 ± 2.3	-430 ± 126	-1800 ± 126	0.018 ± 0.001	0 ± 0.12	0 ± 0.014
P(33)6-3 $^{129}I_2$	1374.0 ± 0.6	-430 ± 72	-1804 ± 72	0.0165 ± 0.0006	0 ± 0.03	0 ± 0.004
P(48)11-3 $^{127}I_2$	1937.67 ± 0.20	-500 ± 22	-2437.67 ± 22.00	0.0204 ± 0.0003	0 ± 0.009	0 ± 0.004
R(48)15-5 $^{127}I_2$	1936.35 ± 0.20	-500 ± 19	-2436.35 ± 19.00	0.0295 ± 0.0002	0 ± 0.009	0 ± 0.004
R(34)17-6 $^{127}I_2$	1932 ± 5	-530	-2462	0.0037 ± 0.0050	0	0

Table 4 : Frequency differences between the hyperfine structure components of the transition P(33)6-3 of $^{127}I_2$ at a wavelength of λ = 633 nm, measured values from ref.[15]. The estimated error of the calculated values is : σ = 0.03 MHz. The frequency reference is component a_{13} of R(127)11-5.

In the same line as the allowed ($\Delta F = +1$) transition (or in the following line), the forbidden ($\Delta F = 0$) transition, having one common level with the allowed one, is given, along with the appropriate cross-over line.

		$\Delta F = +1$				$\Delta F = 0$			Cross-over	
Component		$\Delta\nu_{meas}$[MHz]	I	F-J	$\Delta\nu_{calc}$[MHz]	Comp	F	$\Delta\nu_{calc}$[MHz]	Comp	$\Delta\nu_{calc}$[MHz]
b_1	u		5	-5	-1315.81	f_{2b}	28	-1383.04	c_{2b}	-1349.43
b_2	t		1	0	-1288.14	f_{17b}	32	-384.76	c_{18b}	-836.45
						f_{1b}	33	-1480.89	c_{1b}	-1384.52
b_3	s		5	5	-1262.87	f_{7b}	37	-855.49	c_{5a}	-1059.18
b_4	r		5	-4	-1053.82	f_{2b}	28	-1383.04	c_{3b}	-1218.43
						f_{3b}	29	-1098.19	c_{4b}	-1076.01
b_5	q		3	1	-1003.92	f_{12b}	33	-624.26	c_{19b}	-814.09
						f_{5b}	34	-1044.20	c_{6b}	-1024.06
b_6	p		3	-1	-987.24	f_{9b}	31	-818.95	c_{12b}	-903.09
						f_{4b}	32	-1060.42	c_{7b}	-1023.83
b_7	o		5	4	-940.71	f_{13b}	36	-582.17	c_{22b}	-761.44
						f_{7b}	37	-855.49	c_{13b}	-898.10
b_8	n		5	-3	-880.43	f_{3b}	29	-1098.19	c_{9b}	-989.31
						f_{6b}	30	-950.62	c_{11b}	-915.53
b_9	m		3	-2	-854.62	f_{10b}	30	-709.95	c_{20b}	-782.28
						f_{9b}	31	-818.95	c_{17b}	-836.79

Table 4 cont.

		ΔF = + 1				ΔF = 0			Cross-over	
Component		$\Delta\nu_{meas}$[MHz]	I	F-J	$\Delta\nu_{calc}$[MHz]	Comp	F	$\Delta\nu_{calc}$[MHz]	Comp	$\Delta\nu_{calc}$[MHz]
b_{10}	l		3	2	-846.53	f_{5b}	34	-1044.20	c_{10b}	-945.37
						f_{8b}	35	-849.30	c_{15b}	-847.92
b_{11}	k		3	3	-832.36	f_{8b}	35	-849.30	c_{16b}	-840.83
b_{12}	j	-740.8	3	-3	-740.80	f_{10b}	30	-709.95	c_{23b}	-725.37
b_{13}	i	-703.7	3	0	-703.68	f_{4b}	32	-1060.42	c_{14b}	-882.05
						f_{12b}	33	-624.26	c_{24b}	-663.97
b_{14}	h	-657.0	5	3	-657.01	f_{14b}	35	-472.70	c_{27b}	-564.86
						f_{13b}	36	-582.17	c_{26b}	-619.59
b_{15}	g	-608.0	5	-2	-607.99	f_{6b}	30	-950.62	c_{21b}	-779.31
						f_{11b}	31	-653.57	c_{25b}	-630.78
b_{16}	f	-572.7	1	-1	-572.77	f_{17b}	32	-384.76	c_{30b}	-478.77
b_{17}	e	-547.4	1	1	-547.40	f_{1b}	33	-1480.89	c_{8b}	-1014.15
b_{18}	d	-511.7	5	2	-511.69	f_{18b}	34	-361.96	c_{31b}	-436.83
						f_{14b}	35	-472.70	c_{29b}	-492.20
b_{19}	c	-430.3	5	-1	-430.26	f_{11b}	31	-653.57	c_{28b}	-541.92
						f_{15b}	32	-433.25	c_{32b}	-431.76
b_{20}	b	-415.5	5	0	-415.48	f_{15b}	32	-433.25	c_{33b}	-424.36
						f_{16b}	33	-420.25	c_{34b}	-417.87
b_{21}	a	-393.5	5	1	-393.53	f_{16b}	33	-420.25	c_{35b}	-406.89
						f_{18b}	34	-361.96	c_{36b}	-377.74

Table 5 : Calculated frequency differences between the hyperfine structure components of the transition R(80)1-0 of $^{127}I_2$ at a wavelength of λ = 633 nm. The estimated error may be less than : σ = 2 MHz. Reference : $\nu(d_1) - \nu(a_{13}, R(127)11\text{-}5) = -863 \pm 30$ MHz.

$\Delta F = +1$				$\Delta F = 0$			Cross-over	
Component	I	F-J	$\Delta\nu_{calc}$[MHz]	Comp	F	$\Delta\nu_{calc}$[MHz]	Comp	$\Delta\nu_{calc}$[MHz]
d_1	0	0	0.0					
d_2	4	-4	282.4	f_{7d}	77	463.0	c_{5d}	372.7
d_3	2	1	290.6	f_{11d}	82	860.5	c_{16d}	575.6
				f_{1d}	81	129.1	c_{1d}	209.8
d_4	2	-1	295.2	f_{12d}	80	1035.1	c_{19d}	665.1
				f_{2d}	79	176.6	c_{2d}	235.9
d_5	4	4	303.3	f_{3d}	84	260.8	c_{3d}	282.1
d_6	4	-3	425.9	f_{5d}	78	435.4	c_{7d}	430.7
				f_{7d}	77	463.0	c_{9d}	444.5
d_7	4	-2	435.0	f_{10d}	79	802.7	c_{17d}	618.9
				f_{5d}	78	435.4	c_{8d}	435.2
d_8	4	2	443.2	f_{6d}	83	452.9	c_{10d}	448.1
				f_{4d}	82	361.1	c_{6d}	402.1
d_9	4	3	452.5	f_{3d}	84	260.8	c_{4d}	356.6
				f_{6d}	83	452.9	c_{12d}	452.7
d_{10}	4	0	585.6	f_{9d}	81	777.8	c_{20d}	681.7
				f_{8d}	80	545.5	c_{15d}	565.6
d_{11}	2	-2	724.1	f_{2d}	79	176.6	c_{11d}	450.4

Table 5 cont.

ΔF = + 1				ΔF = 0			Cross-over	
Component	I	F-J	$\Delta\nu_{calc}$[MHz]	Comp	F	$\Delta\nu_{calc}$[MHz]	Comp	$\Delta\nu_{calc}$[MHz]
d_{12}	4	-1	725.7	f_{8d}	80	545.5	c_{18d}	635.6
				f_{10d}	79	802.7	c_{22d}	764.2
d_{13}	4	1	738.4	f_{4d}	82	361.1	c_{14d}	549.7
				f_{9d}	81	777.8	c_{21d}	758.1
d_{14}	2	2	740.6	f_{11d}	82	860.5	c_{23d}	800.6
d_{15}	2	0	878.7	f_{1d}	81	129.1	c_{13d}	503.9
				f_{12d}	80	1035.1	c_{24d}	956.9

Table 6 : Frequency differences between the hyperfine structure components of the transition P(54)8-4 of $^{129}I_2$ at a wavelength of λ = 633 nm, measured values of ref.[7, 16-21]. The estimated error of the calculated values is : σ = 0.056 MHz. The frequency reference is component a_{13} of R(127)11-5.

		ΔF = + 1				ΔF = 0			Cross-over	
Component		$\Delta\nu_{meas}$ [MHz]	I	F-J	$\Delta\nu_{calc}$ [MHz]	Comp	F	$\Delta\nu_{calc}$ [MHz]	Comp	$\Delta\nu_{calc}$ [MHz]
a_1			0	0	-489.72					
a_2	z'	-353.3	6	-6	-354.24	f_{2a}	48	-382.87	c_{1a}	-368.55
a_3	y'	-347.1	4	1	-347.82	f_{14a}	54	-146.07	c_{11a}	-246.95
						f_{3a}	55	-379.57	c_{2a}	-363.69
a_4	x'	-338.3	4	-1	-338.62	f_{8a}	52	-210.94	c_{7a}	-274.78
						f_{1a}	53	-384.18	c_{3a}	-361.40
a_5	w'	-333.1	6	6	-332.92	f_{9a}	59	-192.55	c_{9a}	-262.73
a_6	v'	-265.0	6	-5	-263.90	f_{2a}	48	-382.87	c_{4a}	-323.38
						f_{4a}	49	-280.64	c_{8a}	-272.27
a_7	u'	-249.2	4	2	-248.21	f_{3a}	55	-379.57	c_{5a}	-313.89
						f_{5a}	56	-265.19	c_{10a}	-256.70
a_8	t'	-245.0	4	-2	-243.47	f_{10a}	51	-186.44	c_{16a}	-214.95
						f_{8a}	52	-210.94	c_{15a}	-227.20
a_9	s'	-229.5	6	5	-228.26	f_{11a}	58	-171.75	c_{19a}	-200.01
						f_{9a}	59	-192.55	c_{18a}	-210.40
a_{10}	r'	-211.1	6	-4	-209.74	f_{4a}	49	-280.64	c_{12a}	-245.19
						f_{6a}	50	-255.63	c_{13a}	-232.69
a_{11}	q'	-202.3	4	-3	-201.45	f_{16a}	50	-79.14	c_{25a}	-140.29
						f_{10a}	51	-186.44	c_{20a}	-193.94

Table 6 cont.

ΔF = +1						ΔF = 0			Cross-over	
Component		$\Delta\nu_{meas}$[MHz]	I	F-J	$\Delta\nu_{calc}$[MHz]	Comp	F	$\Delta\nu_{calc}$[MHz]	Comp	$\Delta\nu_{calc}$[MHz]
a_{12}	p'	-197.2	4	0	-196.94	f_{1a}	53	-384.18	c_{6a}	-290.56
						f_{14a}	54	-146.07	c_{22a}	-171.51
a_{13}	o'	-193.8	4	3	-193.52	f_{5a}	56	-265.19	c_{14a}	-229.36
						f_{7a}	57	-227.46	c_{17a}	-210.49
a_{14}	n'	-186.8	6	4	-186.55	f_{20a}	57	16.57	c_{29a}	-84.99
						f_{11a}	58	-171.75	c_{21a}	-179.15
a_{15}	j'	-110.15	4	-4	-110.22	f_{16a}	50	-79.14	c_{28a}	-94.68
a_{16}	i'	-101.83	2	-1	-101.90	f_{23a}	52	88.12	c_{40a}	-6.89
						f_{12a}	53	-165.73	c_{26a}	-133.81
a_{17}	h'	-97.33	2	1	-97.43	f_{24a}	54	160.55	c_{44a}	31.56
						f_{13a}	55	-146.27	c_{27a}	-121.85
a_{18}	g'	-86.84	4	4	-86.87	f_{7a}	57	-227.46	c_{24a}	-157.17
a_{19}	f'	-66.71	6	-3	-66.73	f_{6a}	50	-255.63	c_{23a}	-161.18
						f_{17a}	51	-67.89	c_{31a}	-67.31
a_{20}	e'	-59.82	6	-2	-59.88	f_{17a}	51	-67.89	c_{32a}	-63.89
						f_{15a}	52	-91.70	c_{30a}	-75.79
a_{21}	d'	-42.76	6	2	-42.81	f_{22a}	55	85.38	c_{42a}	21.28
						f_{18a}	56	-44.47	c_{34a}	-43.64
a_{22}	e'	-34.56	6	3	-34.60	f_{18a}	56	-44.47	c_{35a}	-39.53
						f_{20a}	57	16.57	c_{39a}	-9.01

Table 6 cont.

		ΔF = + 1					ΔF = 0		Cross-over	
Component		$\Delta\nu_{meas}$[MHz]	I	F-J	$\Delta\nu_{calc}$[MHz]	Comp	F	$\Delta\nu_{calc}$[MHz]	Comp	$\Delta\nu_{calc}$[MHz]
a_{23}	a'	-2.31	6	0	-2.35	f_{21a}	53	55.40	c_{43a}	26.52
						f_{19a}	54	-19.40	c_{38a}	-10.88
a_{24}	n_2	40.29	6	-1	40.28	f_{15a}	52	-91.70	c_{37a}	-25.71
						f_{21a}	53	55.40	c_{45a}	47.84
a_{25}	n_1	40.29	2	-2	40.32	f_{23a}	52	88.12	c_{46a}	64.22
a_{26}	m_2	52.83	6	1	52.79	f_{19a}	54	-19.40	c_{41a}	16.69
						f_{22a}	55	85.38	c_{47a}	69.08
a_{27}	m_1	54.69	2	2	54.69	f_{13a}	55	-146.27	c_{33a}	-45.79
a_{28}	k	95.90	2	0	95.95	f_{12a}	53	-165.73	c_{36a}	-34.89
						f_{24a}	54	160.55	c_{48a}	128.25

Table 7 : Frequency differences between the hyperfine structure components of the transition P(69)12-6 of $^{129}I_2$ at a wavelength of λ = 633 nm, measured values of ref.[18, 20]. The estimated error of the calculated values is : σ = 0.39 MHz. The frequency reference is component a_{13} of R(127)11-5.

		$\Delta F = +1$				$\Delta F = 0$			Cross-over	
Component		$\Delta\nu_{meas}$[MHz]	I	F-J	$\Delta\nu_{calc}$[MHz]	Comp	F	$\Delta\nu_{calc}$[MHz]	Comp	$\Delta\nu_{calc}$[MHz]
b_1	b"'	194.99	7	-7	195.01	f_{2b}	62	152.88	c_{2b}	173.95
b_2	a"'	211.95	1	0	211.67	f_{32b}	68	911.76	c_{35b}	561.71
						f_{1b}	69	38.89	c_{1b}	125.28
b_3	z"	227.92	7	7	227.96	f_{8b}	75	436.05	c_{7b}	332.01
b_4	s"	330.45	7	-6	330.26	f_{2b}	62	152.88	c_{3b}	241.57
						f_{5b}	63	298.31	c_{6b}	314.28
b_5	r"	352.85	3	1	354.46	f_{30b}	69	809.51	c_{38b}	581.99
						f_{4b}	70	258.45	c_{4b}	306.46
b_6	q"	360.77	3	-1	360.38	f_{25b}	67	732.58	c_{32b}	546.48
						f_{3b}	68	253.12	c_{5b}	306.75
b_7	p"	383.96	7	6	383.76	f_{17b}	74	575.42	c_{17b}	479.59
						f_{8b}	75	436.05	c_{10b}	409.90
b_8	k"	433.72	7	-5	434.20	f_{5b}	63	298.31	c_{8b}	366.25
						f_{6b}	64	391.37	c_{11b}	412.79
b_9	i_1"	454.73	5	2	453.83	f_{20b}	70	652.14	c_{34b}	552.98
						f_{9b}	71	438.09	c_{13b}	445.96
b_{10}	i_2"	454.73	5	-2	455.02	f_{14b}	66	513.32	c_{20b}	484.17
						f_{7b}	67	410.57	c_{12b}	432.80
b_{11}	j"	469.67	5	5	469.19	f_{15b}	73	530.31	c_{25b}	499.75

Table 7 cont.

		ΔF = +1				ΔF = 0			Cross-over	
Component		$\Delta\nu_{meas}$[MHz]	I	F-J	$\Delta\nu_{calc}$[MHz]	Comp	F	$\Delta\nu_{calc}$[MHz]	Comp	$\Delta\nu_{calc}$[MHz]
b_{12}	d"	481.29	5	-5	483.29	f_{11b}	64	482.55	c_{19b}	482.92
b_{13}	c"	489.29	5	-4	490.63	f_{11b}	64	482.55	c_{21b}	486.59
						f_{12b}	65	490.02	c_{23b}	490.33
b_{14}	b"	496.69	5	-3	497.77	f_{12b}	65	490.02	c_{24b}	493.90
						f_{14b}	66	513.32	c_{27b}	505.54
b_{15}	a"	502.59	5	0	503.03	f_{19b}	68	629.93	c_{37b}	566.48
						f_{10b}	69	472.58	c_{22b}	487.81
b_{16}	z'	506.99	5	3	507.72	f_{9b}	71	438.09	c_{15b}	472.90
						f_{13b}	72	507.38	c_{28b}	507.55
b_{17}	y'	513.19	5	4	514.02	f_{13b}	72	507.38	c_{29b}	510.70
						f_{15b}	73	530.31	c_{30b}	522.16
b_{18}			7	5	527.27	f_{22b}	73	662.65	c_{40b}	594.96
						f_{17b}	74	575.42	c_{33b}	551.35
b_{19}			7	-4	571.66	f_{6b}	64	391.37	c_{18b}	481.51
						f_{16b}	65	553.97	c_{36b}	562.81
b_{20}	q'	604.39	5	-1	597.60	f_{7b}	67	410.57	c_{26b}	504.08
						f_{19b}	68	629.93	c_{41b}	613.76
b_{21}			5	1	602.33	f_{10b}	69	472.58	c_{31b}	537.46
						f_{20b}	70	652.14	c_{43b}	627.23

Table 7 cont.

		ΔF = + 1				ΔF = 0			Cross-over	
Component		$\Delta\nu_{meas}$[MHz]	I	F-J	$\Delta\nu_{calc}$[MHz]	Comp	F	$\Delta\nu_{calc}$[MHz]	Comp	$\Delta\nu_{calc}$[MHz]
b_{22}	o'	630.59	7	4	628.14	f_{26b}	72	746.07	c_{50b}	687.11
						f_{22b}	73	662.65	c_{44b}	645.39
b_{23}	n'	633.89	7	-3	631.58	f_{16b}	65	553.97	c_{39b}	592.77
						f_{18b}	66	602.13	c_{42b}	616.86
b_{24}	m'	642.49	3	-2	640.24	f_{23b}	66	696.41	c_{48b}	668.33
						f_{25b}	67	732.58	c_{49b}	686.41
b_{25}	l'	656.59	3	2	656.20	f_{4b}	70	258.45	c_{14b}	457.32
						f_{21b}	71	656.32	c_{45b}	656.26
b_{26}	k'	661.19	3	3	661.33	f_{21b}	71	656.32	c_{46b}	658.82
b_{27}	j'	677.79	3	-3	681.45	f_{23b}	66	696.41	c_{51b}	688.93
b_{28}	i'	693.89	3	0	696.90	f_{3b}	68	253.12	c_{16b}	475.01
						f_{30b}	69	809.51	c_{56b}	753.20
b_{29}	h'	712.39	7	3	716.02	f_{27b}	71	778.87	c_{54b}	747.44
						f_{26b}	72	746.07	c_{53b}	731.04
b_{30}	g'	723.49	7	-2	727.56	f_{18b}	66	602.13	c_{47b}	664.85
						f_{24b}	67	710.01	c_{52b}	718.78
b_{31}	f'	735.69	1	-1	739.19	f_{32b}	68	911.76	c_{64b}	825.47
b_{32}	e'	748.09	1	1	750.56	f_{1b}	69	38.89	c_{9b}	394.72
b_{33}	d'	760.69	7	2	762.11	f_{31b}	70	814.40	c_{59b}	788.26
						f_{27b}	71	778.87	c_{57b}	770.49

Table 7 cont.

		ΔF = + 1					ΔF = 0		Cross-over	
Component		$\Delta\nu_{meas}$[MHz]	I	F-J	$\Delta\nu_{calc}$[MHz]	Comp	F	$\Delta\nu_{calc}$[MHz]	Comp	$\Delta\nu_{calc}$[MHz]
b_{34}	c'	787.49	7	-1	787.58	f_{24b}	67	710.01	c_{55b}	748.79
						f_{28b}	68	787.30	c_{58b}	787.44
b_{35}	b'	792.99	7	0	792.97	f_{28b}	68	787.30	c_{60b}	790.14
						f_{29b}	69	792.40	c_{61b}	792.69
b_{36}	a'	801.29	7	1	800.47	f_{29b}	69	792.40	c_{62b}	796.43
						f_{31b}	70	814.40	c_{63b}	807.44

Table 8 : Frequency differences between the hyperfine structure components of the transition R(60)8-4 of $^{129}I_2$ at a wavelength of λ = 633 nm, measured values of ref.[18]. The estimated error of the calculated values is : σ = 0.68 MHz. The frequency reference is component a_{13} of R(127)11-5.

	$\Delta F = +1$				$\Delta F = 0$			Cross-over	
Component	$\Delta\nu_{meas}$[MHz]	I	F-J	$\Delta\nu_{calc}$[MHz]	Comp	F	$\Delta\nu_{calc}$[MHz]	Comp	$\Delta\nu_{calc}$[MHz]
d_1		0	0	-946.8					
d_2		6	-6	-811.9	f_{6d}	55	-693.0	c_{7d}	-752.5
d_3		4	1	-803.9	f_{9d}	62	-673.9	c_{8d}	-738.9
					f_{1d}	61	-852.6	c_{1d}	-828.2
d_4		4	-1	-796.2	f_{13d}	60	-610.0	c_{11d}	-703.1
					f_{2d}	59	-827.6	c_{2d}	-811.9
d_5		6	6	-788.4	f_{3d}	66	-822.5	c_{3d}	-805.5
d_6		6	-5	-720.5	f_{10d}	56	-650.7	c_{15d}	-685.6
					f_{6d}	55	-693.0	c_{10d}	-706.8
d_7		4	2	-703.9	f_{11d}	63	-633.6	c_{18d}	-668.7
					f_{9d}	62	-673.9	c_{13d}	-688.9
d_8		4	-2	-700.9	f_{2d}	59	-827.6	c_{4d}	-764.2
					f_{4d}	58	-715.8	c_{9d}	-708.3
d_9		6	5	-684.6	f_{3d}	66	-822.5	c_{5d}	-753.6
					f_{5d}	65	-699.3	c_{12d}	-691.9
d_{10}		6	-4	-666.3	f_{19d}	57	-478.8	c_{28d}	-572.6
					f_{10d}	56	-650.7	c_{20d}	-658.5
d_{11}		4	-3	-658.5	f_{4d}	58	-715.8	c_{14d}	-687.1
					f_{8d}	57	-688.6	c_{16d}	-673.5

Table 8 cont.

ΔF = + 1					ΔF = 0			Cross-over	
Component	$\Delta\nu_{meas}$[MHz]	I	F-J	$\Delta\nu_{calc}$[MHz]	Comp	F	$\Delta\nu_{calc}$[MHz]	Comp	$\Delta\nu_{calc}$[MHz]
d_{12}		4	0	-653.5	f_{1d}	61	-852.6	c_{6d}	-753.0
					f_{13d}	60	-610.0	c_{22d}	-631.7
d_{13}		4	3	-649.2	f_{17d}	64	-511.2	c_{27d}	-580.2
					f_{11d}	63	-633.6	c_{21d}	-641.4
d_{14}		6	4	-642.4	f_{5d}	65	-699.3	c_{17d}	-670.9
					f_{7d}	64	-691.4	c_{19d}	-666.9
d_{15}		4	-4	-566.9	f_{8d}	57	-688.6	c_{23d}	-627.8
d_{16}		2	-1	-558.3	f_{24d}	60	-299.4	c_{43d}	-428.9
					f_{14d}	59	-604.4	c_{26d}	-581.4
d_{17}		2	1	-553.6	f_{23d}	62	-355.3	c_{40d}	-454.4
					f_{12d}	61	-615.7	c_{25d}	-584.6
d_{18}		4	4	-542.9	f_{17d}	64	-511.2	c_{29d}	-527.1
d_{19}		6	-3	-522.6	f_{16d}	58	-515.3	c_{30d}	-518.9
					f_{19d}	57	-478.8	c_{34d}	-500.7
d_{20}		6	-2	-515.9	f_{22d}	59	-385.5	c_{41d}	-450.7
					f_{16d}	58	-515.3	c_{31d}	-515.6
d_{21}		6	2	-499.0	f_{18d}	63	-490.3	c_{35d}	-494.6
					f_{15d}	62	-530.5	c_{32d}	-514.8
d_{22}		6	3	-491.2	f_{7d}	64	-691.4	c_{24d}	-591.3
					f_{18d}	63	-490.3	c_{36d}	-490.7

Table 8 cont.

		ΔF = + 1					ΔF = 0		Cross-over	
Component		$\Delta\nu_{meas}$[MHz]	I	F-J	$\Delta\nu_{calc}$[MHz]	Comp	F	$\Delta\nu_{calc}$[MHz]	Comp	$\Delta\nu_{calc}$[MHz]
d_{23}	A'	458.5	6	0	-458.4	f_{21d}	61	-387.7	c_{44d}	-423.1
						f_{20d}	60	-473.4	c_{39d}	-465.9
d_{24}	N	415.0	2	-2	-415.9	f_{14d}	59	-604.4	c_{33d}	-510.2
d_{25}	N	415.0	6	-1	-415.5	f_{20d}	60	-473.4	c_{42d}	-444.5
						f_{22d}	59	-385.5	c_{45d}	-400.5
d_{26}	M	403.1	6	1	-403.5	f_{15d}	62	-530.5	c_{38d}	-467.0
						f_{21d}	61	-387.7	c_{46d}	-395.6
d_{27}	M	403.1	2	2	-401.4	f_{23d}	62	-355.3	c_{47d}	-378.3
d_{28}	K	360.1	2	0	-360.1	f_{12d}	61	-615.7	c_{37d}	-487.9
						f_{24d}	60	-299.4	c_{48d}	-329.8

Table 9 : Frequency differences between the hyperfine structure components of the transition P(33)6-3 of $^{129}I_2$ at a wavelength of λ = 633 nm, measured values of ref.[18, 22]. The estimated error of the calculated values is : σ = 0.047 MHz. The frequency reference is component a_{13} of R(127)11-5.

		$\Delta F = +1$				$\Delta F = 0$			Cross-over	
Component		$\Delta\nu_{meas}$[MHz]	I	F-J	$\Delta\nu_{calc}$[MHz]	Comp	F	$\Delta\nu_{calc}$[MHz]	Comp	$\Delta\nu_{calc}$[MHz]
e_1	A	968.45	7	-7	968.47	f_{2e}	26	930.84	c_{2e}	949.65
e_2	B	988.29	1	0	988.31	f_{32e}	32	1743.05	c_{38e}	1365.68
						f_{1e}	33	819.02	c_{1e}	903.66
e_3	C	1006.12	7	7	1006.14	f_{9e}	39	1229.89	c_{7e}	1118.01
e_4	D	1090.86	7	-6	1090.88	f_{2e}	26	930.84	c_{3e}	1010.86
						f_{4e}	27	1059.21	c_{4e}	1075.04
e_5	E	1129.15	3	1	1126.79	f_{30e}	33	1584.86	c_{37e}	1355.83
						f_{5e}	34	1096.15	c_{6e}	1111.47
e_6	F	1144.95	3	-1	1143.56	f_{26e}	31	1497.80	c_{33e}	1320.68
						f_{3e}	32	1040.33	c_{5e}	1091.95
e_7	G	1179.05	7	6	1175.66	f_{19e}	38	1369.51	c_{23e}	1272.58
						f_{9e}	39	1229.89	c_{13e}	1202.77
e_8	H	1196.25	7	-5	1194.60	f_{4e}	27	1059.21	c_{8e}	1126.90
						f_{6e}	28	1153.01	c_{10e}	1173.80
e_9	I	1227.15	3	2	1226.81	f_{5e}	34	1096.15	c_{9e}	1161.48
						f_{7e}	35	1159.65	c_{12e}	1193.23
e_{10}	J	1237.65	5	-2	1238.07	f_{14e}	30	1288.75	c_{20e}	1263.41
						f_{8e}	31	1195.55	c_{14e}	1216.81
e_{11}	K	1249.15	5	5	1249.46	f_{16e}	37	1310.49	c_{24e}	1279.98

Table 9 cont.

		ΔF = + 1					ΔF = 0		Cross-over	
Component		$\Delta\nu_{meas}$[MHz]	I	F-J	$\Delta\nu_{calc}$[MHz]	Comp	F	$\Delta\nu_{calc}$[MHz]	Comp	$\Delta\nu_{calc}$[MHz]
e_{12}	L	1257.25	5	-5	1257.72	f_{11e}	28	1256.24	c_{16e}	1256.98
e_{13}	M	1261.15	5	-4	1261.63	f_{11e}	28	1256.24	c_{18e}	1258.93
						f_{12e}	29	1257.54	c_{19e}	1259.58
e_{14}	N	1275.65	5	-3	1276.34	f_{12e}	29	1257.54	c_{22e}	1266.94
						f_{14e}	30	1288.75	c_{25e}	1282.54
e_{15}	O	1280.65	5	0	1281.33	f_{20e}	32	1405.47	c_{34e}	1343.40
						f_{10e}	33	1250.71	c_{21e}	1266.02
e_{16}	P	1283.85	5	3	1284.20	f_{24e}	35	1487.54	c_{41e}	1385.87
						f_{13e}	36	1281.62	c_{26e}	1282.91
e_{17}	Q	1293.25	5	4	1294.85	f_{13e}	36	1281.62	c_{28e}	1288.24
						f_{16e}	37	1310.49	c_{30e}	1302.67
e_{18}			7	5	1322.86	f_{21e}	37	1460.83	c_{43e}	1391.84
						f_{19e}	38	1369.51	c_{35e}	1346.18
e_{19}			7	-4	1329.79	f_{6e}	28	1153.01	c_{15e}	1241.40
						f_{15e}	29	1310.42	c_{32e}	1320.11
e_{20}			5	-1	1375.41	f_{8e}	31	1195.55	c_{26e}	1285.48
						f_{20e}	32	1405.47	c_{42e}	1390.44
e_{21}			5	1	1380.98	f_{10e}	33	1250.71	c_{31e}	1315.85
						f_{18e}	34	1363.68	c_{39e}	1372.33

Table 9 cont.

ΔF = + 1					ΔF = 0			Cross-over	
Component	$\Delta\nu_{meas}$[MHz]	I	F-J	$\Delta\nu_{calc}$[MHz]	Comp	F	$\Delta\nu_{calc}$[MHz]	Comp	$\Delta\nu_{calc}$[MHz]
e_{22}		7	-3	1392.90	f_{15e}	29	1310.42	c_{36e}	1351.66
					f_{17e}	30	1362.62	c_{40e}	1377.76
e_{23}		3	-2	1412.95	f_{22e}	30	1468.51	c_{46e}	1440.73
					f_{26e}	31	1497.80	c_{48e}	1455.38
e_{24}		7	4	1427.14	f_{27e}	36	1535.87	c_{51e}	1481.50
					f_{21e}	37	1460.83	c_{47e}	1443.98
e_{25}		5	2	1438.35	f_{18e}	34	1363.68	c_{44e}	1401.01
					f_{24e}	35	1487.54	c_{50e}	1462.94
e_{26}		3	3	1445.23	f_{7e}	35	1159.65	c_{29e}	1302.44
e_{27}		3	-3	1455.46	f_{22e}	30	1468.51	c_{49e}	1461.99
e_{28}		3	0	1475.05	f_{3e}	32	1040.33	c_{17e}	1257.69
					f_{30e}	33	1584.86	c_{56e}	1529.96
e_{29}		7	-2	1490.72	f_{17e}	30	1362.62	c_{45e}	1426.67
					f_{23e}	31	1485.26	c_{52e}	1487.99
e_{30}		7	3	1509.66	f_{29e}	35	1566.59	c_{58e}	1538.13
					f_{27e}	36	1535.87	c_{55e}	1522.76
e_{31}		7	-1	1510.91	f_{23e}	31	1485.26	c_{53e}	1498.08
					f_{25e}	32	1492.74	c_{54e}	1501.83
e_{32}		1	1	1531.99	f_{1e}	33	819.02	c_{11e}	1175.50

Table 9 cont.

ΔF = + 1					ΔF = 0			Cross-over	
Component	$\Delta\nu_{meas}$[MHz]	I	F-J	$\Delta\nu_{calc}$[MHz]	Comp	F	$\Delta\nu_{calc}$[MHz]	Comp	$\Delta\nu_{calc}$[MHz]
e_{33}		7	2	1552.34	f_{31e}	34	1592.70	c_{61e}	1572.52
					f_{29e}	35	1566.59	c_{59e}	1559.47
e_{34}		1	-1	1562.91	f_{32e}	32	1743.05	c_{64e}	1652.98
e_{35}		7	0	1568.38	f_{25e}	32	1492.74	c_{57e}	1530.56
					f_{28e}	33	1564.76	c_{60e}	1566.57
e_{36}		7	1	1583.16	f_{28e}	33	1564.76	c_{62e}	1573.96
					f_{31e}	34	1592.70	c_{63e}	1587.93

Table 10 : Frequency differences between the hyperfine structure components of the transition P(48)11-3 of $^{127}I_2$ at a wavelength of λ = 612 nm, measured values of ref.[23, 24]. The estimated error of the calculated values is : σ = 0.39 MHz. The frequency reference is component a_7 of R(47)9-2.

		$\Delta F = +1$				$\Delta F = 0$			Cross-over	
Component		$\Delta\nu_{meas}$[MHz]	I	F-J	$\Delta\nu_{calc}$[MHz]	Comp	F	$\Delta\nu_{calc}$[MHz]	Comp	$\Delta\nu_{calc}$[MHz]
b_1			0	0	-1040.0					
b_2			2	1	-751.8	f_{12b}	48	-14.6	c_{19b}	-383.2
						f_{2b}	49	-861.4	c_{2b}	-806.6
b_3			4	-4	-745.9	f_{3b}	44	-783.3	c_{3b}	-764.6
b_4			2	-1	-740.8	f_{11b}	46	-211.5	c_{15b}	-476.1
						f_{1b}	47	-884.8	c_{1b}	-812.8
b_5			4	4	-724.9	f_{7b}	51	-533.6	c_{6b}	-629.2
b_6	n	-617.5	4	-3	-610.1	f_{3b}	44	-783.3	c_{4b}	-696.7
						f_{5b}	45	-616.2	c_{7b}	-613.1
b_7	m	-603.5	4	-2	-601.0	f_{5b}	45	-616.2	c_{8b}	-608.6
						f_{4b}	46	-673.0	c_{5b}	-637.0
b_8	l	-595.2	4	2	-594.8	f_{10b}	49	-222.2	c_{17b}	-408.5
						f_{6b}	50	-593.1	c_{9b}	-594.0
b_9	k	-578.5	4	3	-577.1	f_{6b}	50	-593.1	c_{10b}	-585.1
						f_{7b}	51	-533.6	c_{12b}	-555.3
b_{10}	hij	-453.8	4	0	-454.4	f_{9b}	47	-282.0	c_{20b}	-368.2
						f_{8b}	48	-490.7	c_{16b}	-472.6
b_{11}	g	-315.3	2	-2	-316.1	f_{11b}	46	-211.5	c_{22b}	-263.8

Table 10 cont.

ΔF = +1						ΔF = 0			Cross-over	
Component		$\Delta\nu_{meas}$[MHz]	I	F-J	$\Delta\nu_{calc}$[MHz]	Comp	F	$\Delta\nu_{calc}$[MHz]	Comp	$\Delta\nu_{calc}$[MHz]
b_{12}	f	-315.3	4	-1	-315.9	f_{4b}	46	-673.0	c_{14b}	-494.5
						f_{9b}	47	-282.0	c_{21b}	-299.0
b_{13}	e	-298.6	4	1	-298.7	f_{8b}	48	-490.7	c_{18b}	-394.7
						f_{10b}	49	-222.2	c_{23b}	-260.4
b_{14}	d	-295.6	2	2	-295.8	f_{2b}	49	-861.4	c_{11b}	-578.6
b_{15}	abc	-163.3	2	0	-163.3	f_{1b}	47	-884.8	c_{13b}	-524.1
						f_{12b}	48	-14.6	c_{24b}	-89.0

Table 11 : Frequency differences between the hyperfine structure components of the transition R(48)15-5 of $^{127}I_2$ at a wavelength of λ = 612 nm, measured values of ref.[23, 24]. The estimated error of the calculated values is : σ = 1.1 MHz. The frequency reference is component a_7 of R(47)9-2.

		$\Delta F = +1$				$\Delta F = 0$			Cross-over	
Component		$\Delta\nu_{meas}$[MHz]	I	F-J	$\Delta\nu_{calc}$[MHz]	Comp	F	$\Delta\nu_{calc}$[MHz]	Comp	$\Delta\nu_{calc}$[MHz]
d_1	stu	-514.5	0	0	-513.8					
d_2	r	-237.1	4	-4	-237.4	f_{6d}	45	-63.9	c_{5d}	-150.7
d_3	q	-228.1	2	1	-228.1	f_{11d}	50	338.5	c_{16d}	55.2
						f_{1d}	49	-383.8	c_{1d}	-306.0
d_4	p	-219.0	2	-1	-218.5	f_{12d}	48	-504.2	c_{19d}	142.9
						f_{2d}	47	-331.5	c_{2d}	-275.0
d_5	o	-211.3	4	4	-211.5	f_{3d}	52	-250.9	c_{3d}	-231.2
d_6	n	-97.6	4	-3	-96.8	f_{5d}	46	-81.5	c_{7d}	-89.2
						f_{6d}	45	-63.9	c_{9d}	-80.4
d_7	m		4	-2	-83.0	f_{10d}	47	274.7	c_{17d}	95.8
						f_{5d}	46	-81.5	c_{8d}	-82.3
d_8	l	-71.2	4	2	-74.0	f_{7d}	51	-57.9	c_{11d}	-66.0
						f_{4d}	50	-152.0	c_{6d}	-113.0
d_9	k	-59.9	4	3	-59.3	f_{3d}	52	-250.9	c_{4d}	-155.1
						f_{7d}	51	-57.9	c_{12d}	-58.6
d_{10}	hij	67.7	4	0	66.8	f_{9d}	49	259.1	c_{20d}	163.0
						f_{8d}	48	29.7	c_{15d}	48.2
d_{11}	g	199.6	2	-2	198.6	f_{2d}	47	-331.5	c_{10d}	-66.4

Table 11 cont.

		ΔF = + 1				ΔF = 0			Cross-over	
Component		$\Delta\nu_{meas}$[MHz]	I	F-J	$\Delta\nu_{calc}$[MHz]	Comp	F	$\Delta\nu_{calc}$[MHz]	Comp	$\Delta\nu_{calc}$[MHz]
d_{12}	f	205.1	4	-1	202.4	f_{8d}	48	29.7	c_{18d}	116.0
						f_{10d}	47	274.7	c_{21d}	238.5
d_{13}	e	213.9	4	1	221.3	f_{4d}	50	-152.0	c_{14d}	34.6
						f_{9d}	49	259.1	c_{22d}	240.2
d_{14}	d	216.4	2	2	221.8	f_{11d}	50	338.5	c_{23d}	280.1
d_{15}	abc	358.4	2	0	354.6	f_{1d}	49	-383.8	c_{13d}	-14.6
						f_{12d}	48	504.2	c_{24d}	429.4

Table 12 : Calculated frequency differences between hyperfine structure components of the transition R(34)17-6 of $^{127}I_2$ at a wavelength of λ = 612 nm. The estimated error may be less than : σ = 2 MHz. Reference : $\nu(e_1) - \nu(a_7, R(47)9-2) = 162 \pm 30$ MHz.

$\Delta F = +1$				$\Delta F = 0$			Cross-over	
Component	I	F-J	$\Delta\nu_{calc}$[MHz]	Comp	F	$\Delta\nu_{calc}$[MHz]	Comp	$\Delta\nu_{calc}$[MHz]
e_1	0	0	0.0					
e_2	4	-4	278.8	f_{6e}	31	450.2	c_{5e}	364.5
e_3	2	1	280.8	f_{11e}	36	861.0	c_{16e}	570.9
				f_{1e}	35	119.6	c_{1e}	200.2
e_4	2	-1	298.3	f_{12e}	34	1025.0	c_{19e}	661.7
				f_{2e}	33	184.0	c_{2e}	241.1
e_5	4	4	299.8	f_{3e}	38	257.2	c_{3e}	278.5
e_6	4	-3	413.4	f_{5e}	32	434.9	c_{7e}	424.2
				f_{6e}	31	450.2	c_{8e}	431.8
e_7	4	-2	430.6	f_{10e}	33	789.0	c_{17e}	609.8
				f_{5e}	32	434.9	c_{9e}	432.7
e_8	4	2	435.8	f_{7e}	37	458.8	c_{10e}	447.3
				f_{4e}	36	353.9	c_{6e}	394.8
e_9	4	3	454.3	f_{3e}	38	257.2	c_{4e}	355.7
				f_{7e}	37	458.8	c_{12e}	456.5
e_{10}	4	0	578.5	f_{9e}	35	776.7	c_{20e}	677.6
				f_{8e}	34	541.5	c_{15e}	560.0
e_{11}	4	-1	711.8	f_{8e}	34	541.5	c_{18e}	626.7
				f_{10e}	33	789.0	c_{21e}	750.4

Table 12 cont.

ΔF = + 1					ΔF = 0			Cross-over
Component	I	F-J	$\Delta\nu_{calc}$[MHz]	Comp	F	$\Delta\nu_{calc}$[MHz]	Comp	$\Delta\nu_{calc}$[MHz]
e_{12}	2	-2	712.4	f_{2e}	33	184.0	c_{11e}	448.2
e_{13}	4	1	734.3	f_{4e}	36	353.9	c_{14e}	544.1
				f_{9e}	35	776.7	c_{22e}	755.5
e_{14}	2	2	736.7	f_{11e}	36	861.0	c_{23e}	798.8
e_{15}	2	0	868.6	f_{1e}	35	119.6	c_{13e}	494.1
				f_{12e}	34	1025.0	c_{24e}	946.8

Figure Captions

Fig. 1 : Sum profiles of the third derivatives of two Lorentzian lines having the same amplitudes and linewidths (HWHM). The two Lorentzian lines are spaced by the indicated multiples x_2 of their linewidths.

Fig. 2 : Absolute shift of the middle zero-crossing (z.c.) point of the third derivative of a Lorentz profile due to the overlapping by another one, as a function of the separation x_2 of the two profiles. Both axes are given in units of the linewidth (HWHM). The sign of the z.c. shift is positive for : $0 < x_2 < 1$, negative for : $x_2 > 1$. At $x_2 = 0$ and $x_2 = 1$, the z.c. shift is zero. The parameter b represents the amplitude of the overlapping profile relative to the overlapped one.

Fig. 3 : Absolute shift of the middle zero-crossing point of the third derivative of a Lorentz profile due to the overlapping by another one, as a function of its amplitude b relative to the overlapped one. The parameter x_2 represents the separation of the two profiles. Further conditions as in Fig. 2.

Fig. 4-9 : Positions of the calculated hyperfine structure components of P(33)6-3 of $^{127}I_2$ at λ = 633 nm on a frequency scale. The vertical lines represent : the $\Delta F = \pm 1$ transitions above, the cross-over lines, across, and the $\Delta F = 0$ transitions below the frequency axis.

Fig. 10-14 : Hyperfine structure components of R(80)1-0 of $^{127}I_2$ at λ = 633 nm. Further conditions as in Fig. 4-9.

Fig. 15-20 : Hyperfine structure components of P(54)8-4 of $^{129}I_2$ at λ = 633 nm. Further conditions as in Fig. 4-9.

Fig. 21-29 : Hyperfine structure components of P(69)12-6 of $^{129}I_2$ at λ = 633 nm. Further conditions as in Fig. 4-9.

Fig. 30-34 : Hyperfine structure components of R(60)8-4 of $^{129}I_2$ at λ = 633 nm. Further conditions as in Fig. 4-9.

Fig. 35-39 : Hyperfine structure components of P(33)6-3 of $^{129}I_2$ at λ = 633 nm. Further conditions as in Fig. 4-9.

Fig. 40-43 : Hyperfine structure components of P(48)11-3 of $^{127}I_2$ at λ = 612 nm. Further conditions as in Fig. 4-9.

Fig. 44-46 : Hyperfine structure components of R(48)15-5 of $^{127}I_2$ at λ = 612 nm. Further conditions as in Fig. 4-9.

Fig. 47-50 : Hyperfine structure components of R(34)17-6 of $^{127}I_2$ at λ = 612 nm. Further conditions as in Fig. 4-9.

Fig. 51 : Synopsis of the main hyperfine structure components of all calculated transitions of $^{127}I_2$ at λ = 633 nm on a frequency scale, the $\Delta F = \pm 1$ transitions being above, and the cross-over lines below, the reference lines.

Fig. 52 : Synopsis of the main hyperfine structure components of all calculated transitions of $^{127}I_2$ and $^{129}I_2$ and of the components of ^{127}I-^{129}I found by experiment [18, 20, 21] at λ = 633 nm. Further conditions as in Fig. 51.

Fig. 53 : As in Fig. 52, with the frequency scale centered on transition P(54)8-4.

Fig. 54 : As in Fig. 52, with the frequency scale centered on transition P(69)12-6.

Fig. 55 : Synopsis of the main hyperfine structure components of all calculated transitions of $^{127}I_2$ at λ = 612 nm. Further conditions as in Fig. 51.

Fig. 56 : Synopsis of the main hyperfine structure components of all calculated transitions of $^{127}I_2$ and $^{129}I_2$ at λ = 612 nm. Further conditions as in Fig. 51.

Fig. 57 : As in Fig. 56, with the frequency scale centered on P(110)10-2.

Fig.1

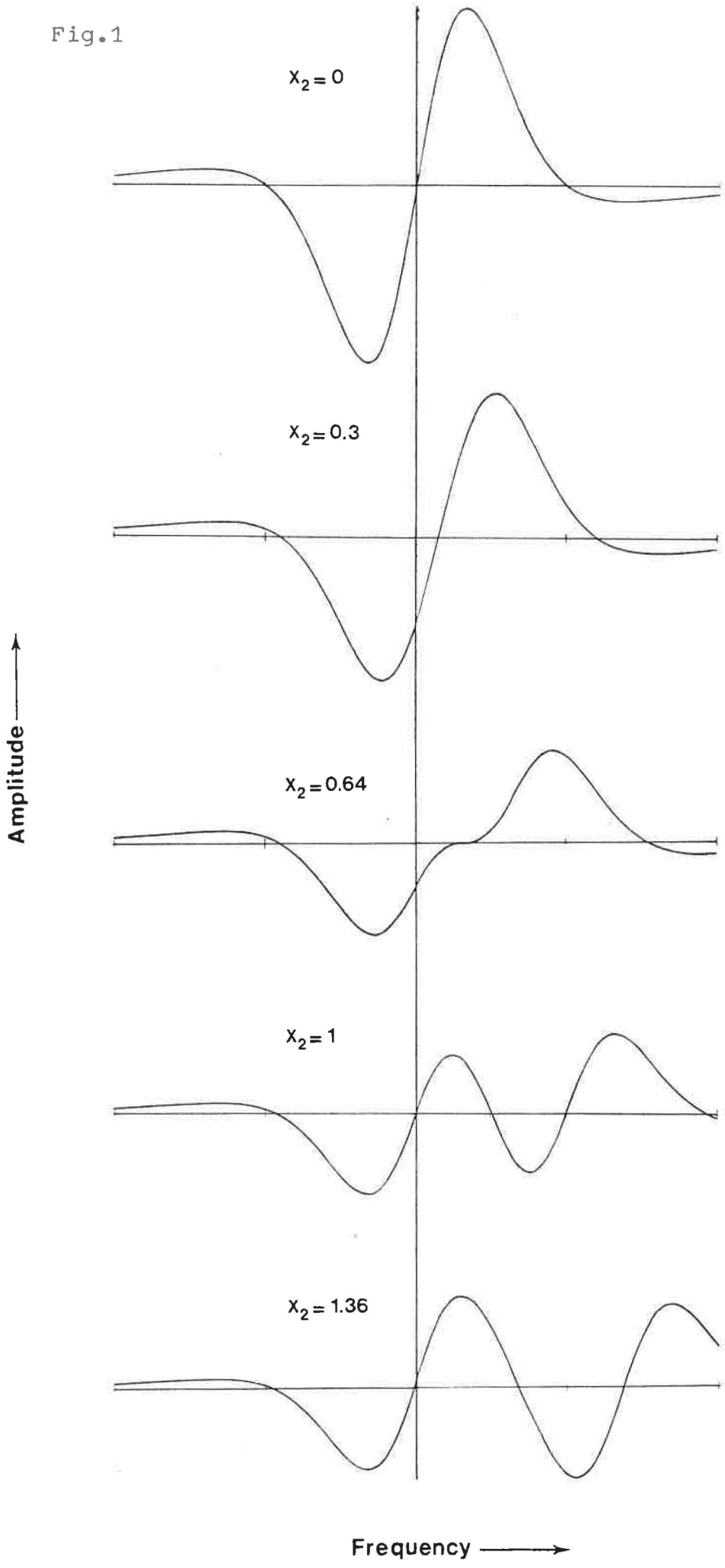

Fig.2

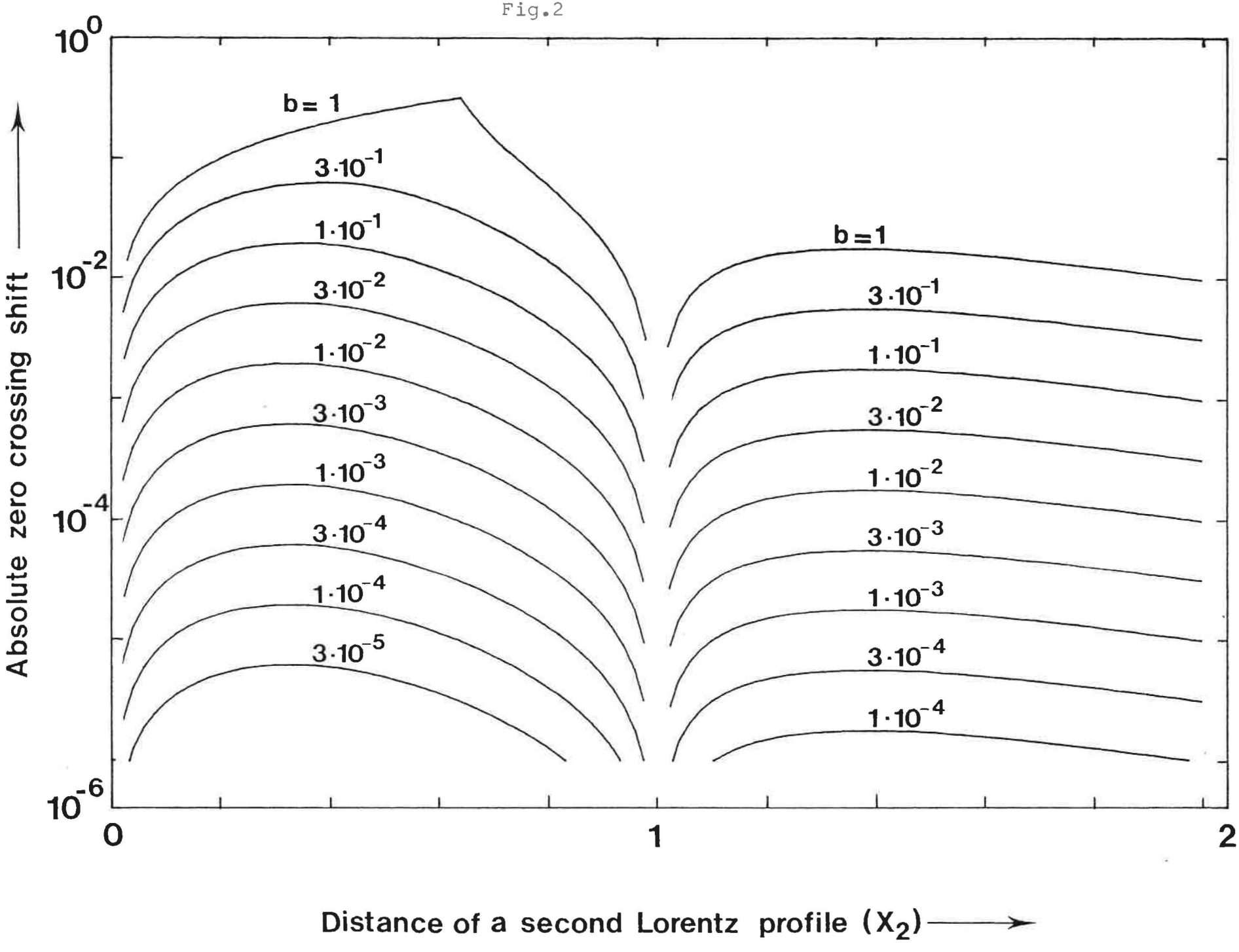
Absolute zero crossing shift
10^0
10^{-2}
10^{-4}
10^{-6}
b= 1
$3\cdot10^{-1}$
$1\cdot10^{-1}$
$3\cdot10^{-2}$
$1\cdot10^{-2}$
$3\cdot10^{-3}$
$1\cdot10^{-3}$
$3\cdot10^{-4}$
$1\cdot10^{-4}$
$3\cdot10^{-5}$
b=1
$3\cdot10^{-1}$
$1\cdot10^{-1}$
$3\cdot10^{-2}$
$1\cdot10^{-2}$
$3\cdot10^{-3}$
$1\cdot10^{-3}$
$3\cdot10^{-4}$
$1\cdot10^{-4}$
0
1
2
Distance of a second Lorentz profile (X_2) ⟶

Fig.3

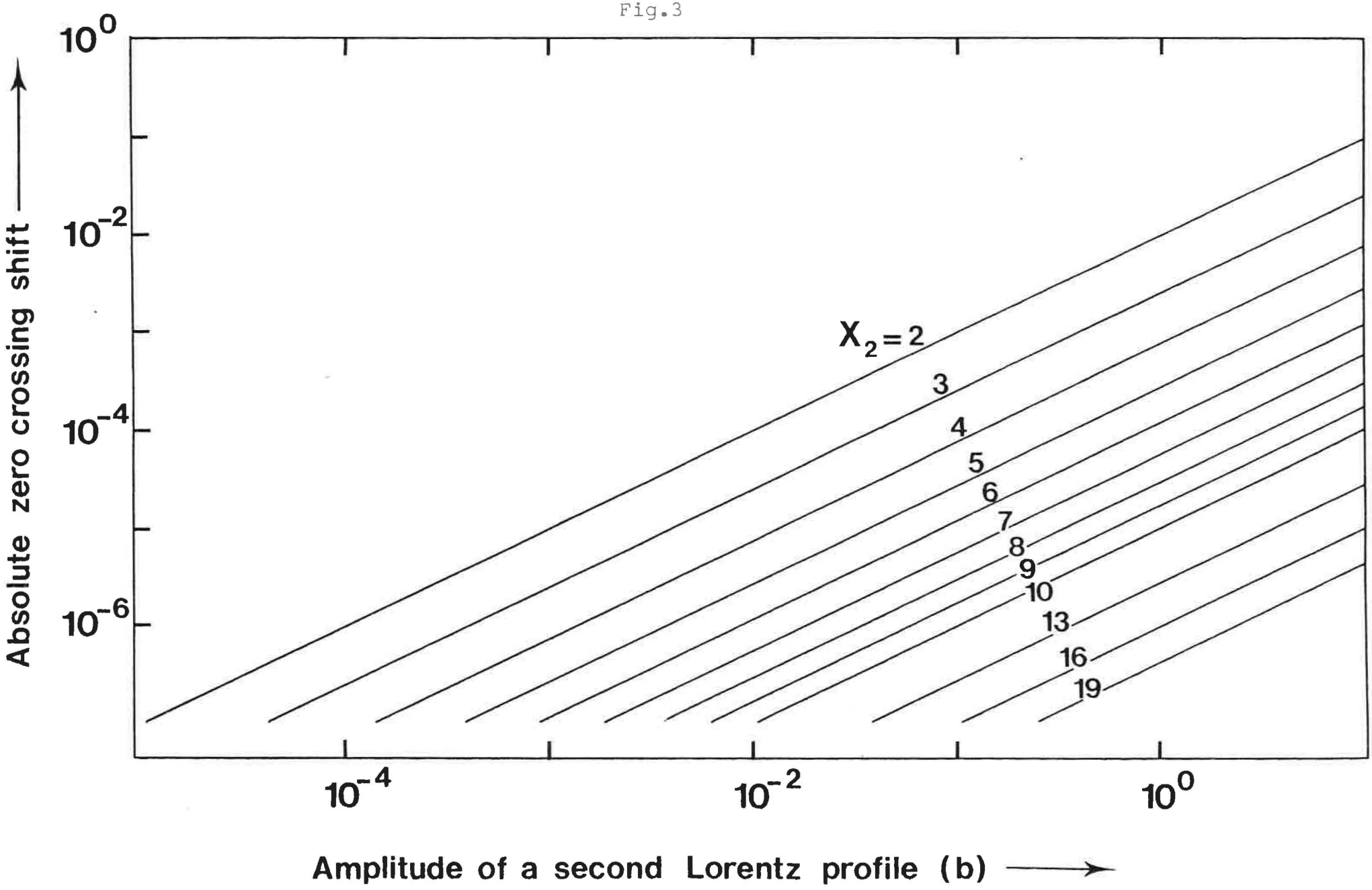
10^0
10^{-2}
10^{-4}
10^{-6}
Absolute zero crossing shift
$X_2 = 2$
3
4
5
6
7
8
9
10
13
16
19
10^{-4}
10^{-2}
10^0
Amplitude of a second Lorentz profile (b)

Fig.4: $^{127}I_2$; P(33)6-3; λ=633 NM

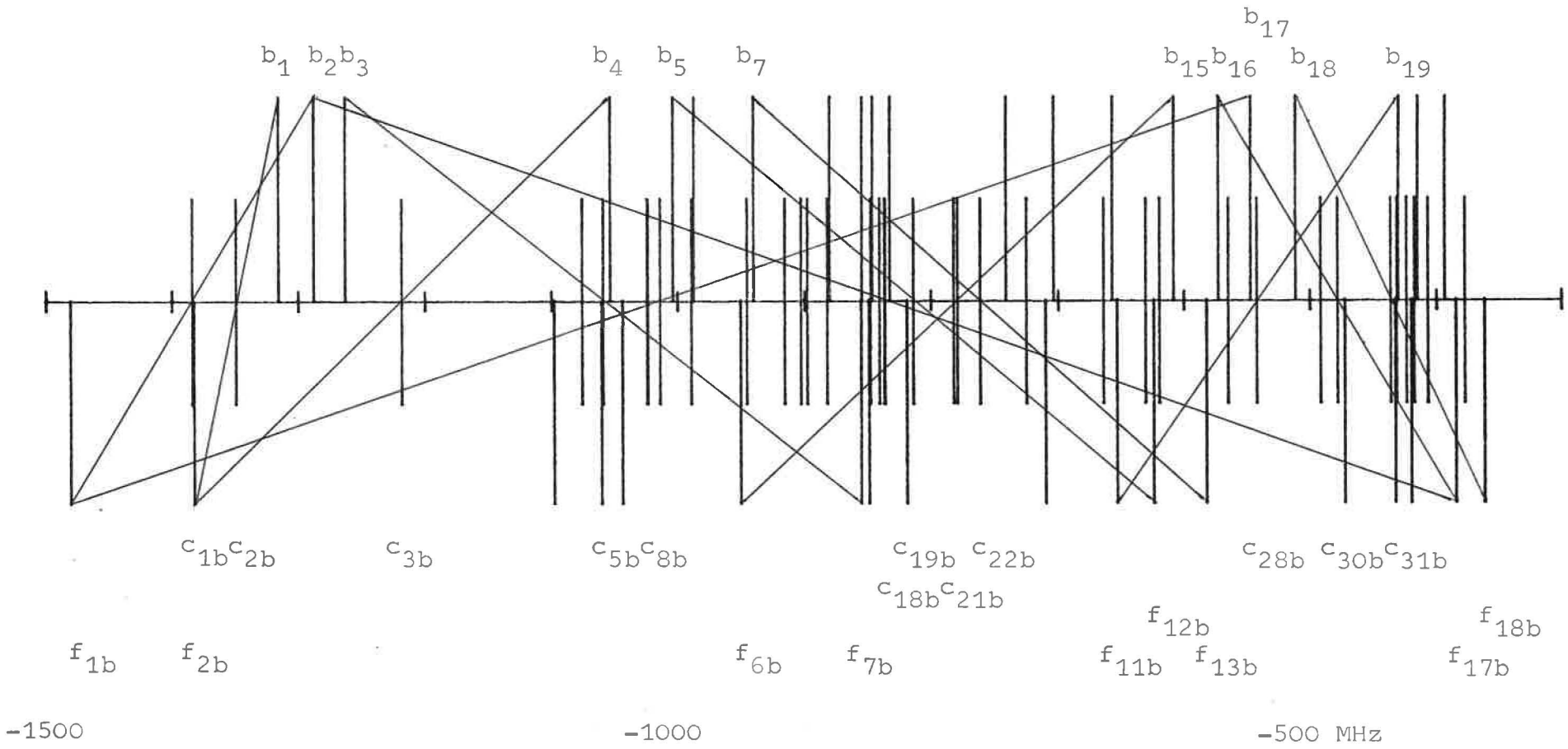

Fig.5: $^{127}I_2$; P(33)6-3; λ=633 NM

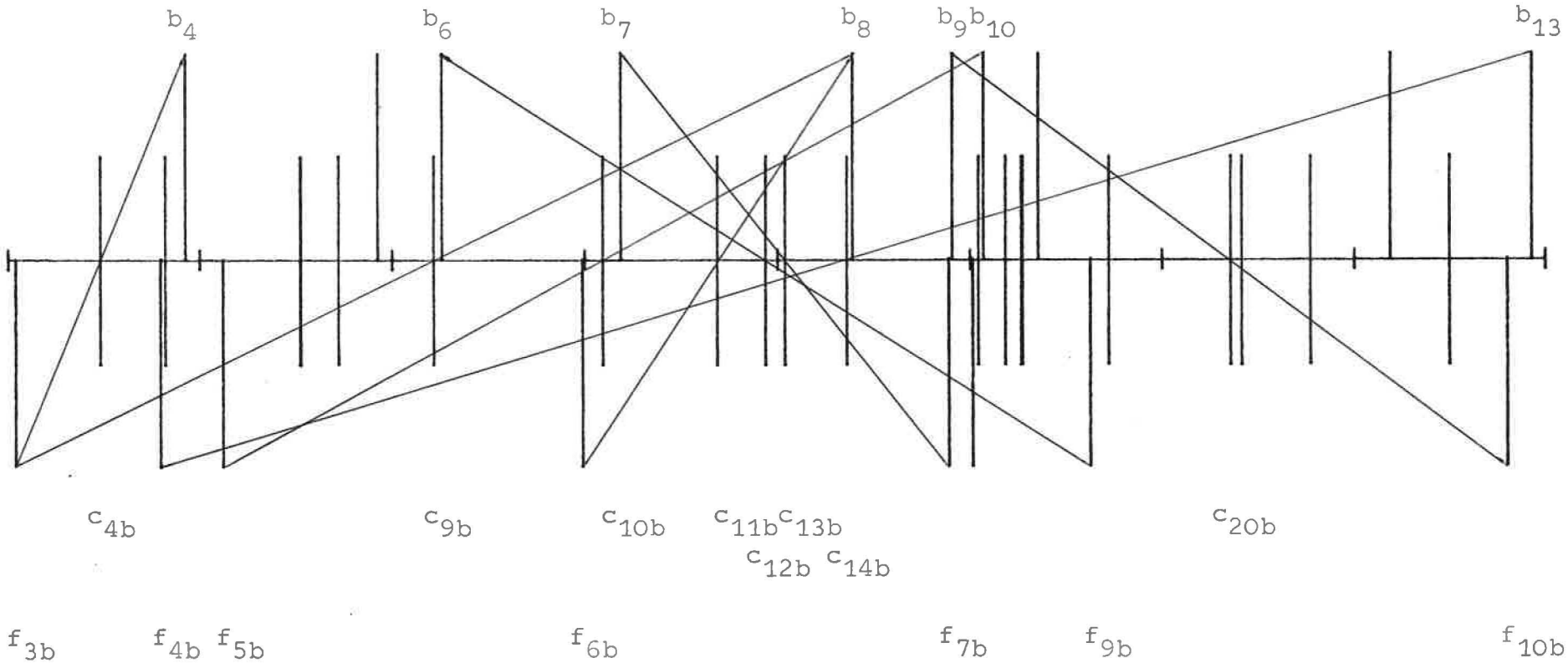

Fig.6: $^{127}I_2$; P(33)6-3; λ=633 NM

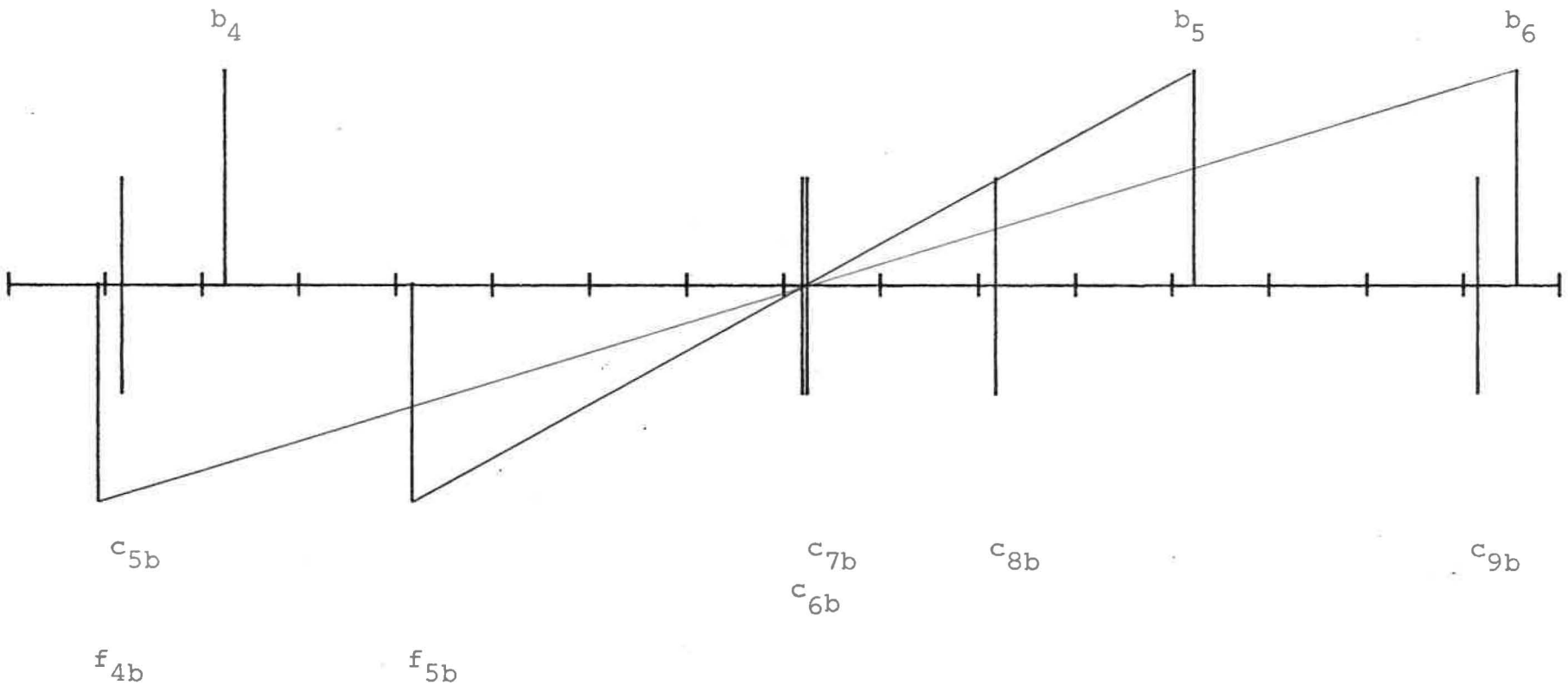

Fig.7: $^{127}I_2$; P(33)6-3; λ=633 NM

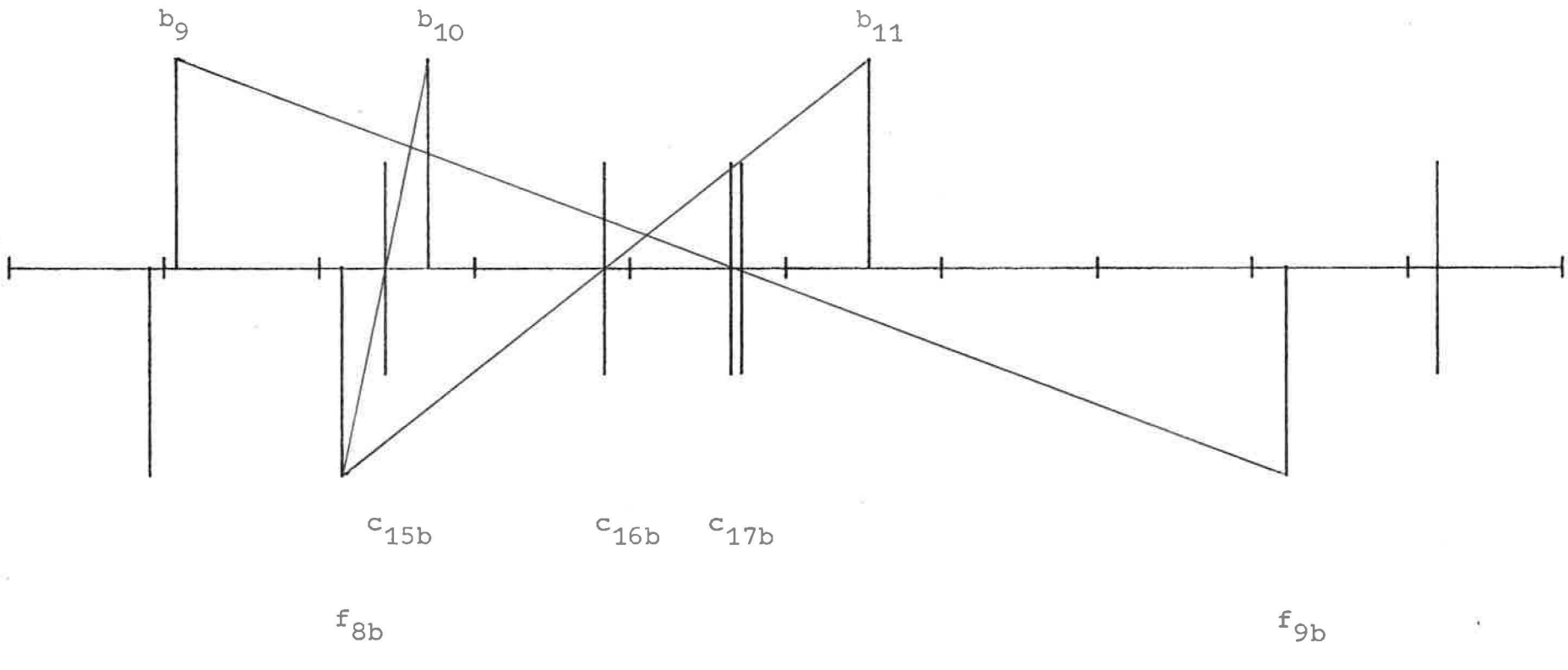

Fig.8: $^{127}I_2$; P(33)6-3; λ=633 NM

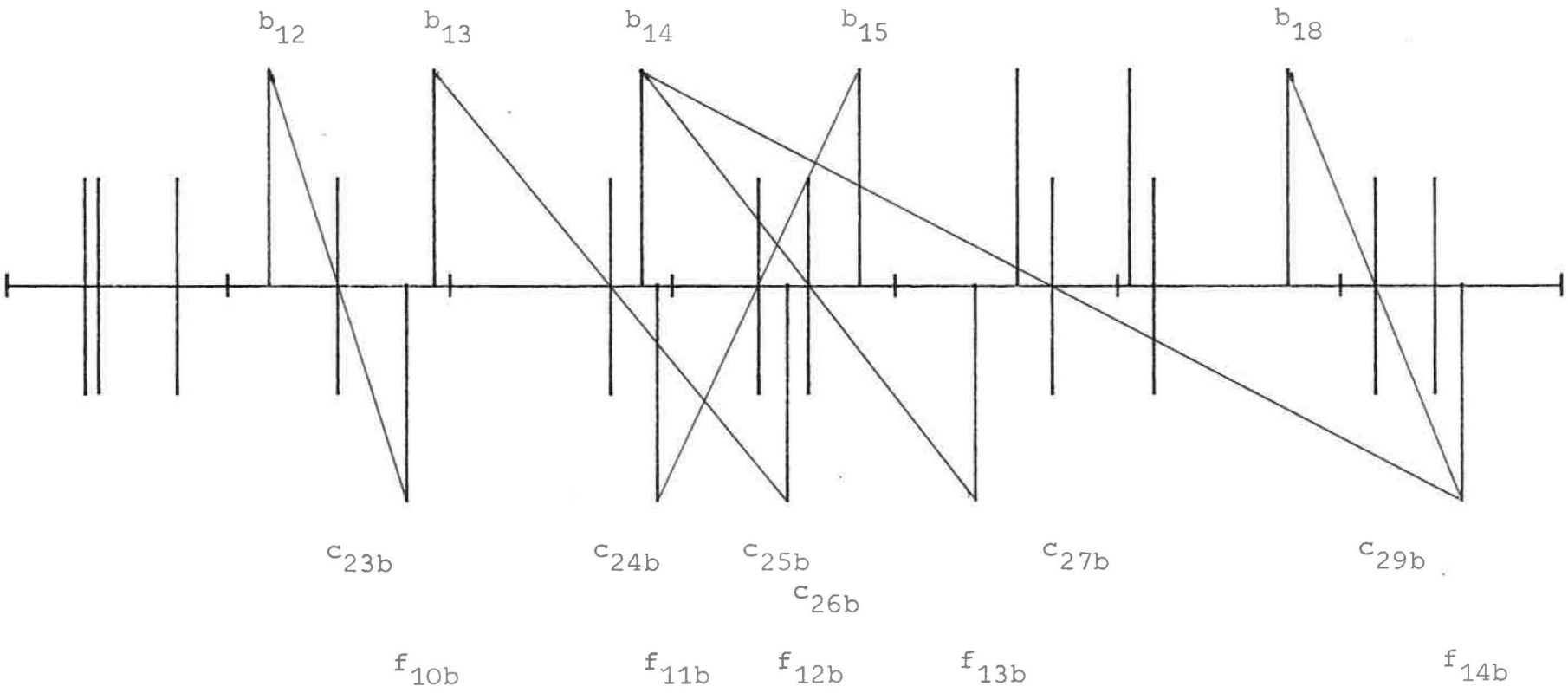

Fig.9: $^{127}I_2$; P(33)6-3; λ=633 NM

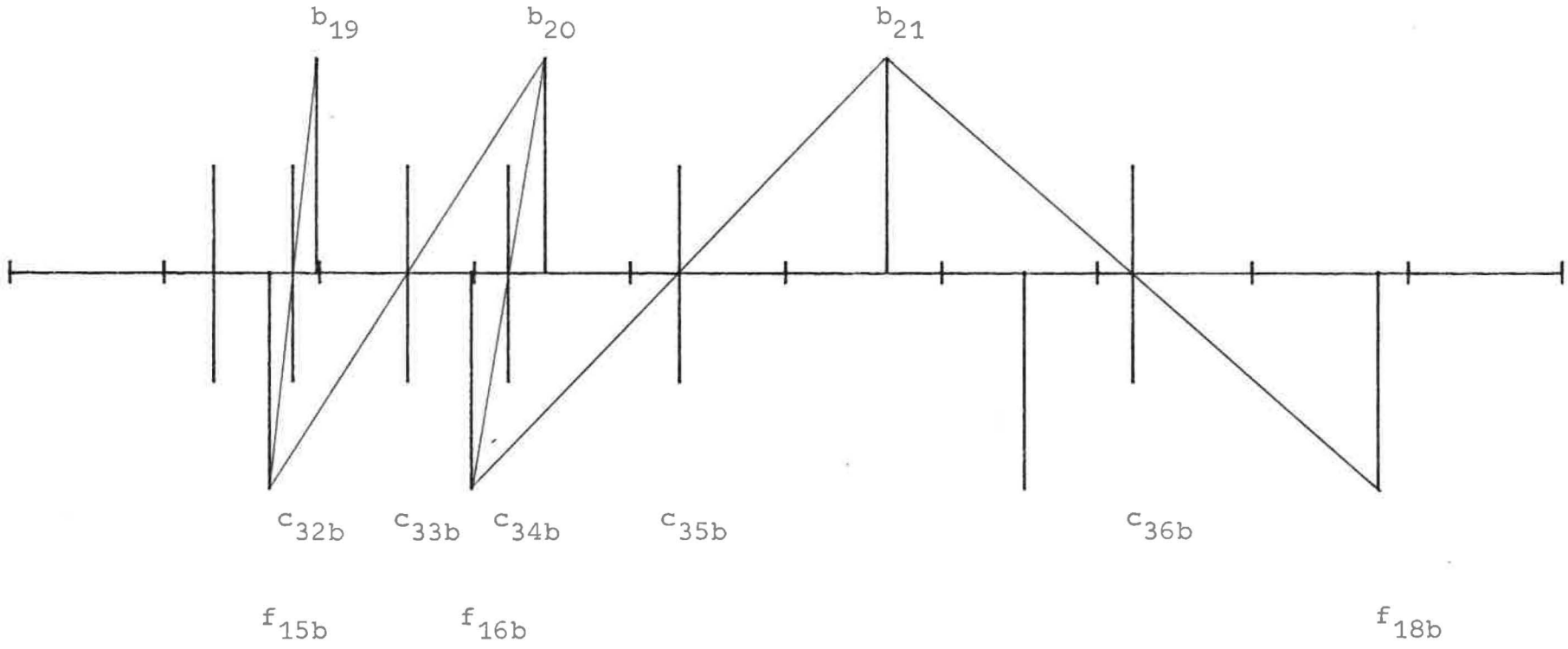

Fig.10: $^{127}I_2$; R(80)1-0; λ=633 NM

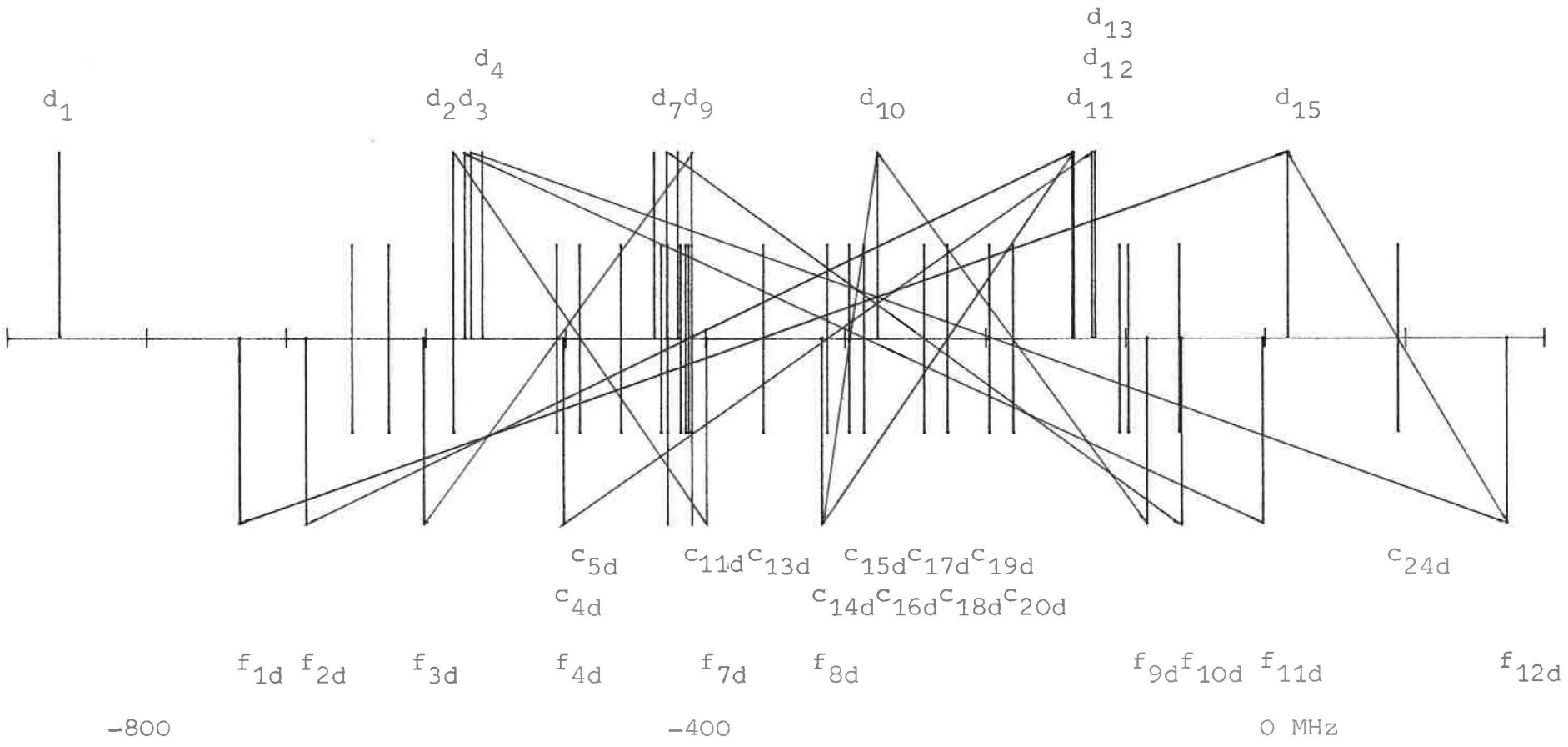

Fig.11: $^{127}I_2$; R(80)1-0; λ=633 NM

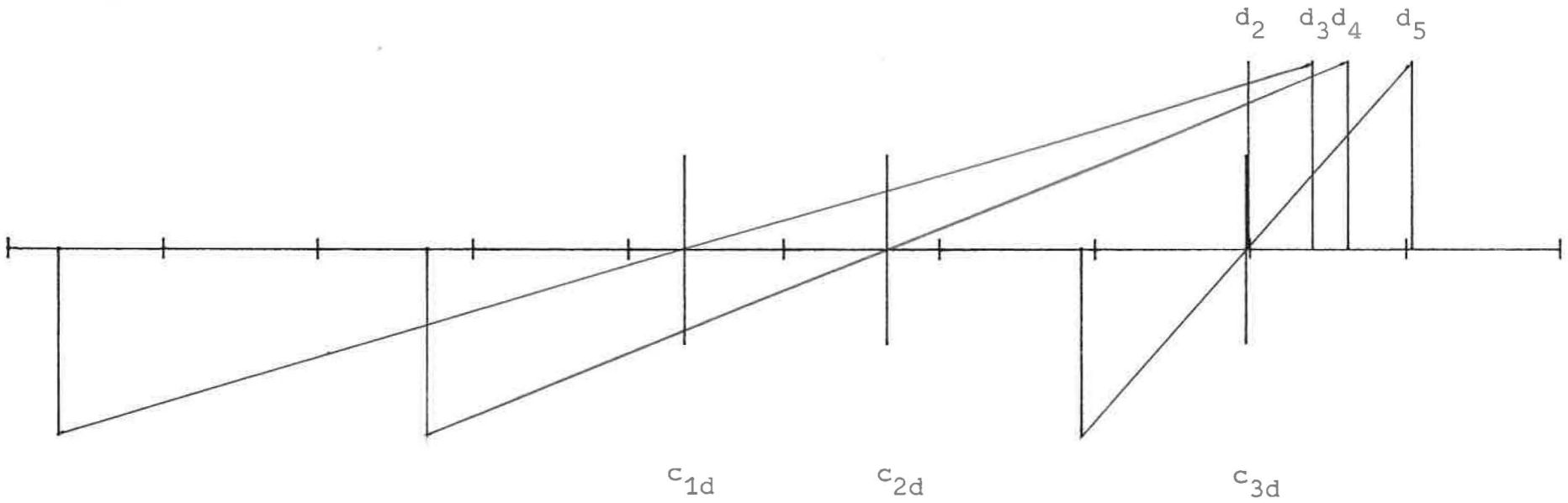

Fig.12: $^{127}I_2$; R(80)1-0; λ=633 NM

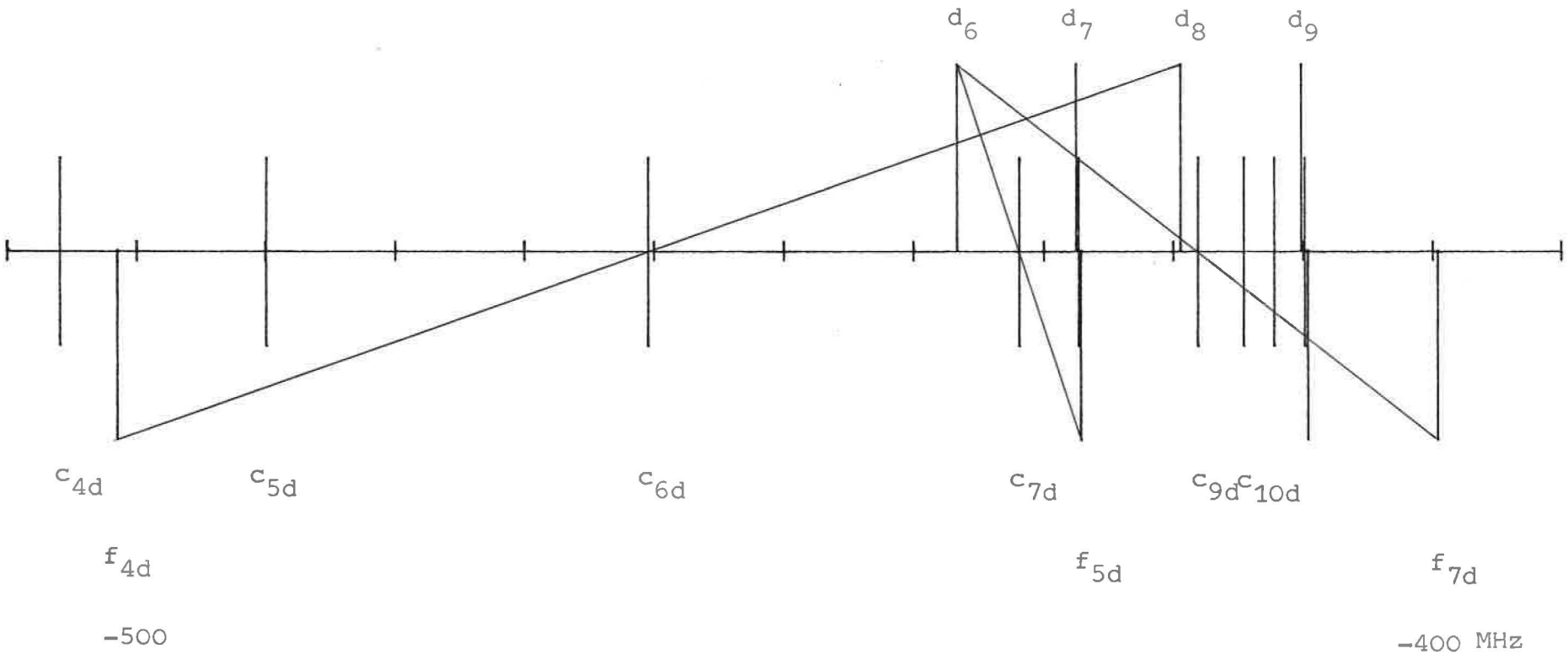

Fig.13: $^{127}I_2$; R(80)1-0; λ=633 NM

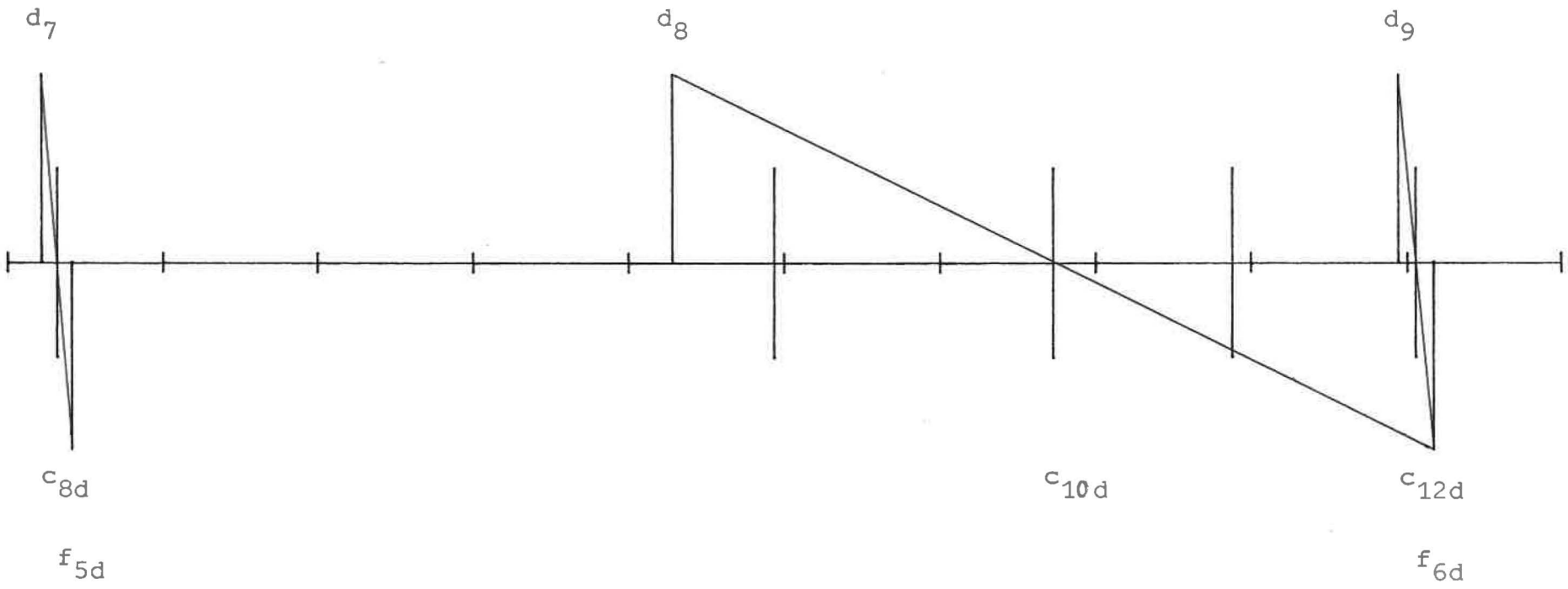

Fig.14: $^{127}I_2$; R(80)1-0; λ=633 NM

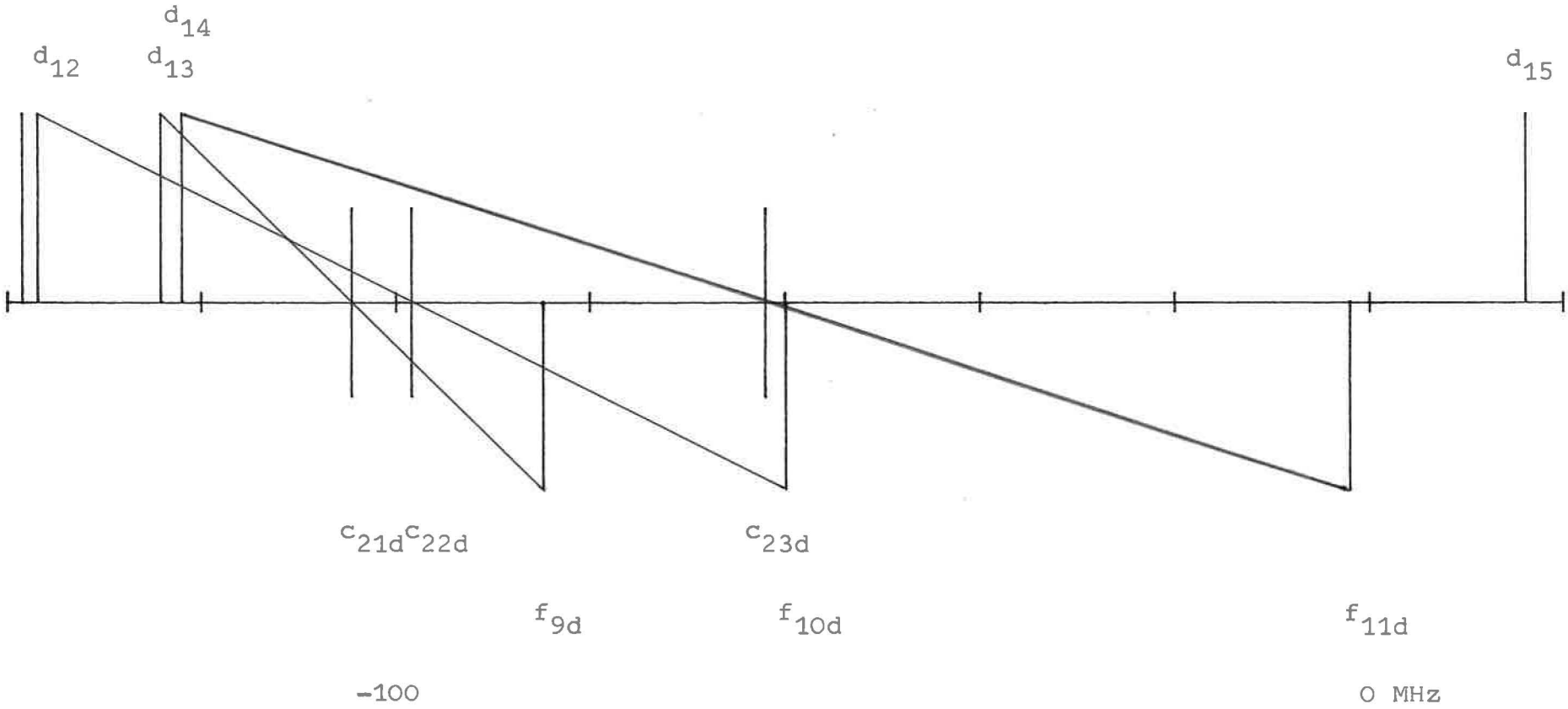

Fig.15: $^{129}I_2$; P(54)8-4; λ=633 NM

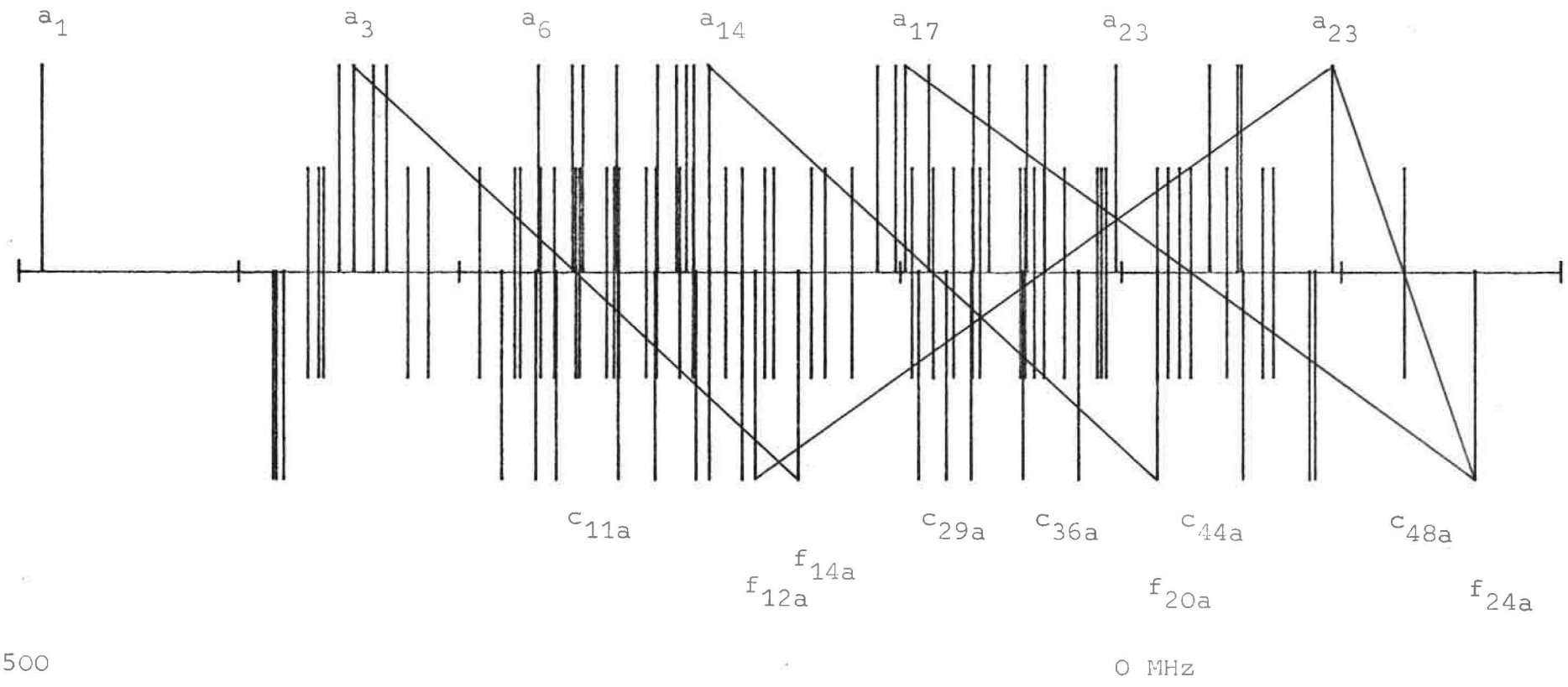

Fig.16: $^{129}I_2$; P(54)8-4; λ=633 NM

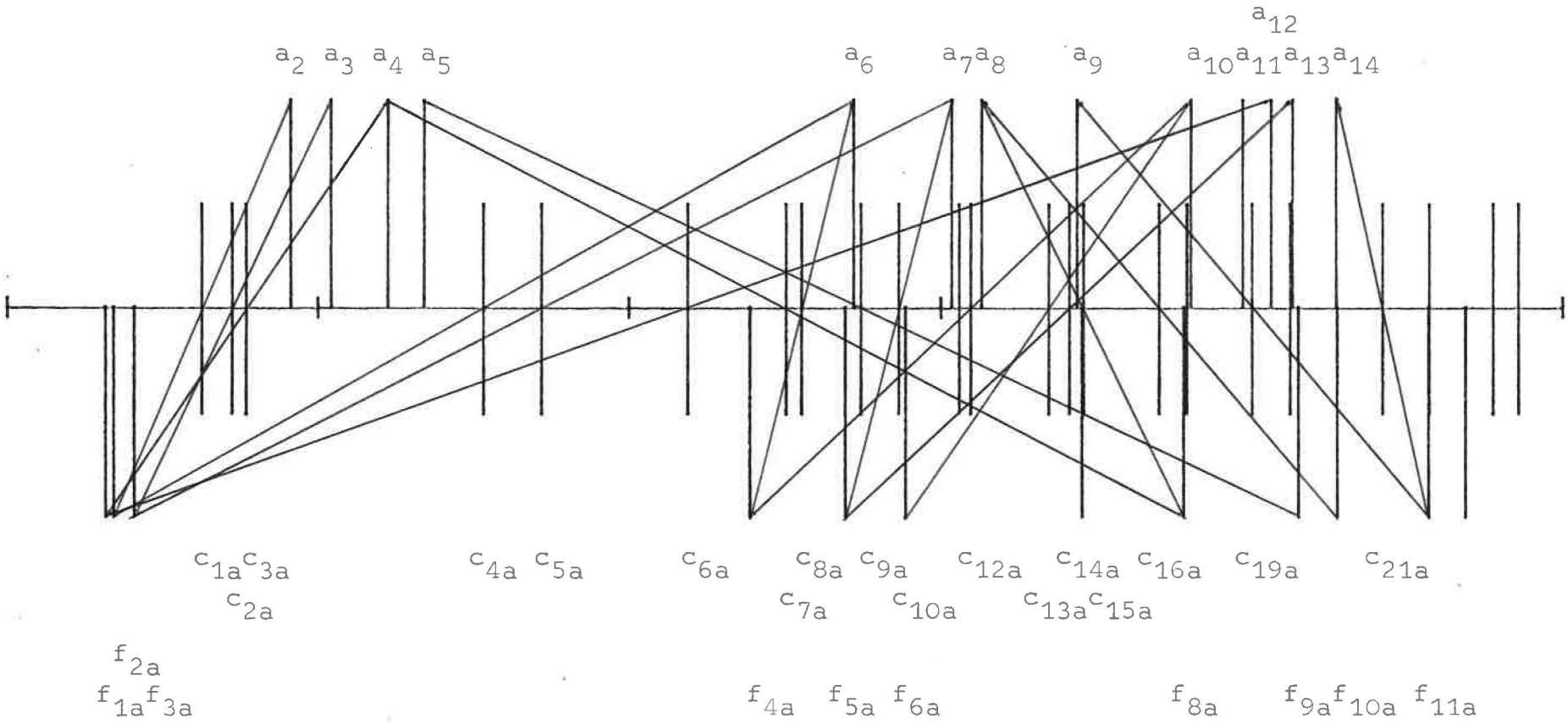

Fig.17: $^{129}I_2$; P(54)8-4; λ=633 NM

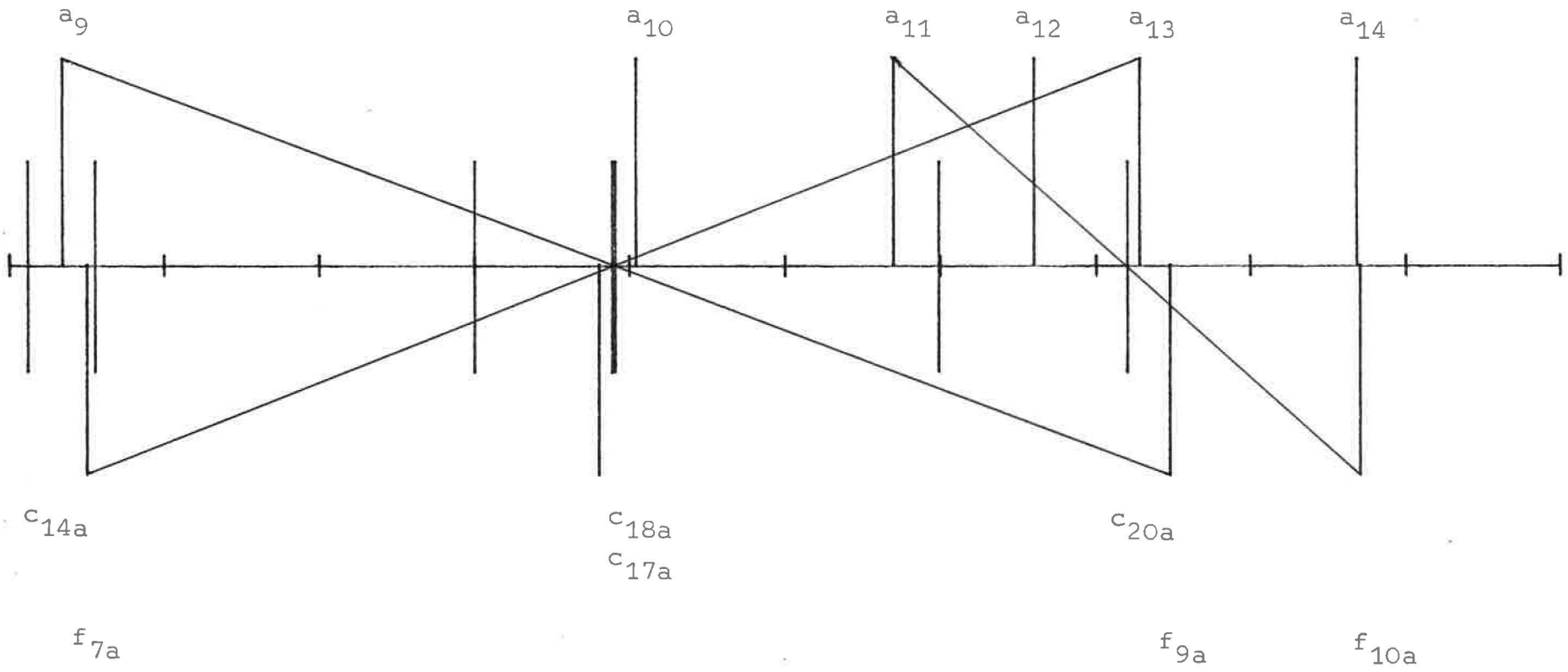

Fig.18: $^{129}I_2$; P(54)8-4; λ=633 NM

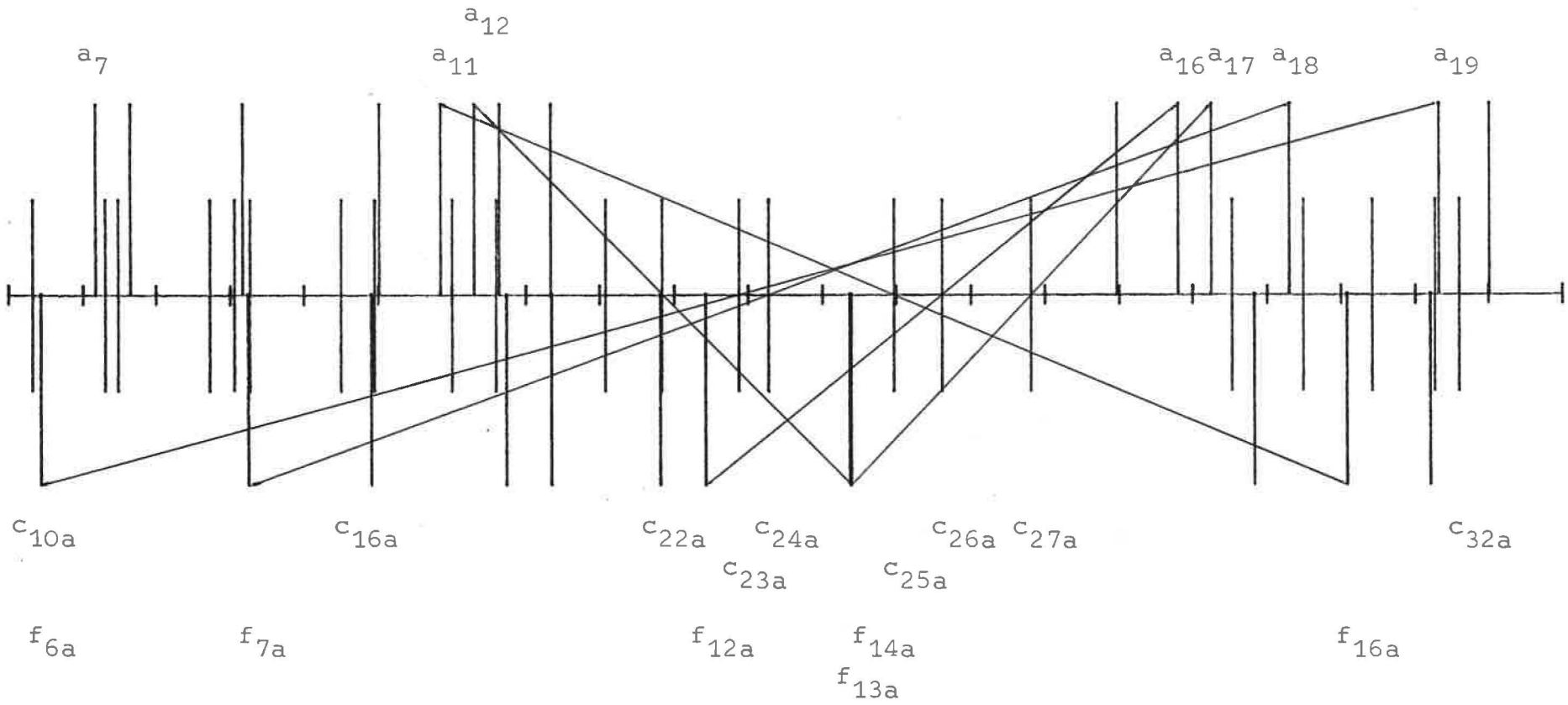

Fig.19: $^{129}I_2$; P(54)8-4; λ =633 NM

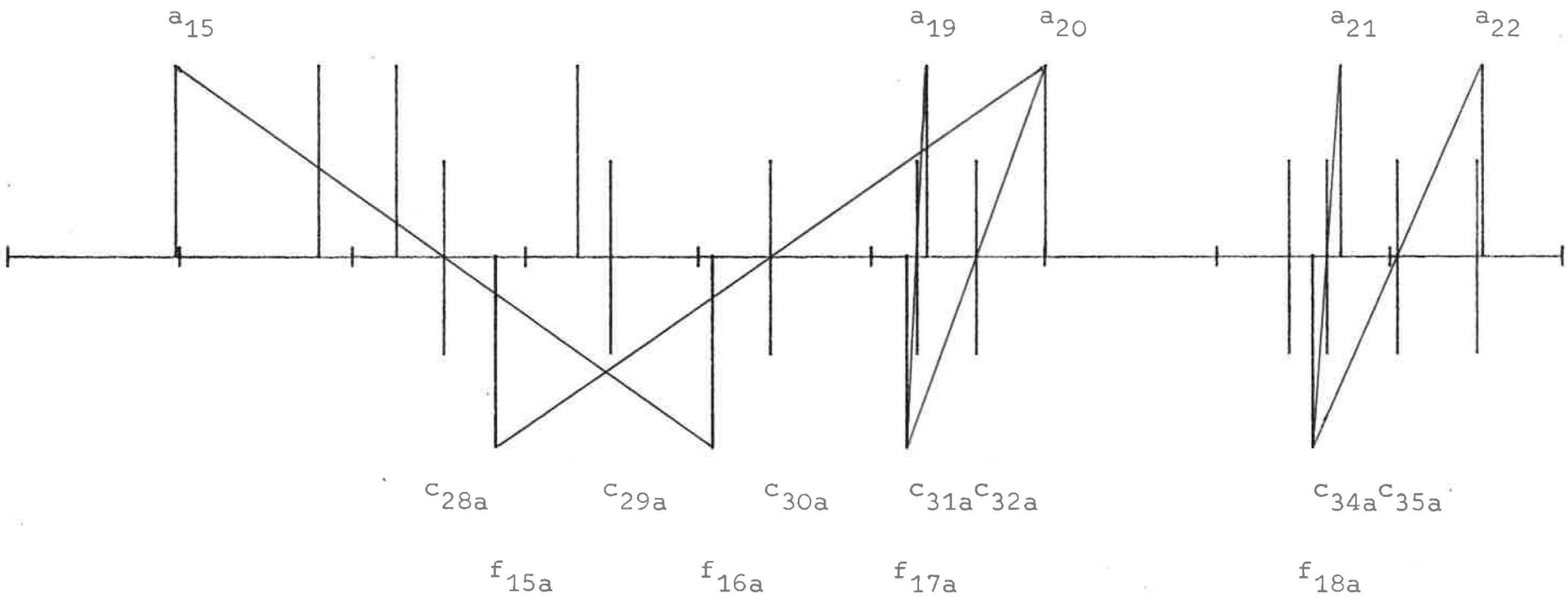

Fig.20: $^{129}I_2$; P(54)8-4; λ=633 NM

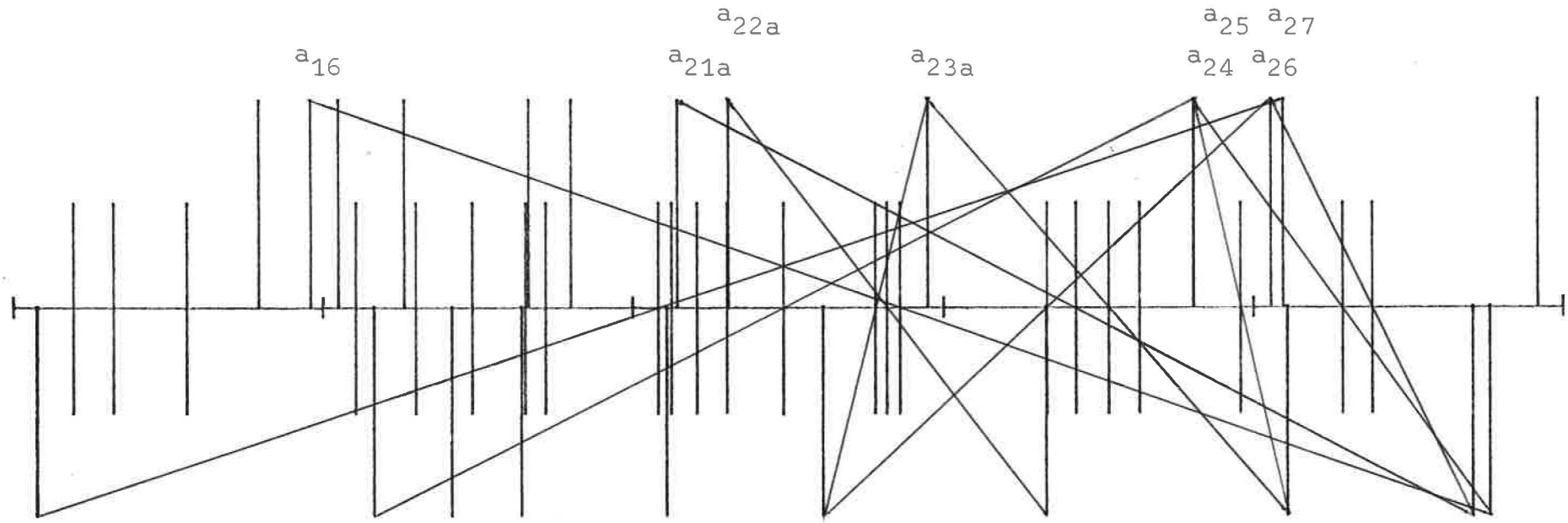

Fig.21: $^{129}I_2$; P(69)12-6; λ=633 NM

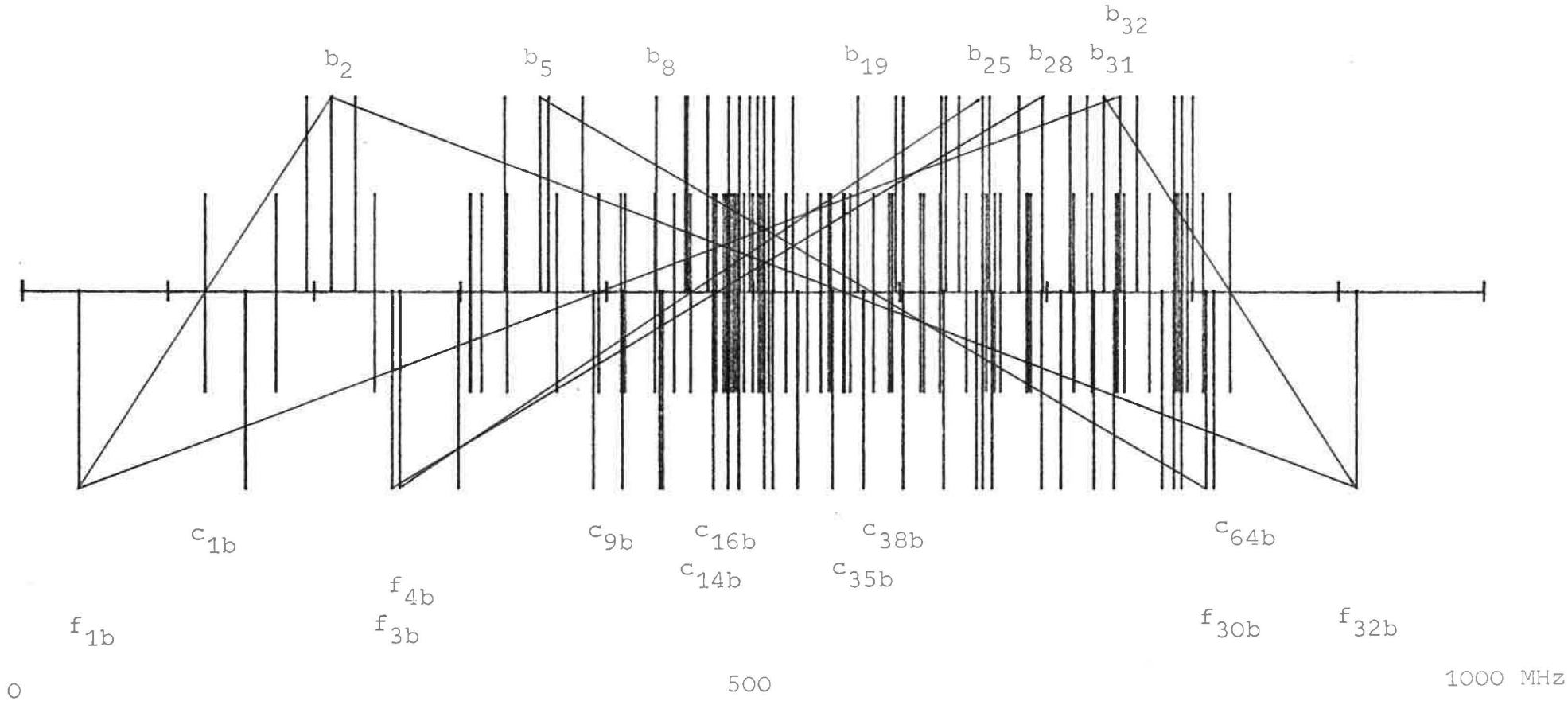

Fig.22: $^{129}I_2$; P(69)12-6; λ =633 NM

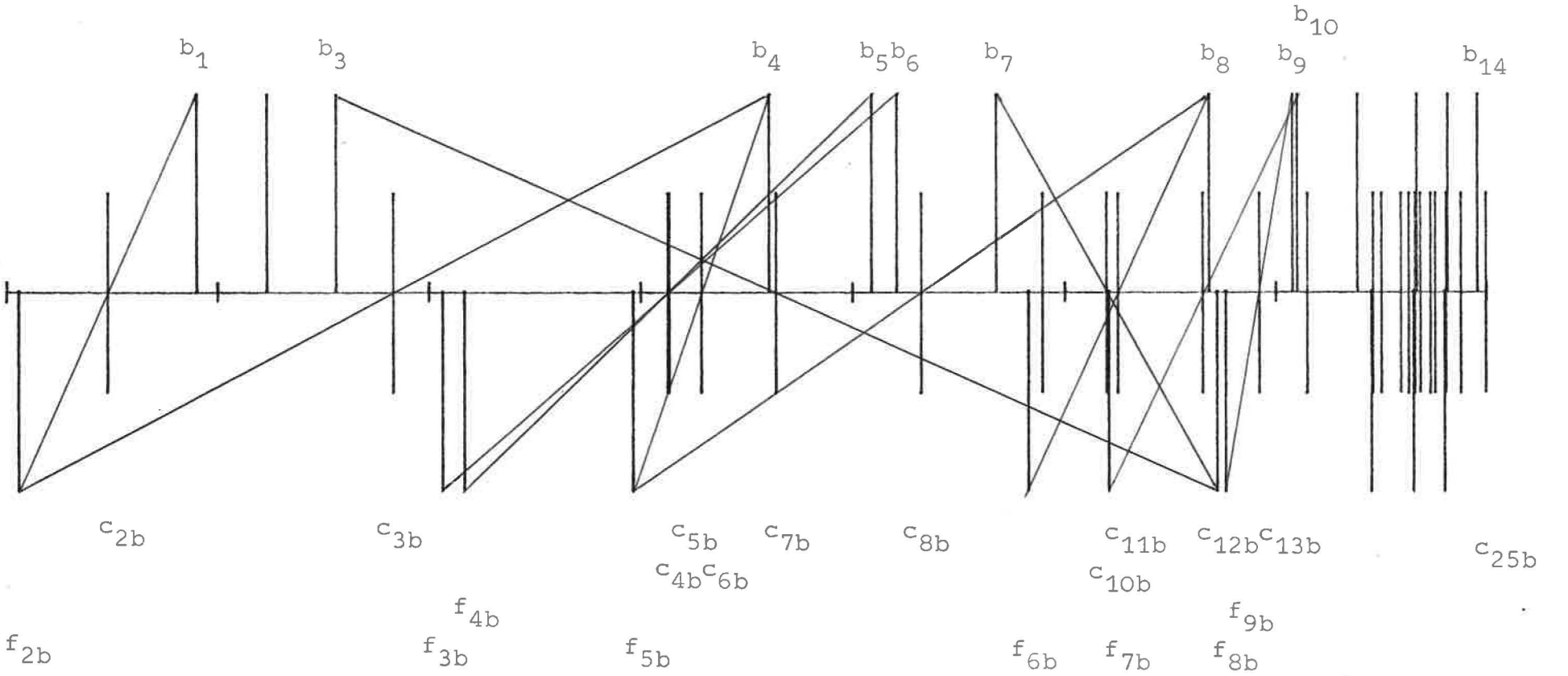

Fig.23: $^{129}I_2$; P(69)12-6; λ=633 NM

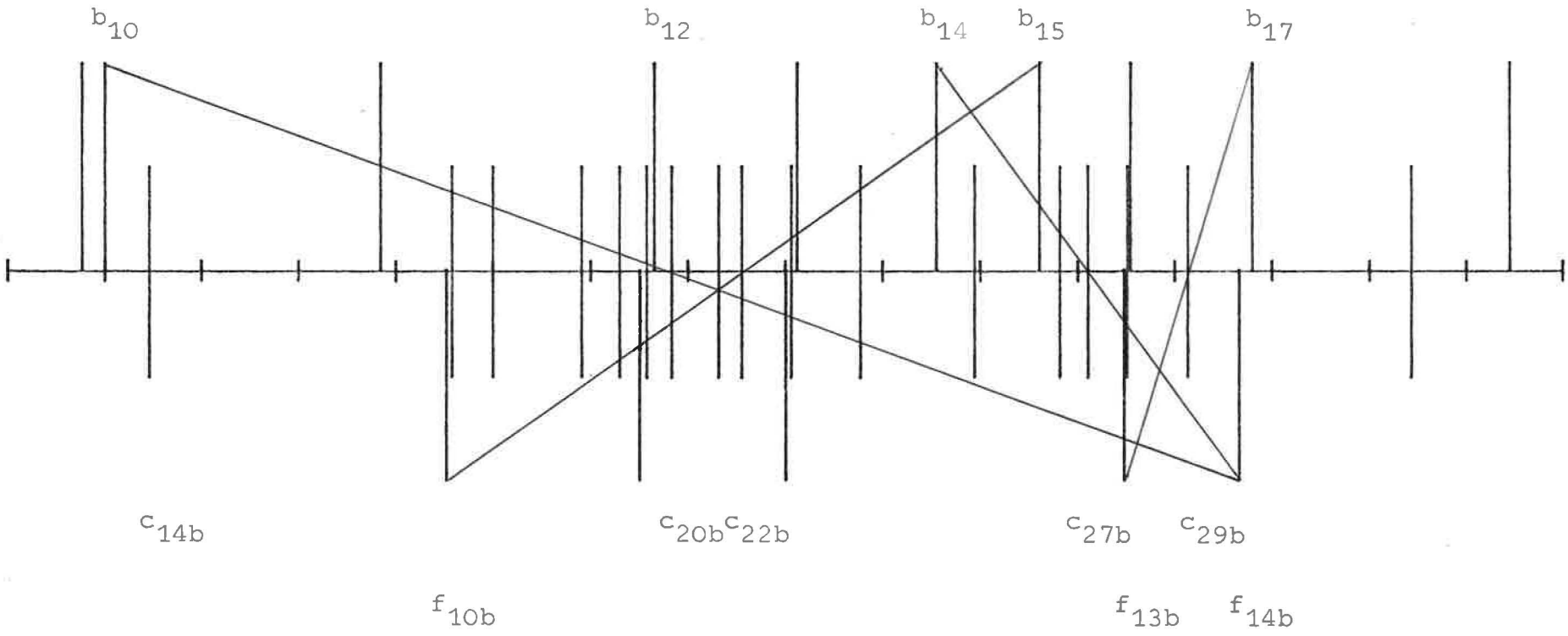

Fig.24: $^{129}I_2$; P(69)12-6; λ=633 NM

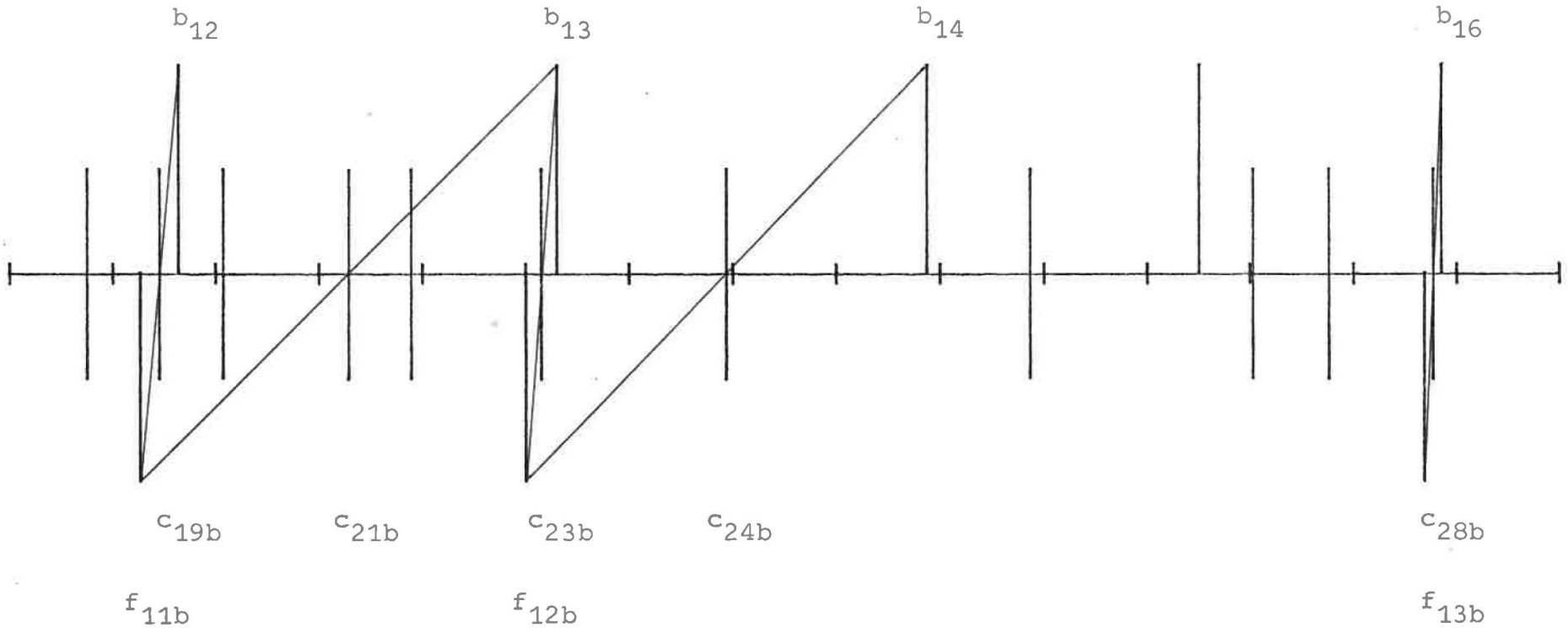

480

500 MHz

Fig.25: $^{129}I_2$; P(69)12-6; λ=633 NM

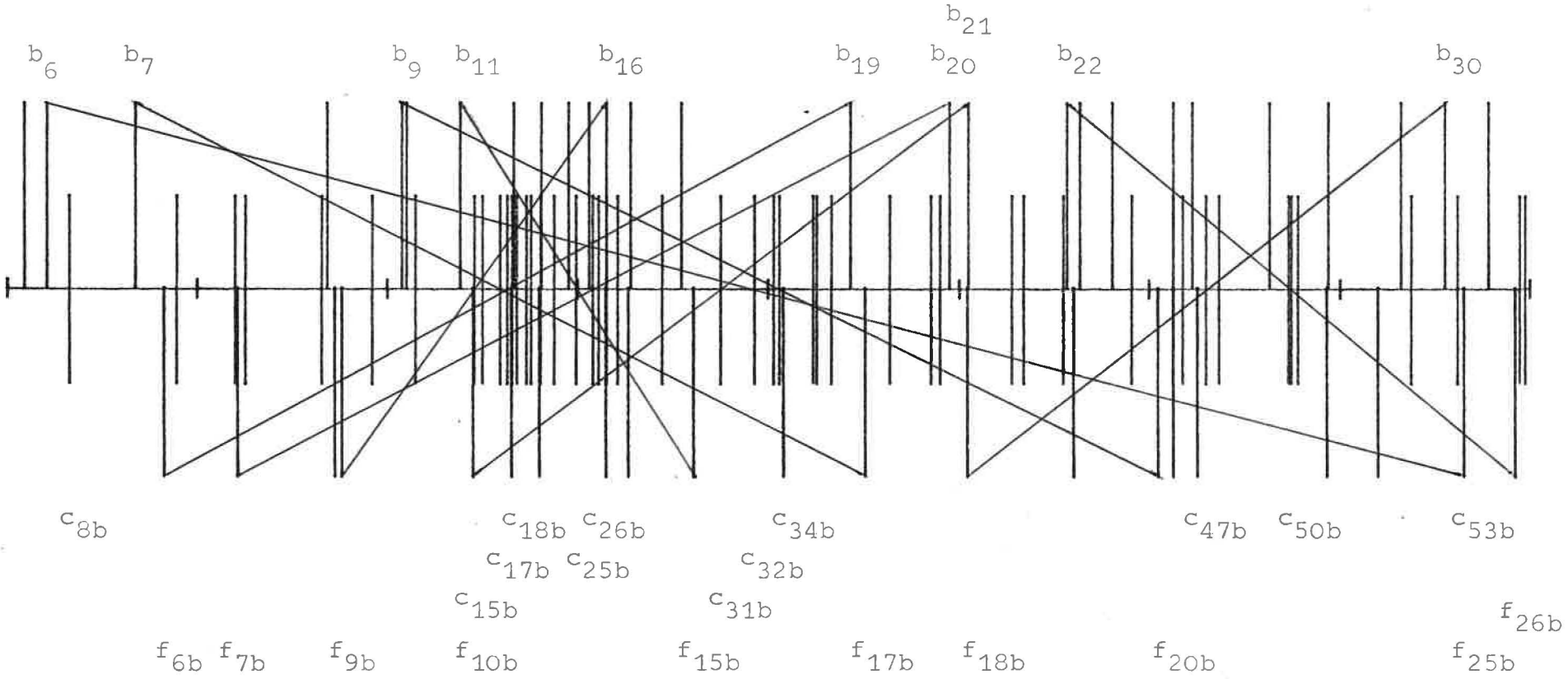

Fig.26: $^{129}I_2$; P(69)12-6; λ=633 NM

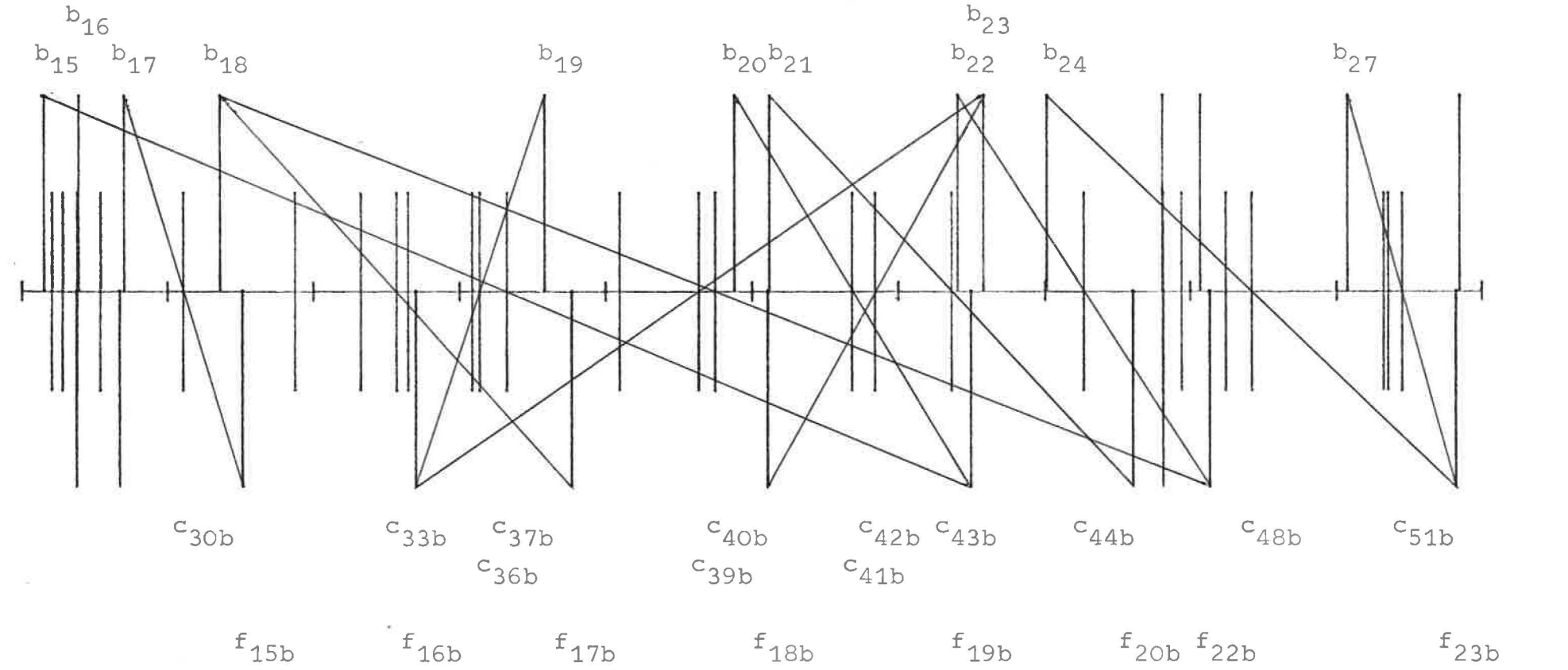

Fig.27: $^{129}I_2$; P(69)12-6; λ=633 NM

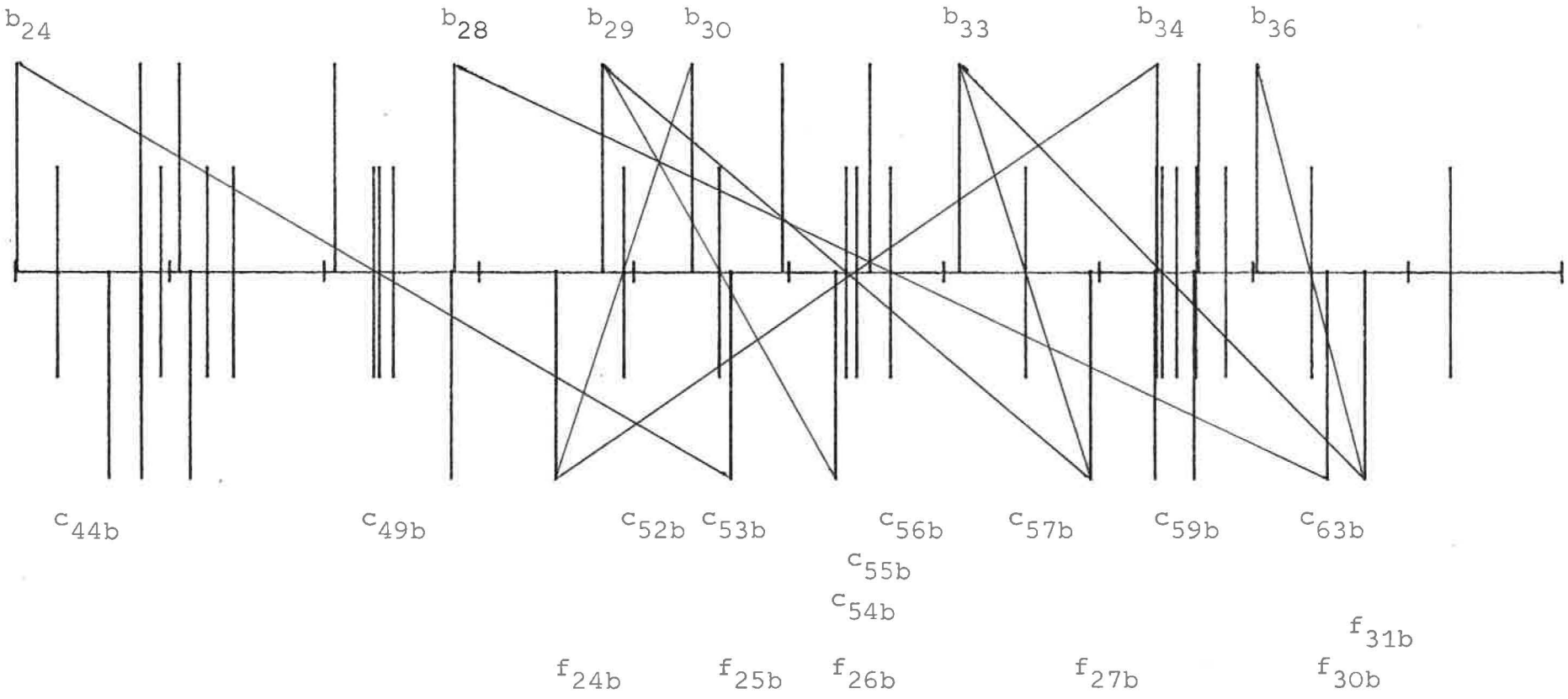

Fig.28: $^{129}I_2$; P(69)12-6; λ=633 NM

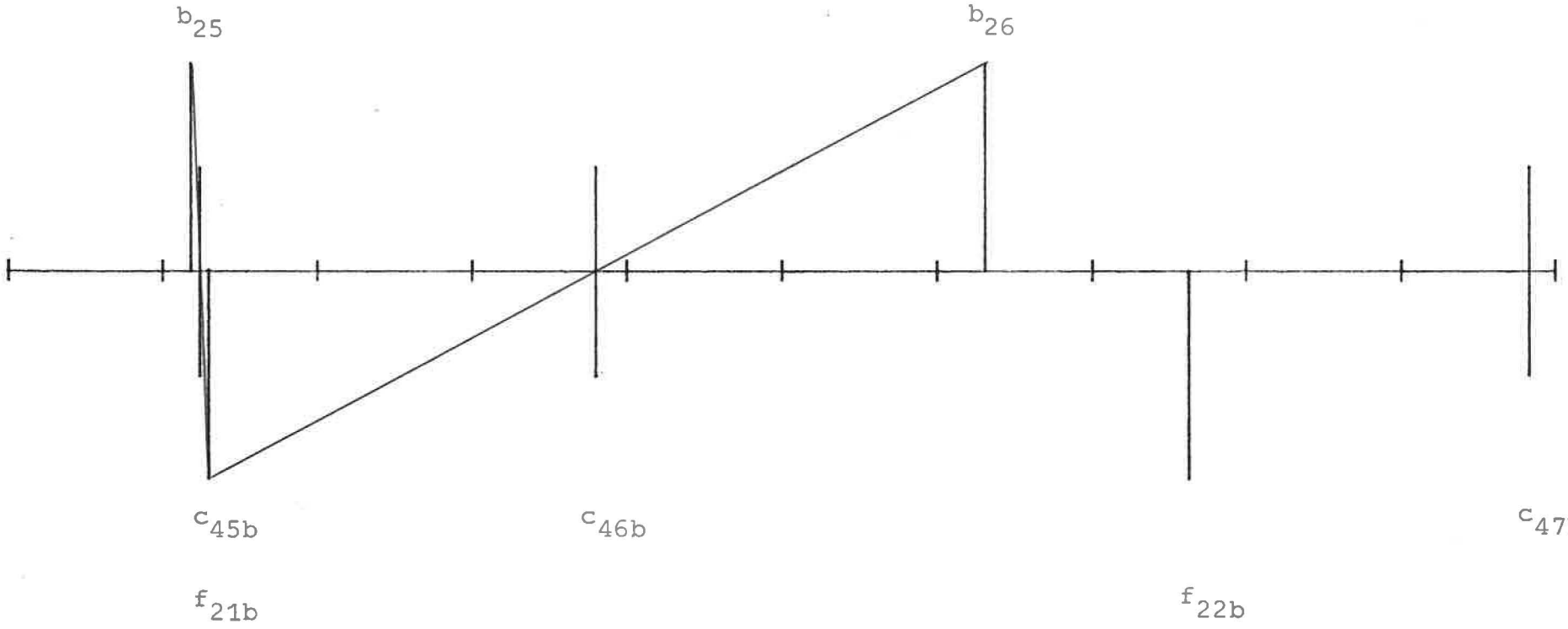

Fig.29: $^{129}I_2$; P(69)12-6; λ=633 NM

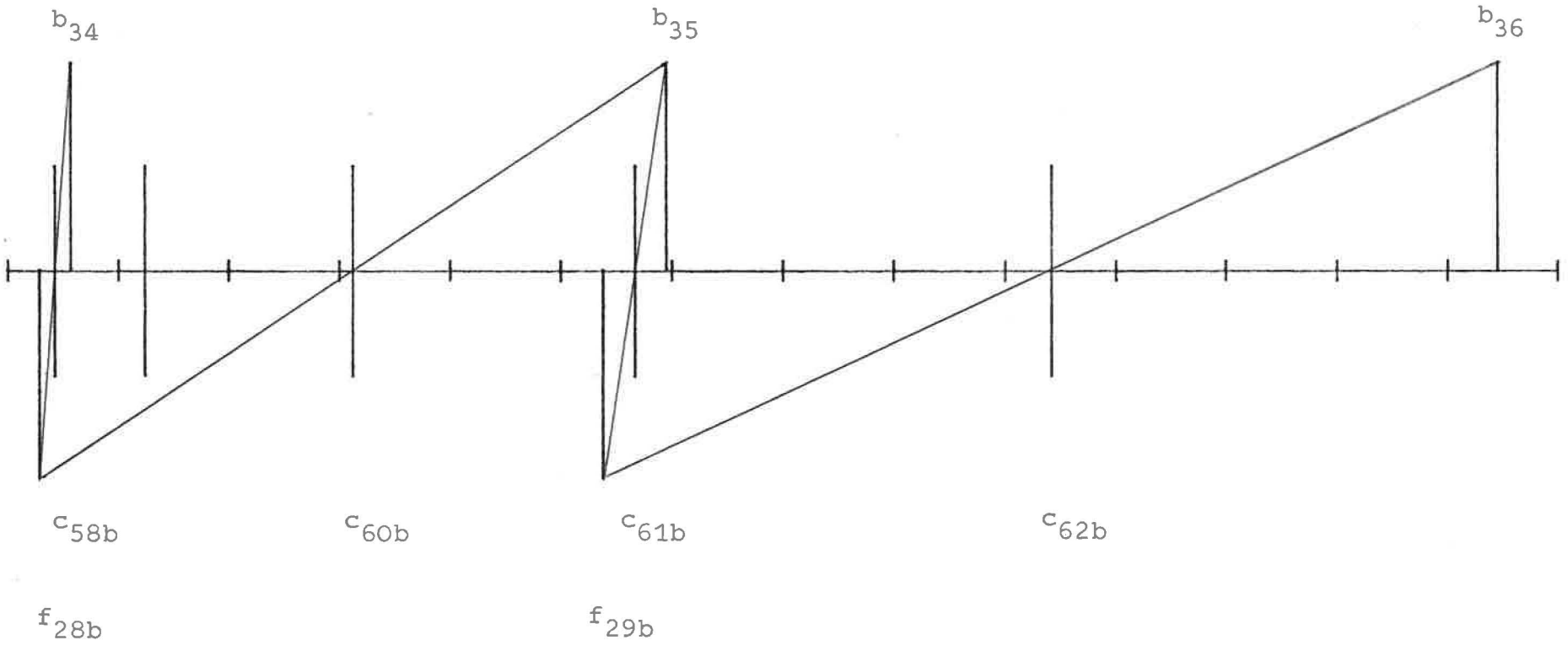

Fig.30: $^{129}I_2$; R(60)8-4; λ=633 NM

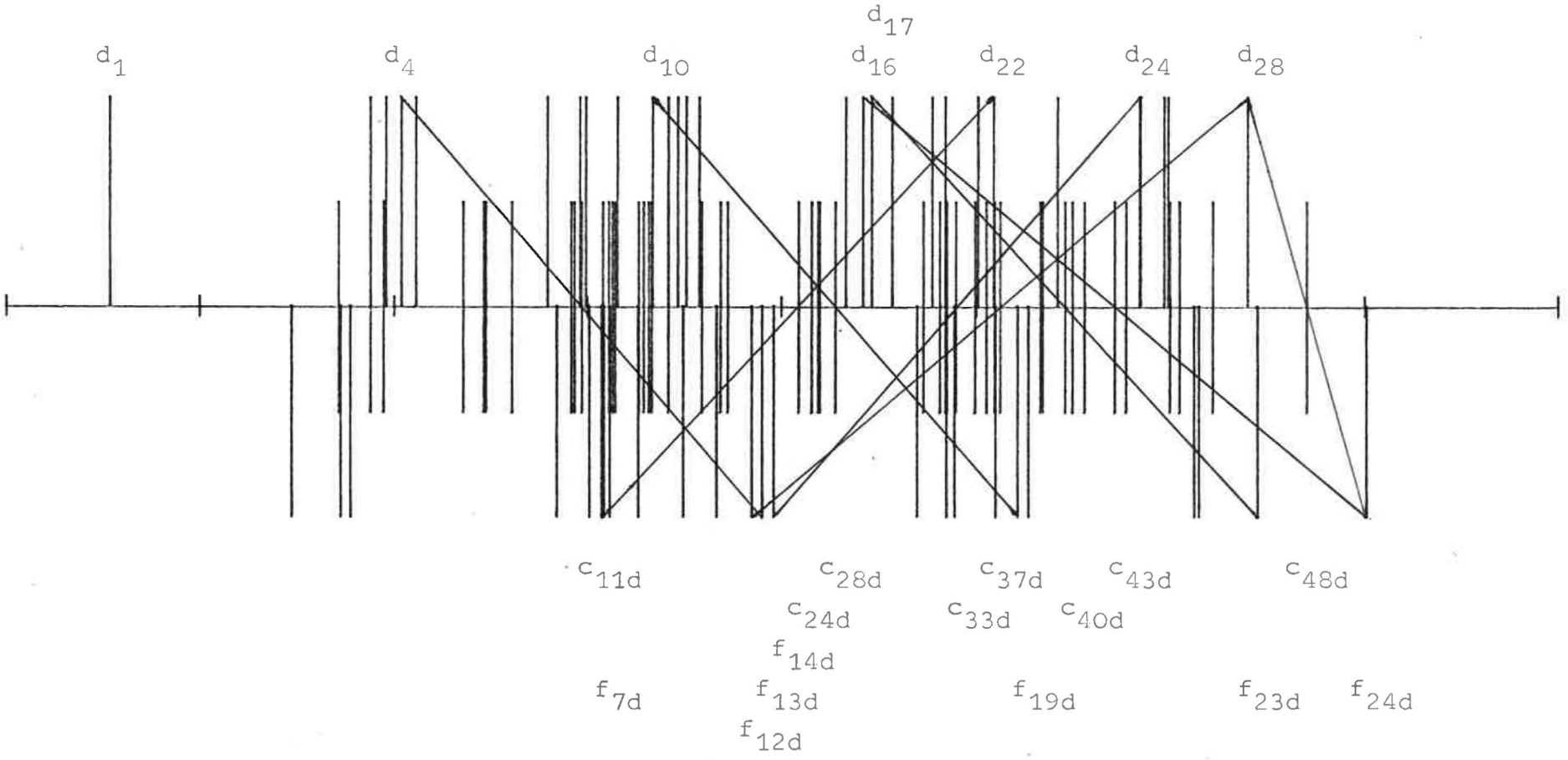

Fig.31: $^{129}I_2$; R(60)8-4; λ=633 NM

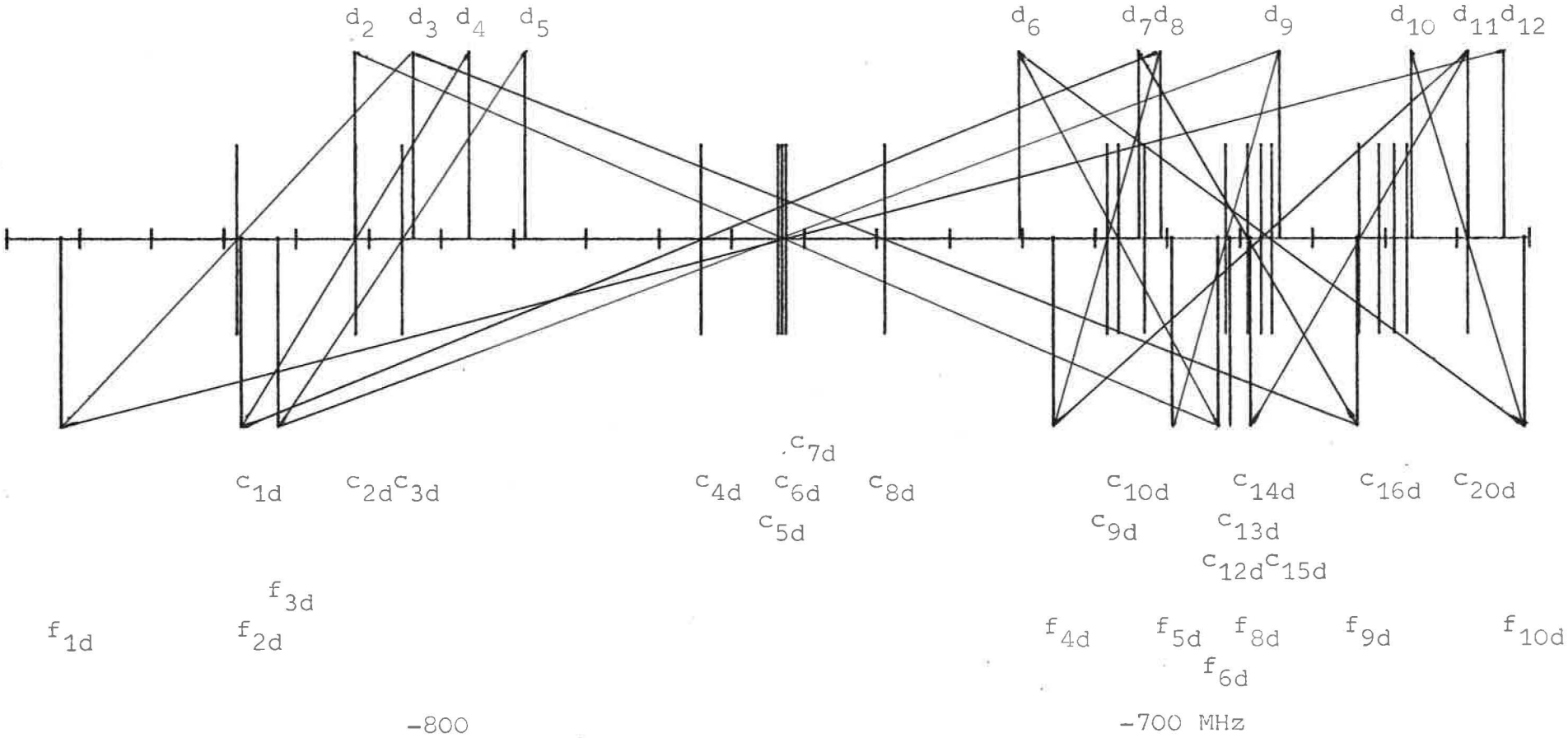

Fig.32: $^{129}I_2$; R(60)8-4; λ=633 NM

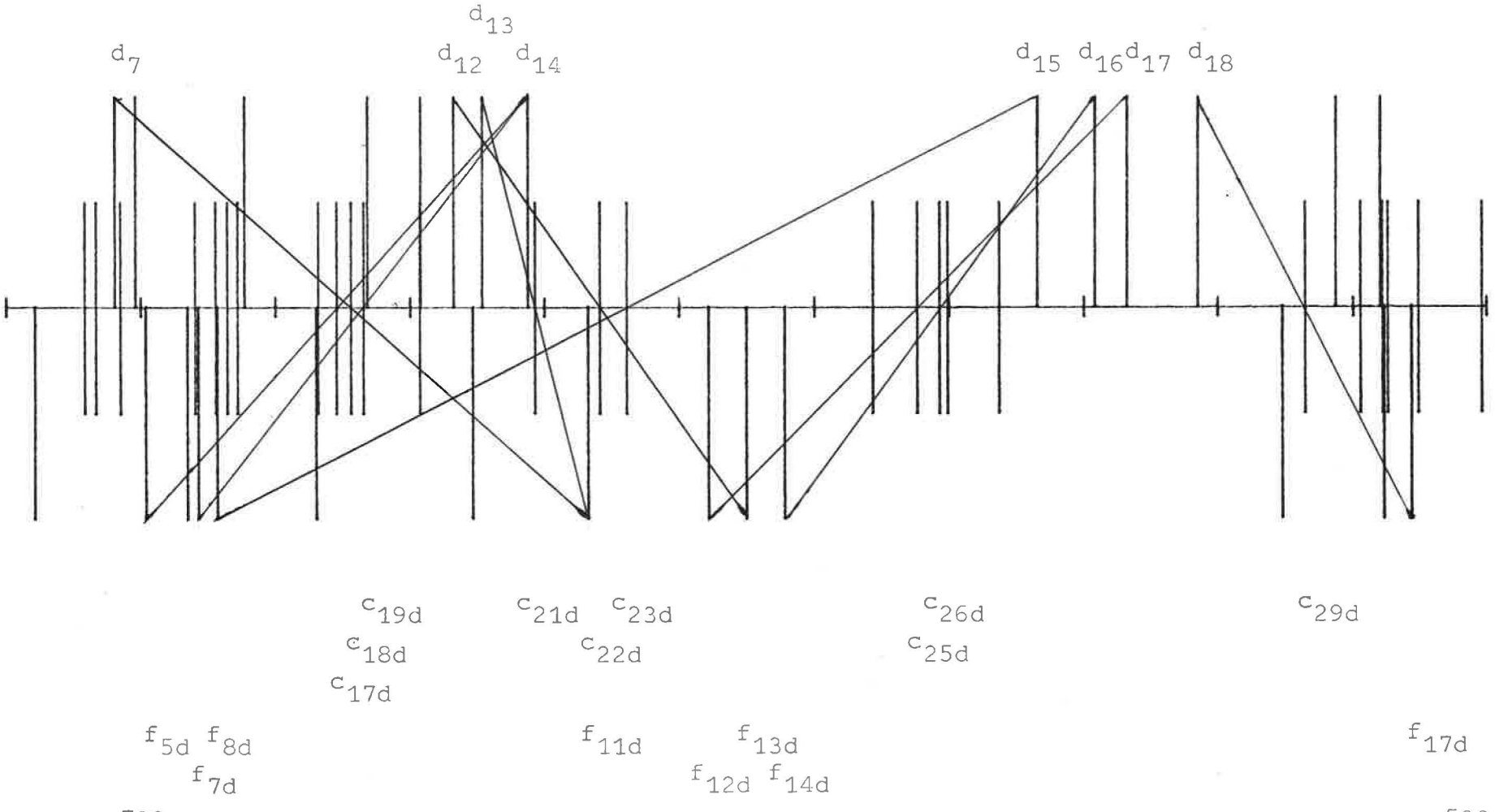

Fig.33: $^{129}I_2$; R(60)8-4; λ=633 NM

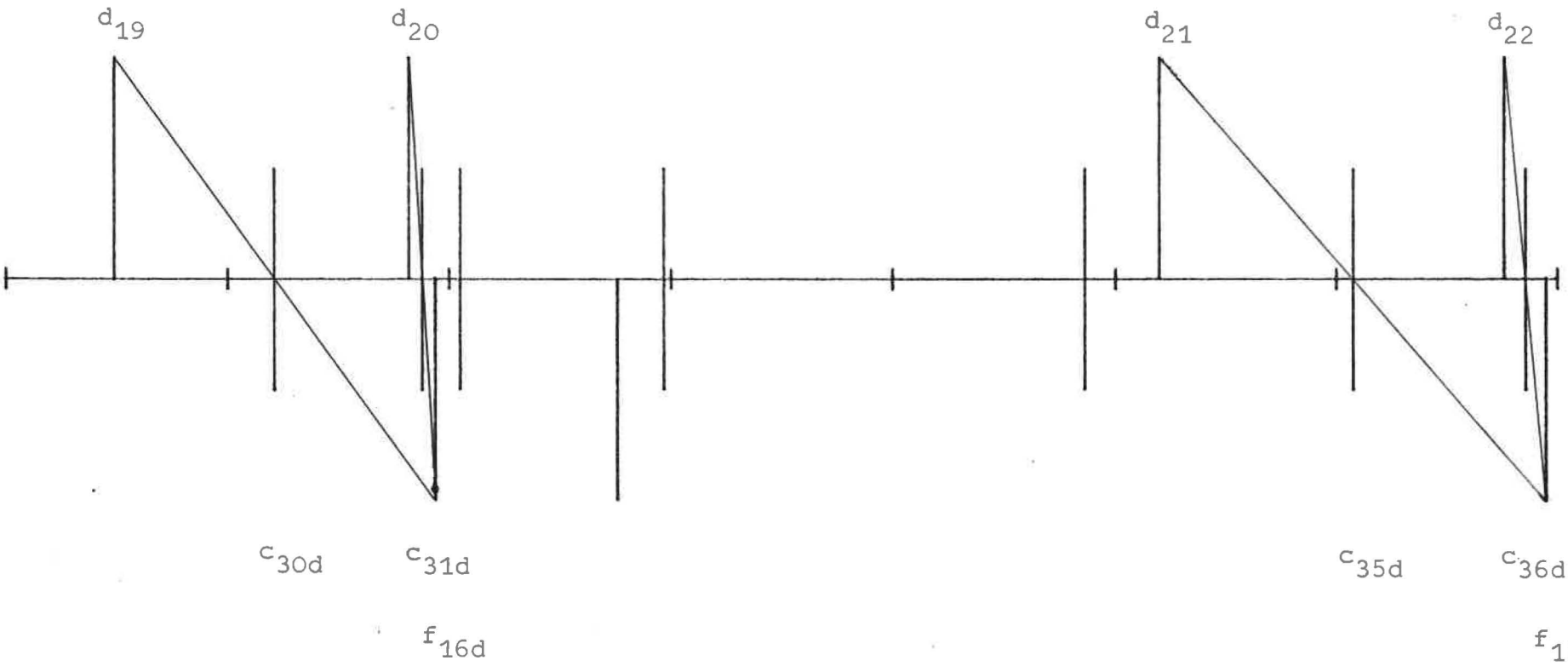

Fig.34: $^{129}I_2$; R(60)8-4; λ=633 NM

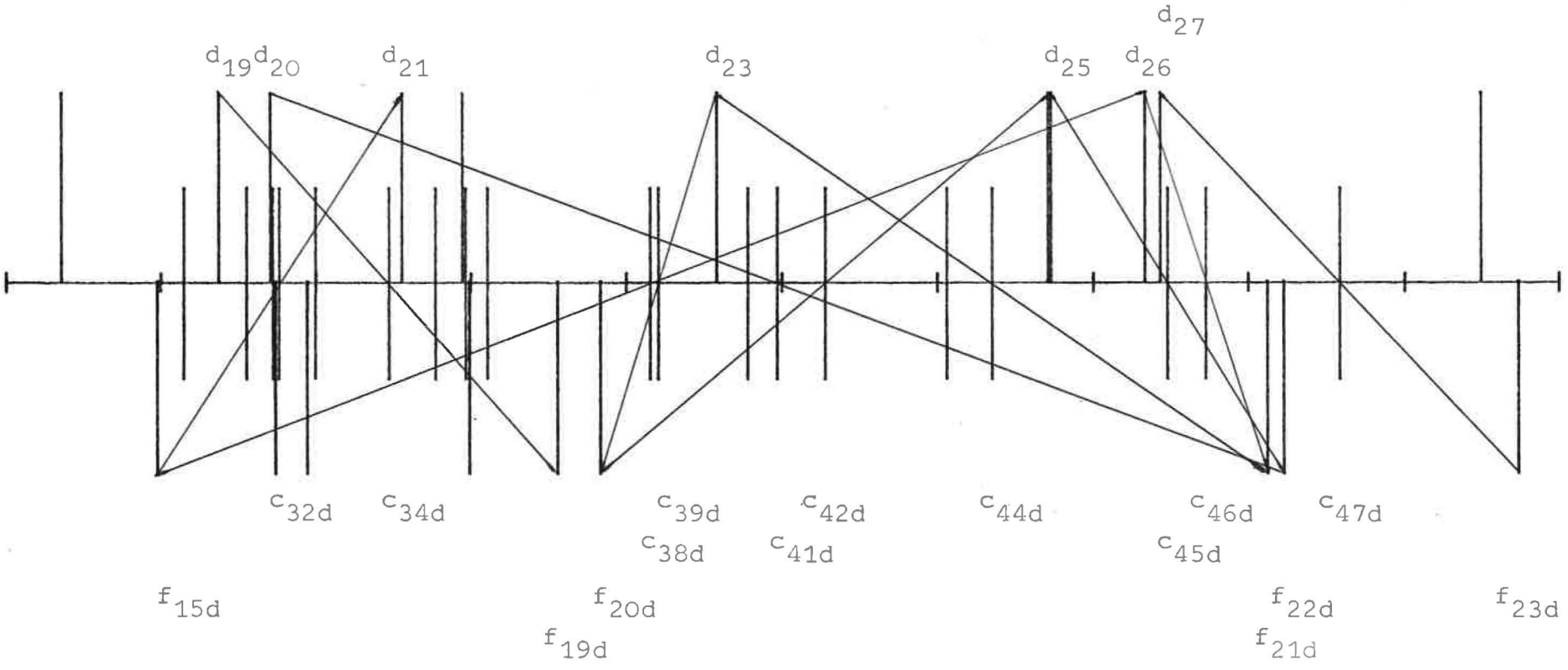

Fig.35: $^{129}I_2$; P(33)6-3; λ=633 NM

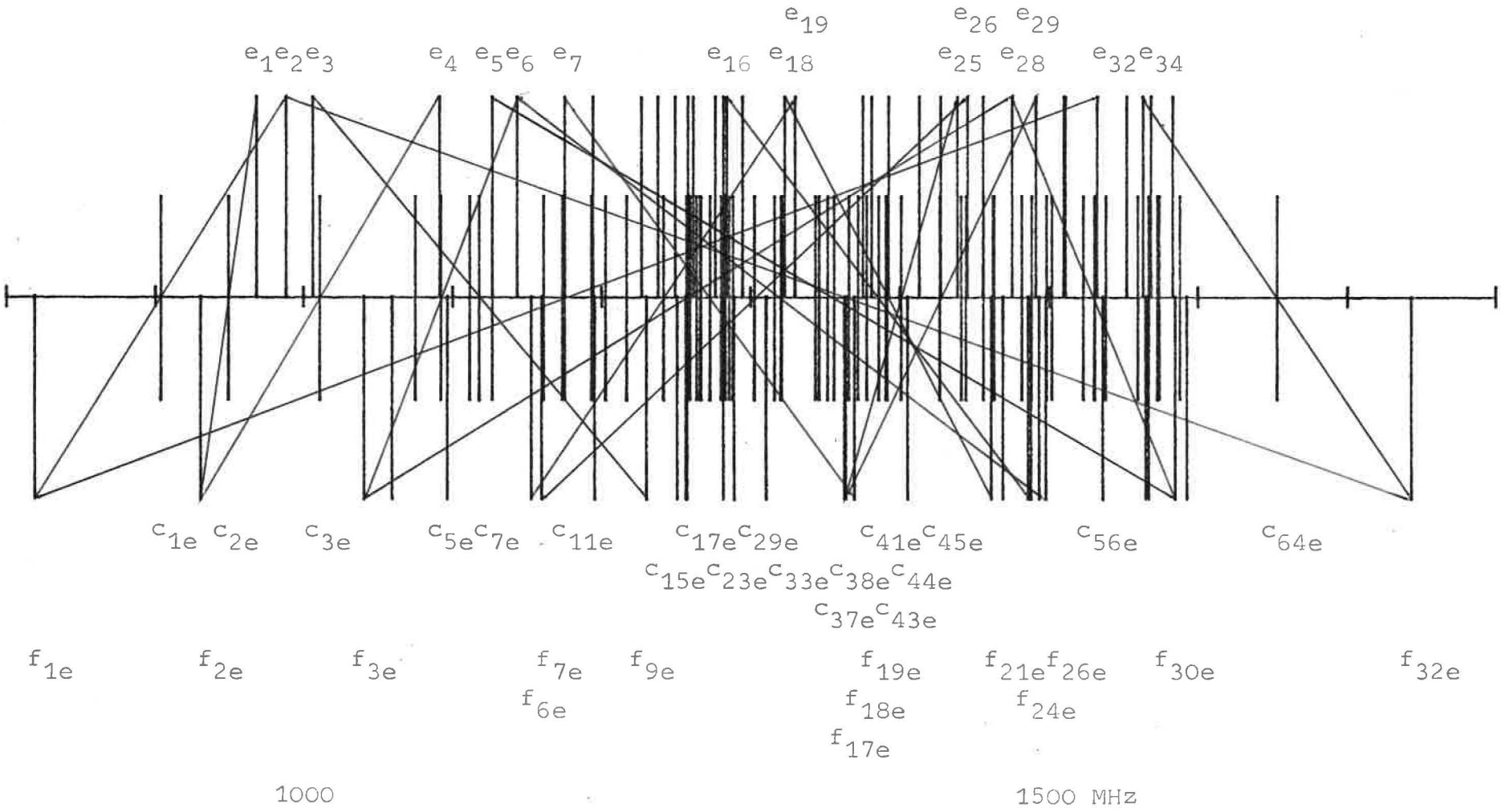

Fig.36: $^{129}I_2$; P(33)6-3; λ=633 NM

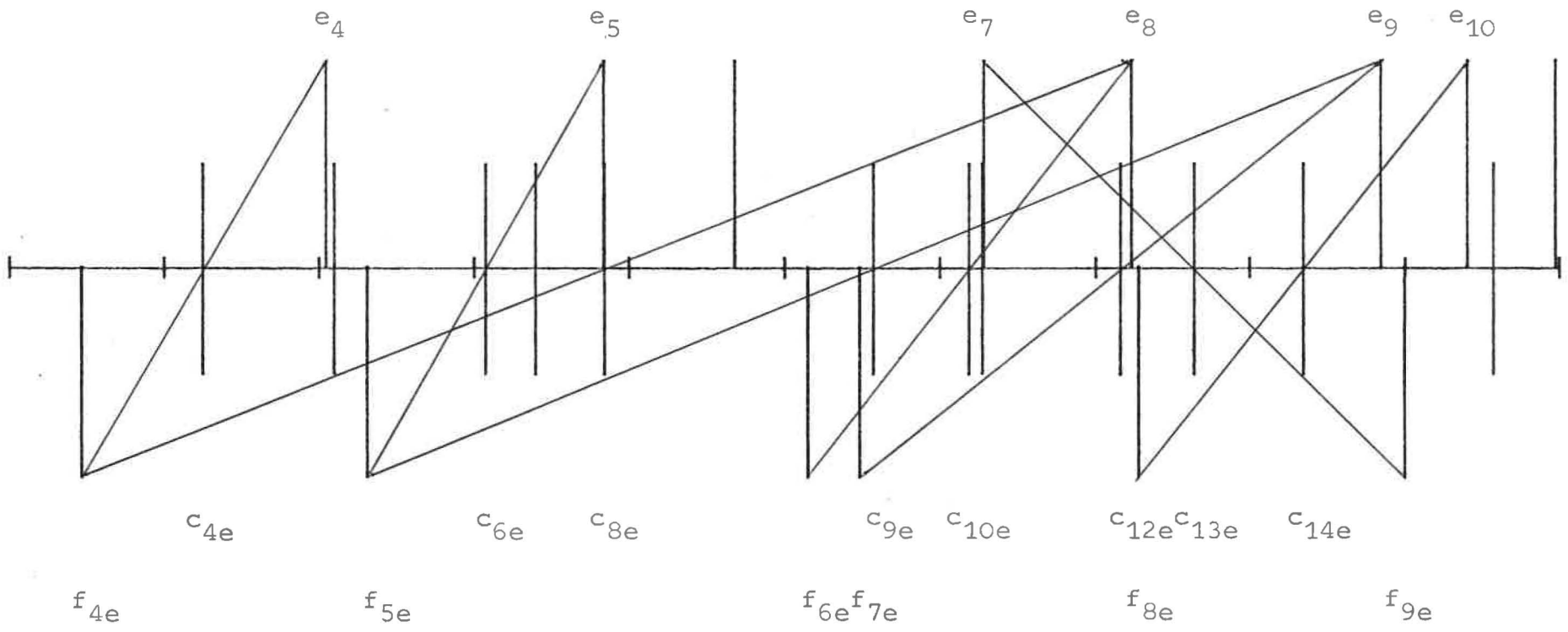

1050 1150 1250 MHz

Fig.37: $^{129}I_2$; P(33)6-3; λ=633 NM

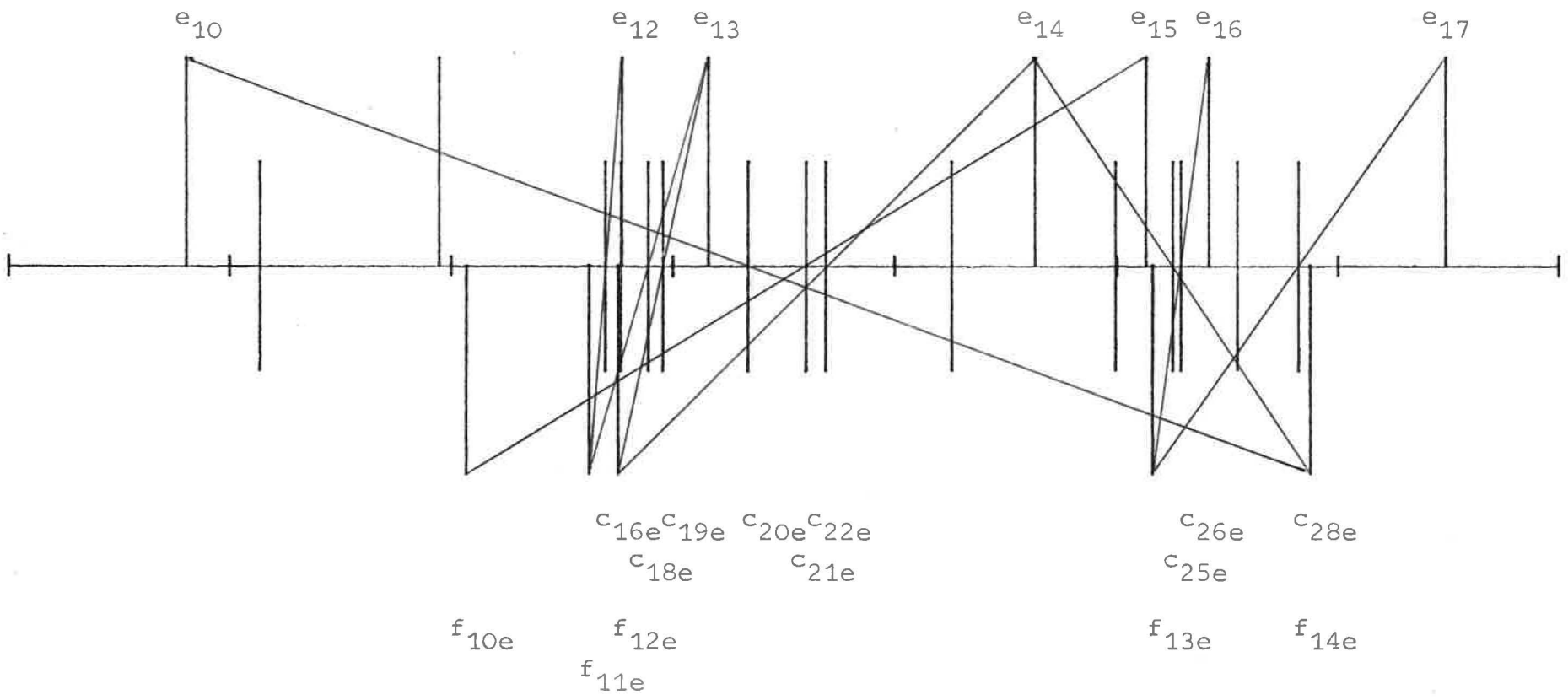

Fig.38: $^{129}I_2$; P(33)6-3; λ=633 NM

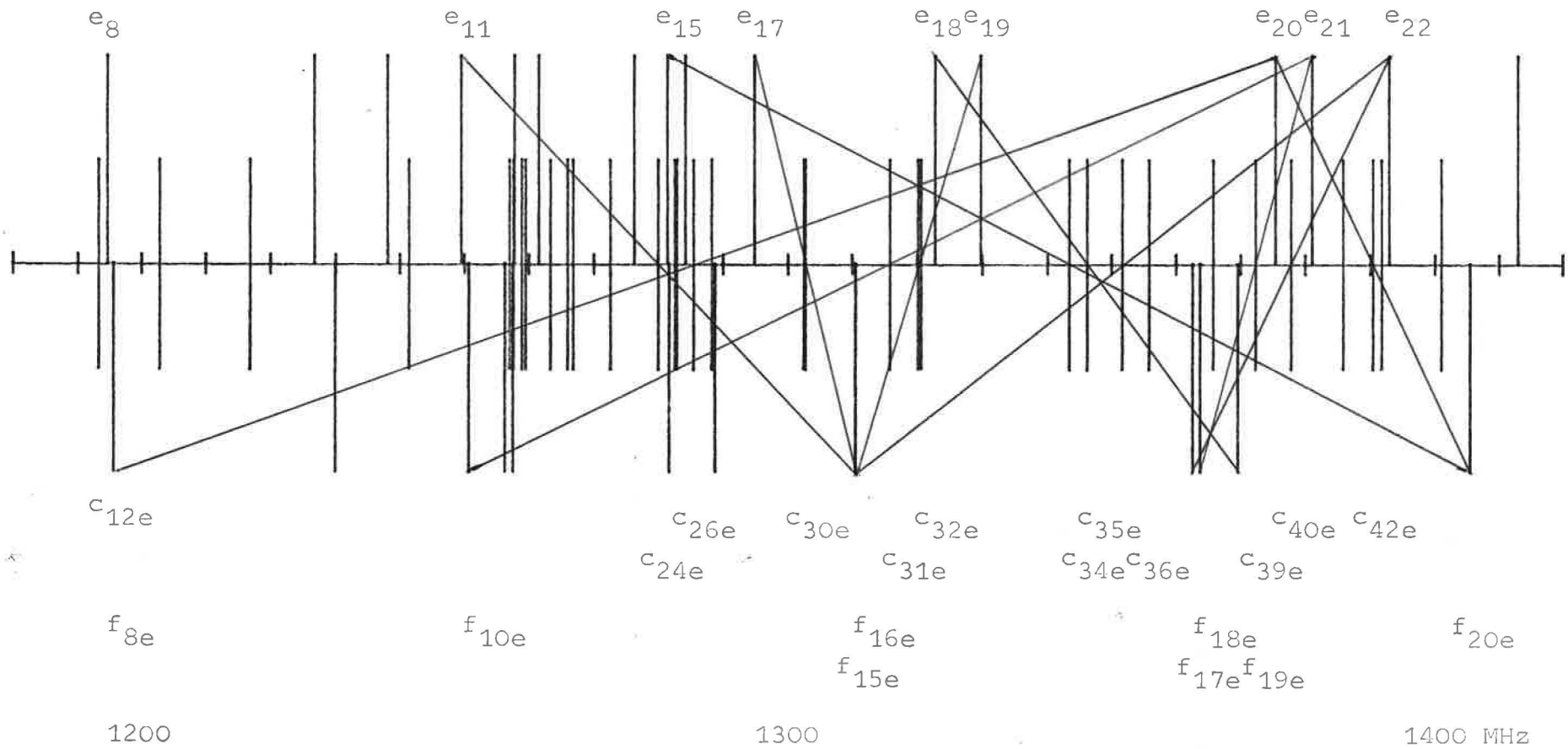

Fig.39: $^{129}I_2$; P(33)6-3; λ=633 NM

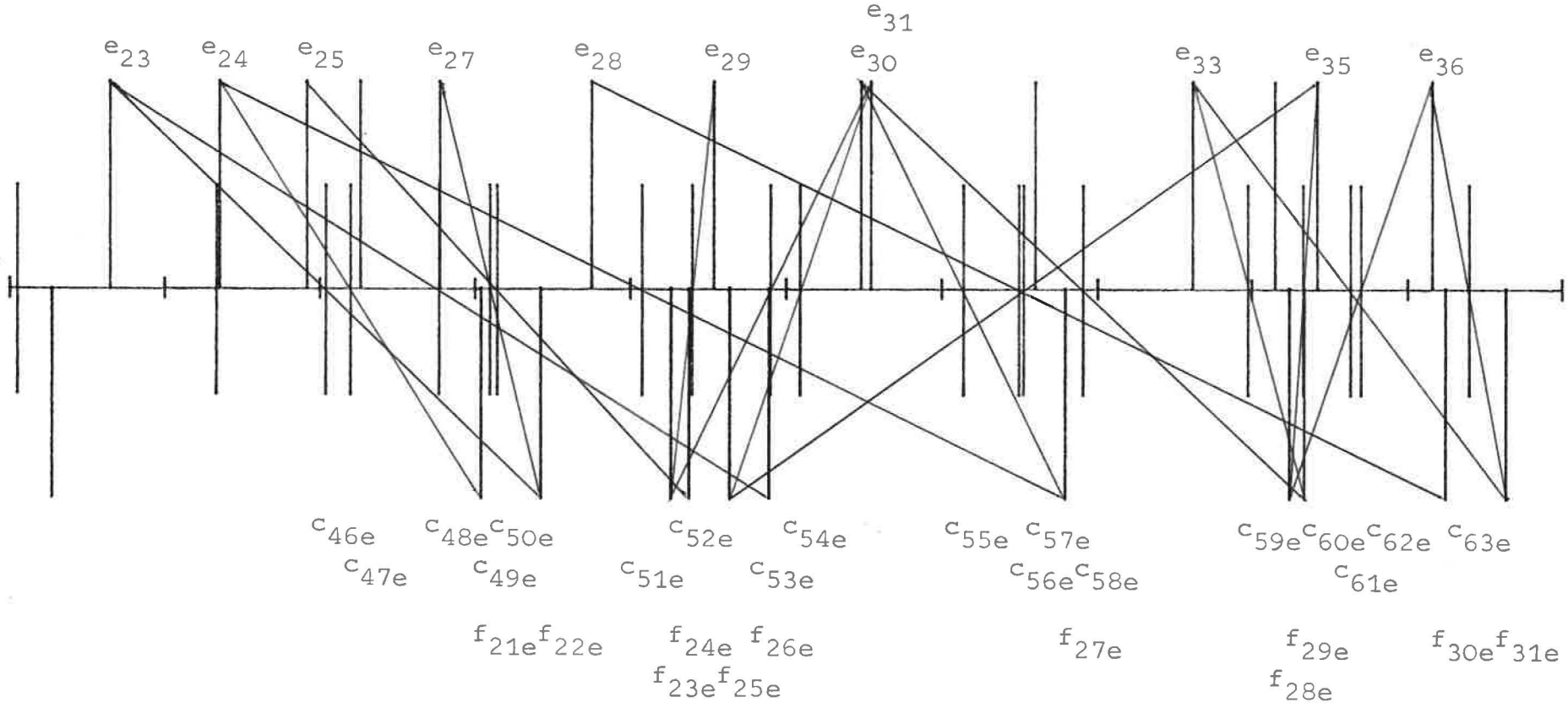

Fig.40: $^{127}I_2$; P(48)11-3; λ=612 NM

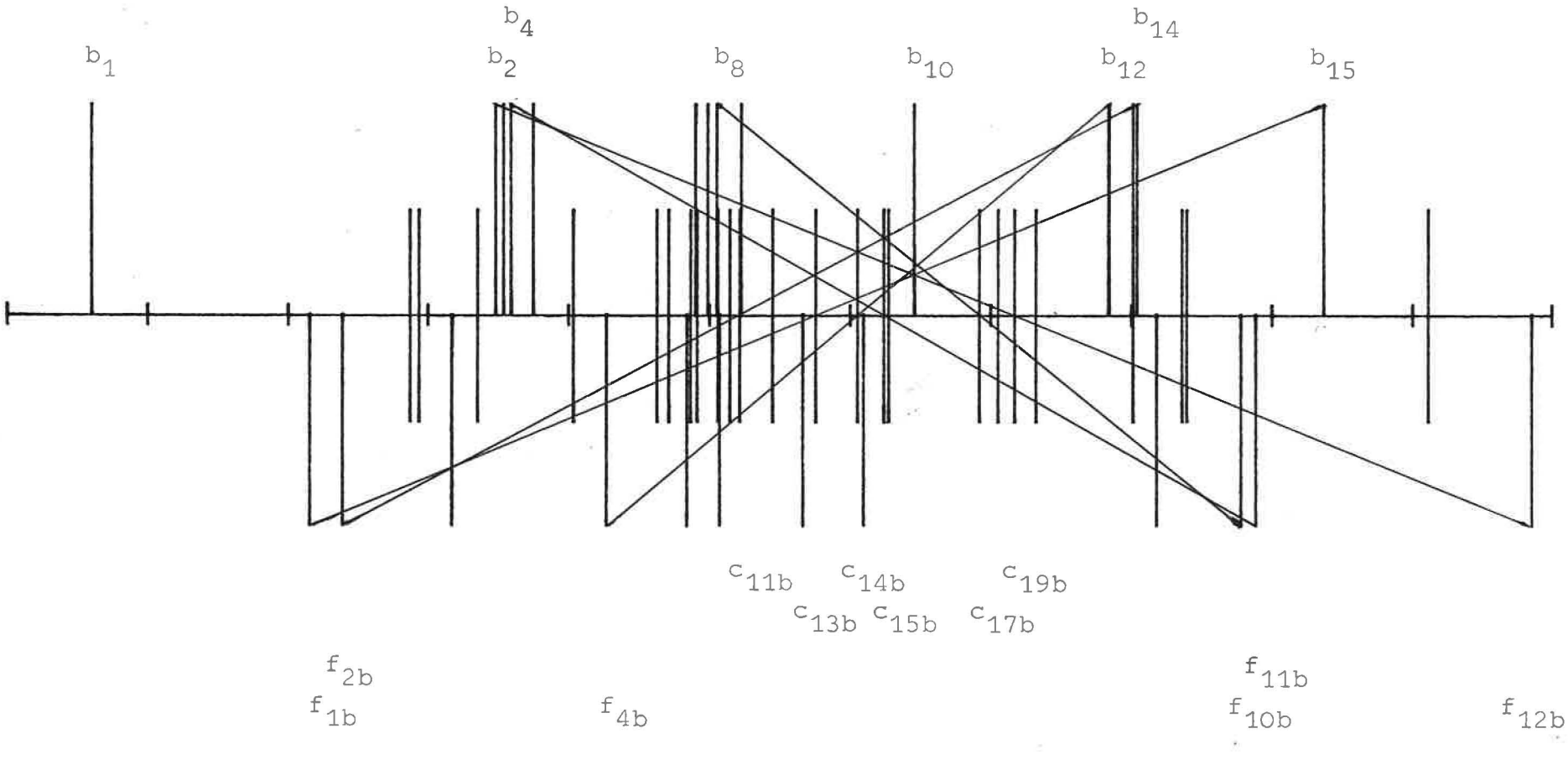

Fig.41: $^{127}I_2$; P(48)11-3; λ=612 NM

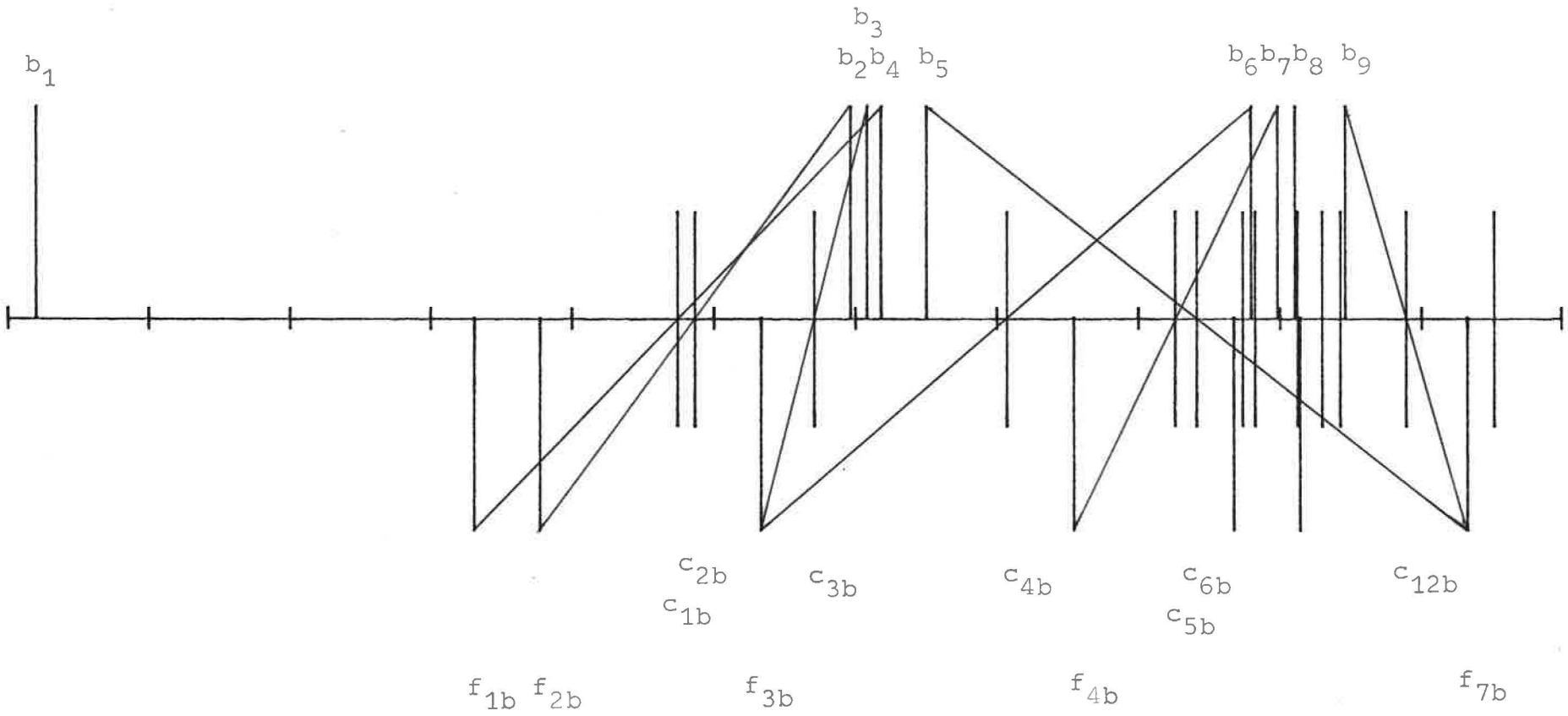

Fig.42: $^{127}I_2$; P(48)11-3; λ=612 NM

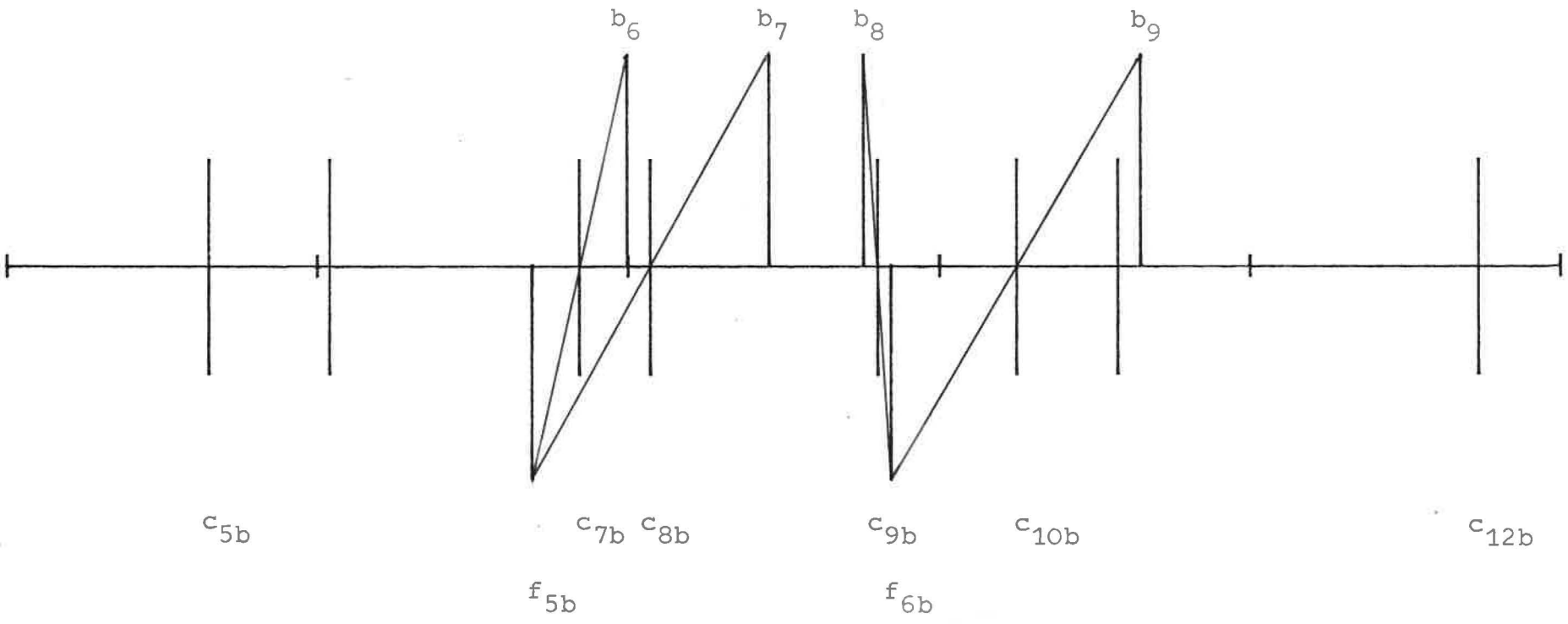

Fig.43: $^{127}I_2$; P(48)11-3; λ=612 NM

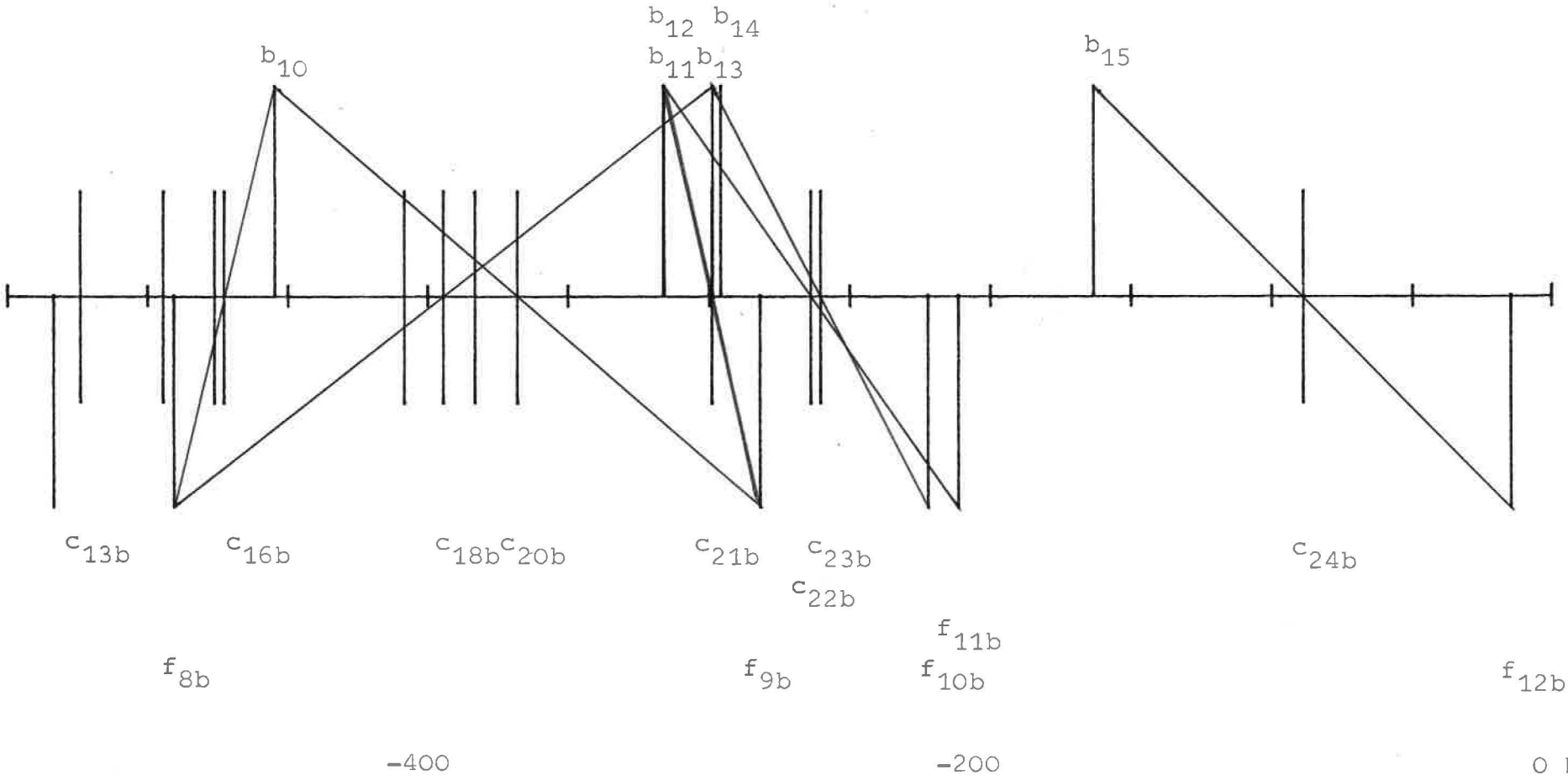

Fig.44: $^{127}I_2$; R(48)15-5; λ=612 NM

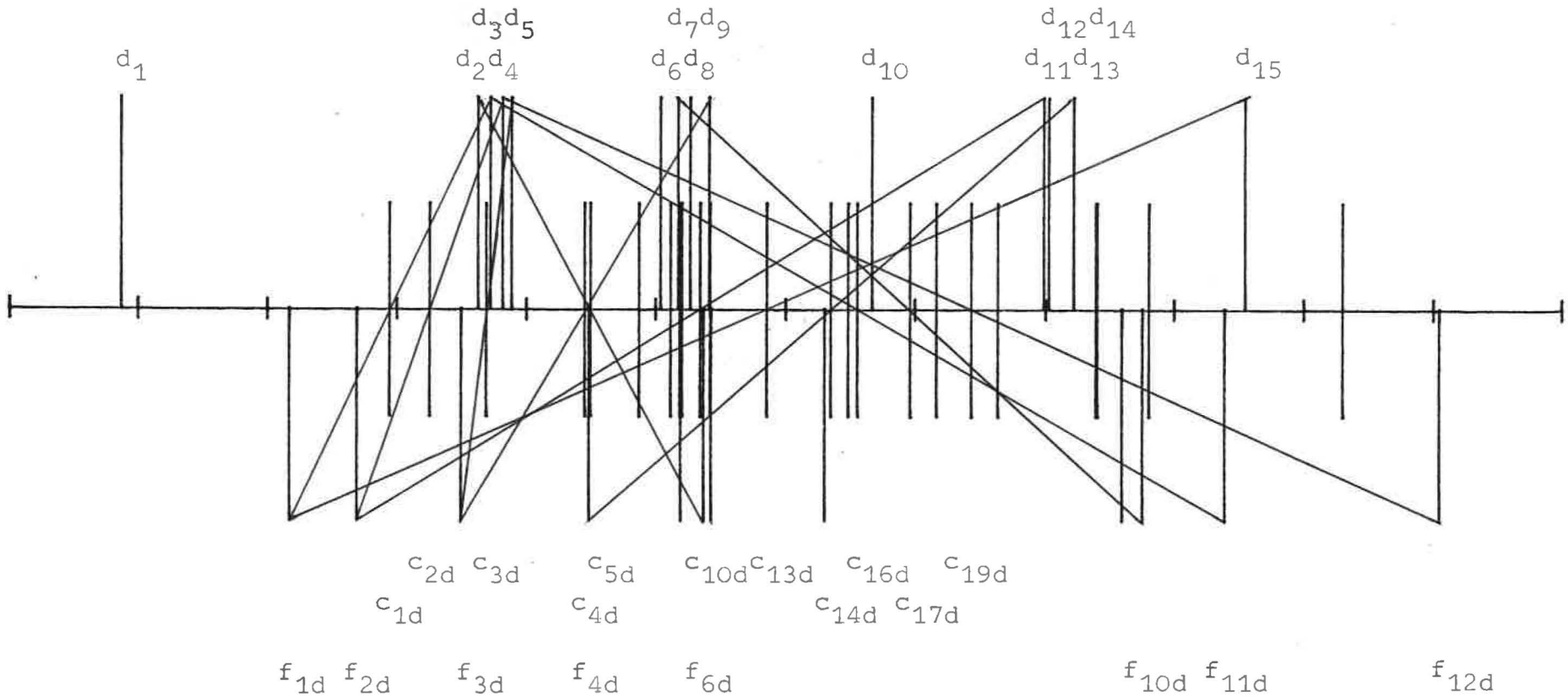

Fig.45: $^{127}I_2$; R(48)15-5; λ=612 NM

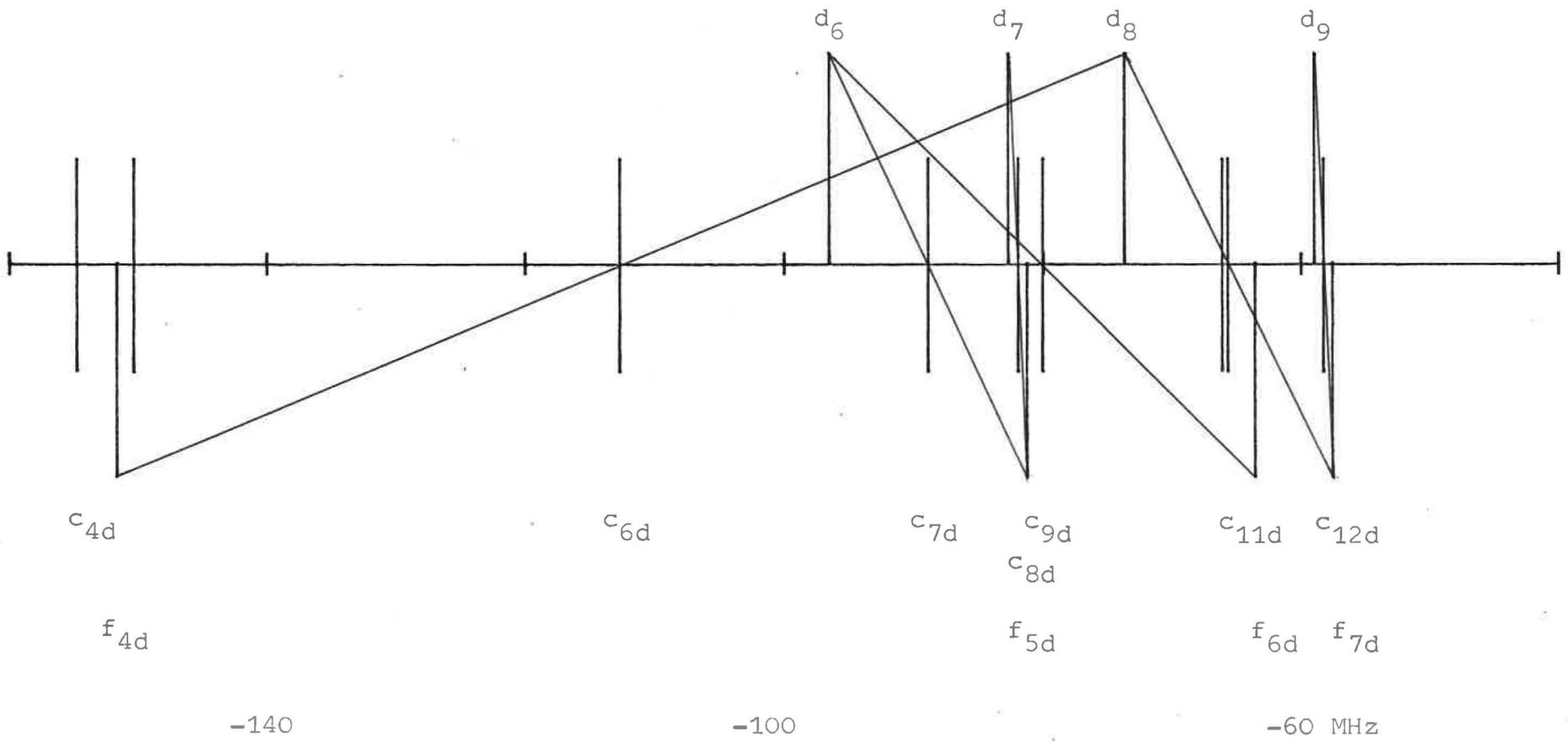

Fig.46: $^{127}I_2$; R(48)15-5; λ=612 NM

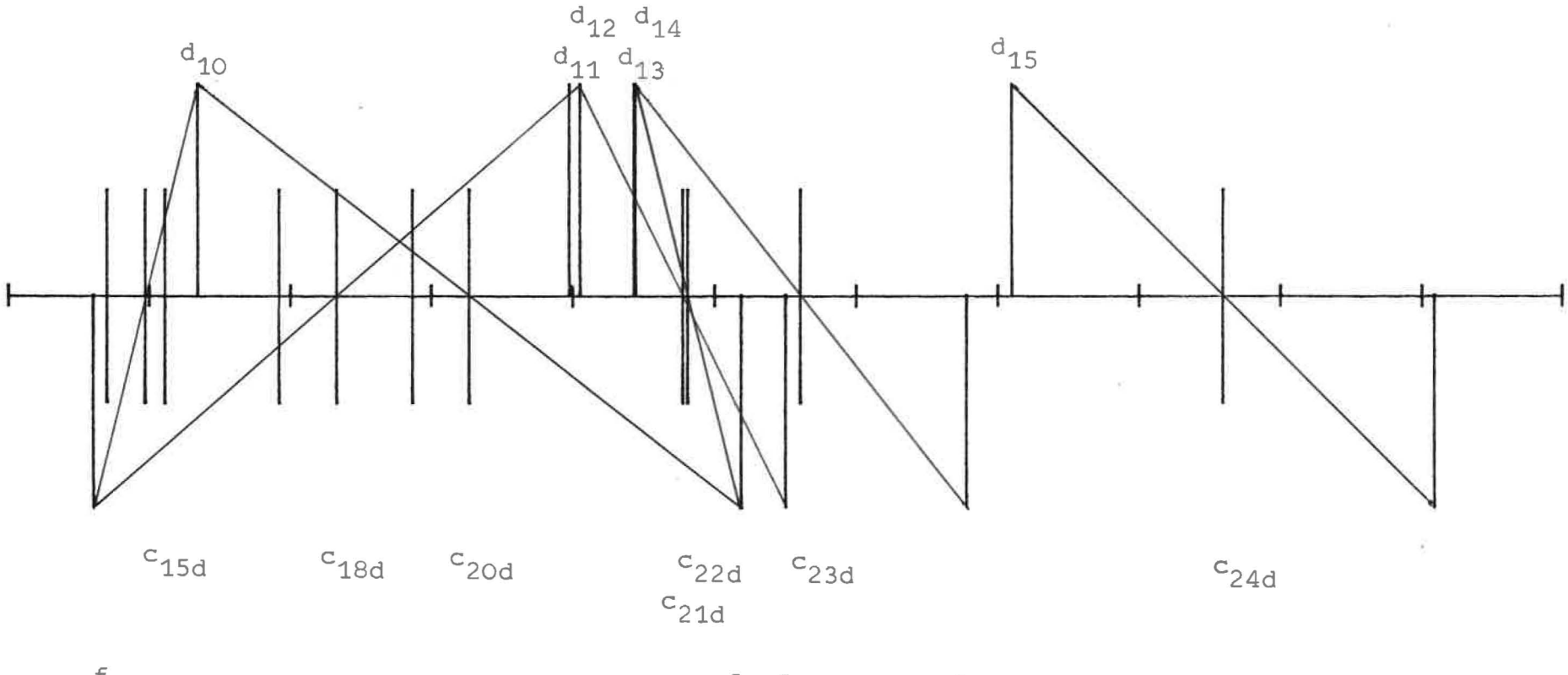

Fig.47: $^{127}I_2$; R(34)17-6; λ=612 NM

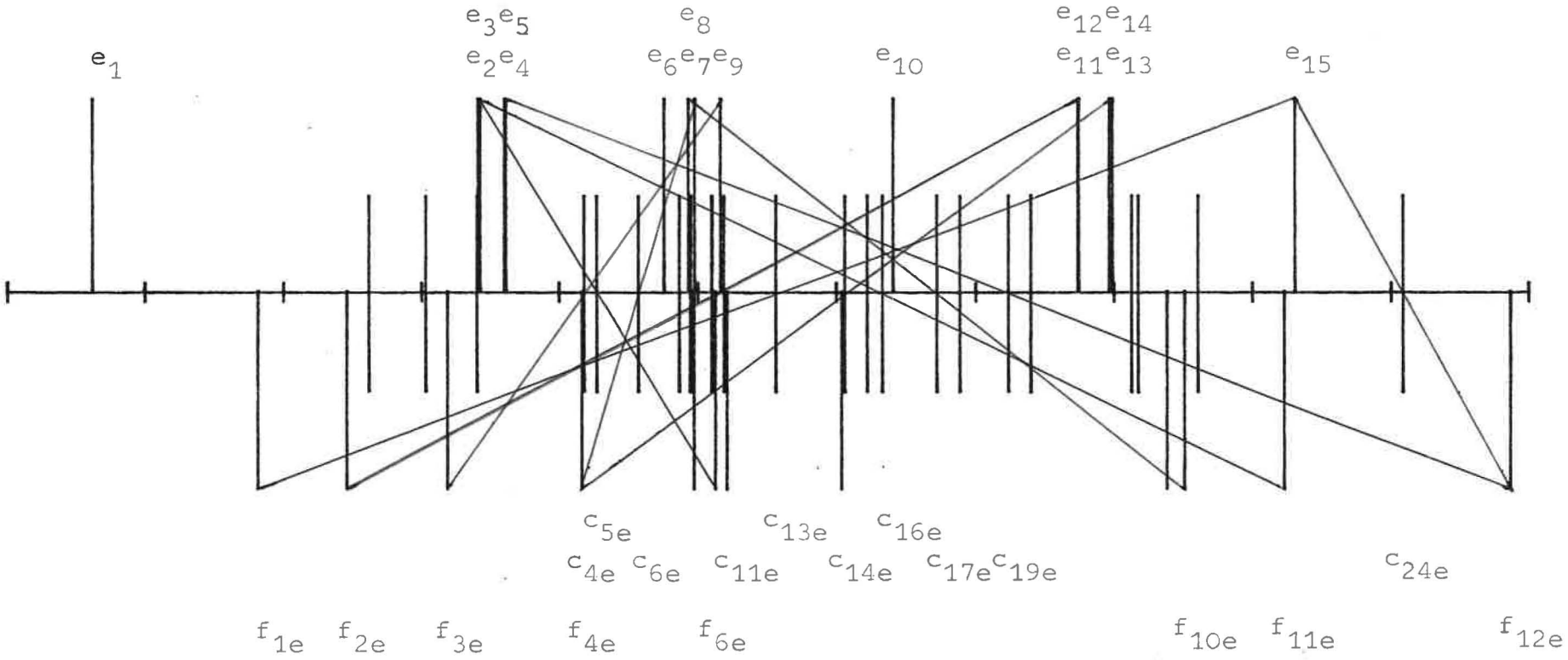

Fig.48: $^{127}I_2$; R(34)17-6; λ=612 NM

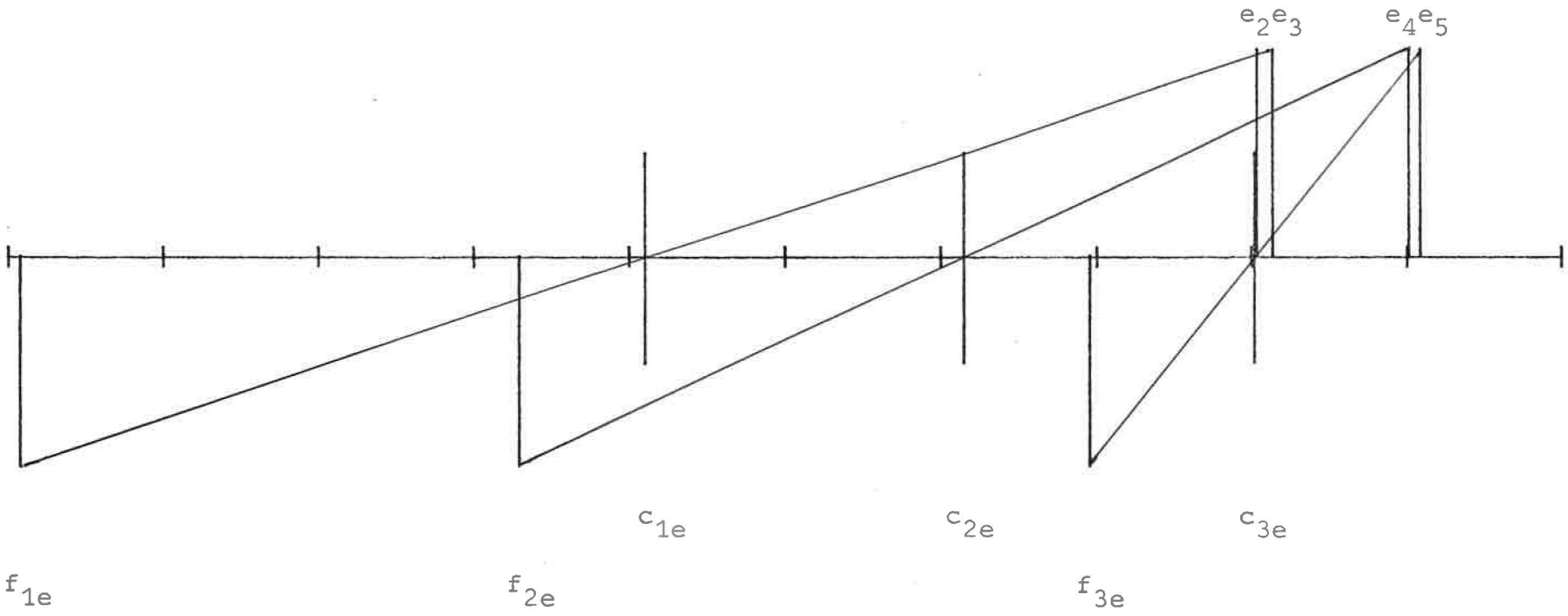

Fig.49: $^{127}I_2$; R(34)17-6; λ=612 NM

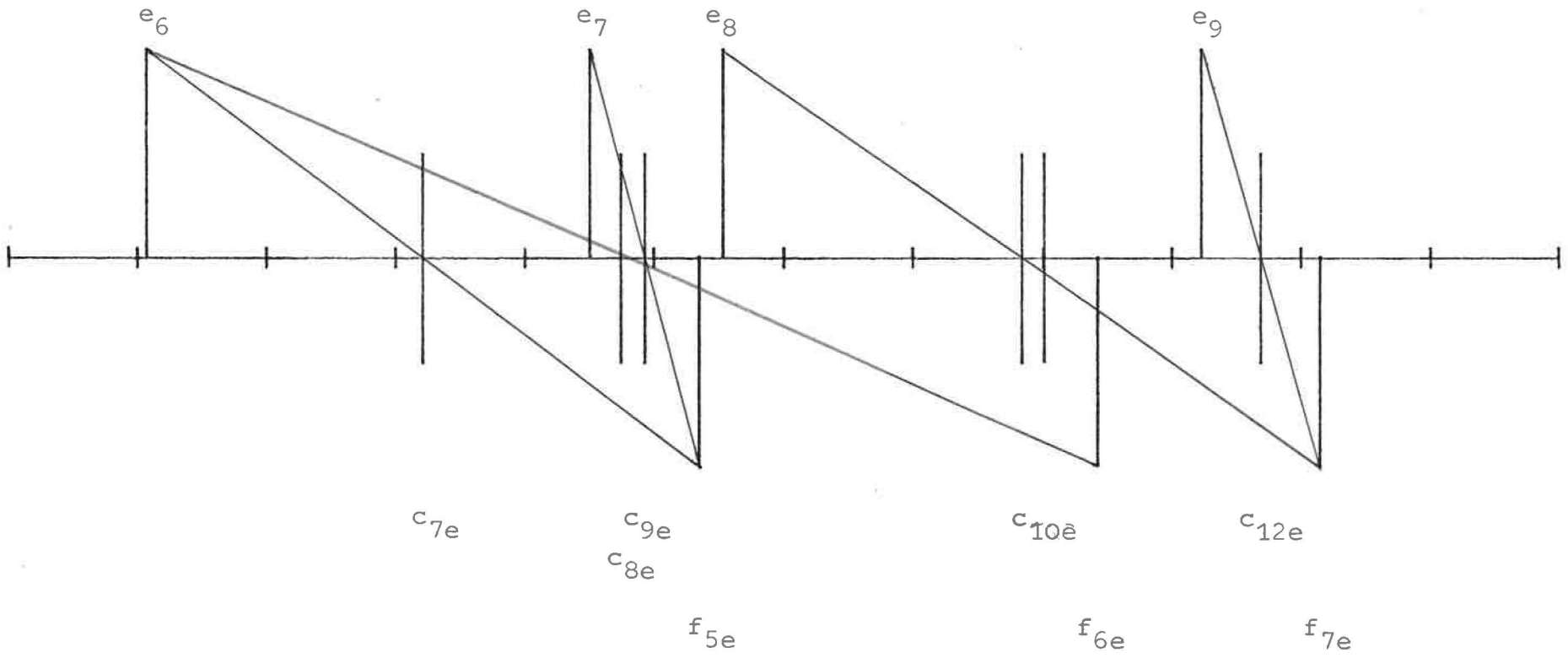

Fig.50: $^{127}I_2$; R(34)17-6; λ=612 NM

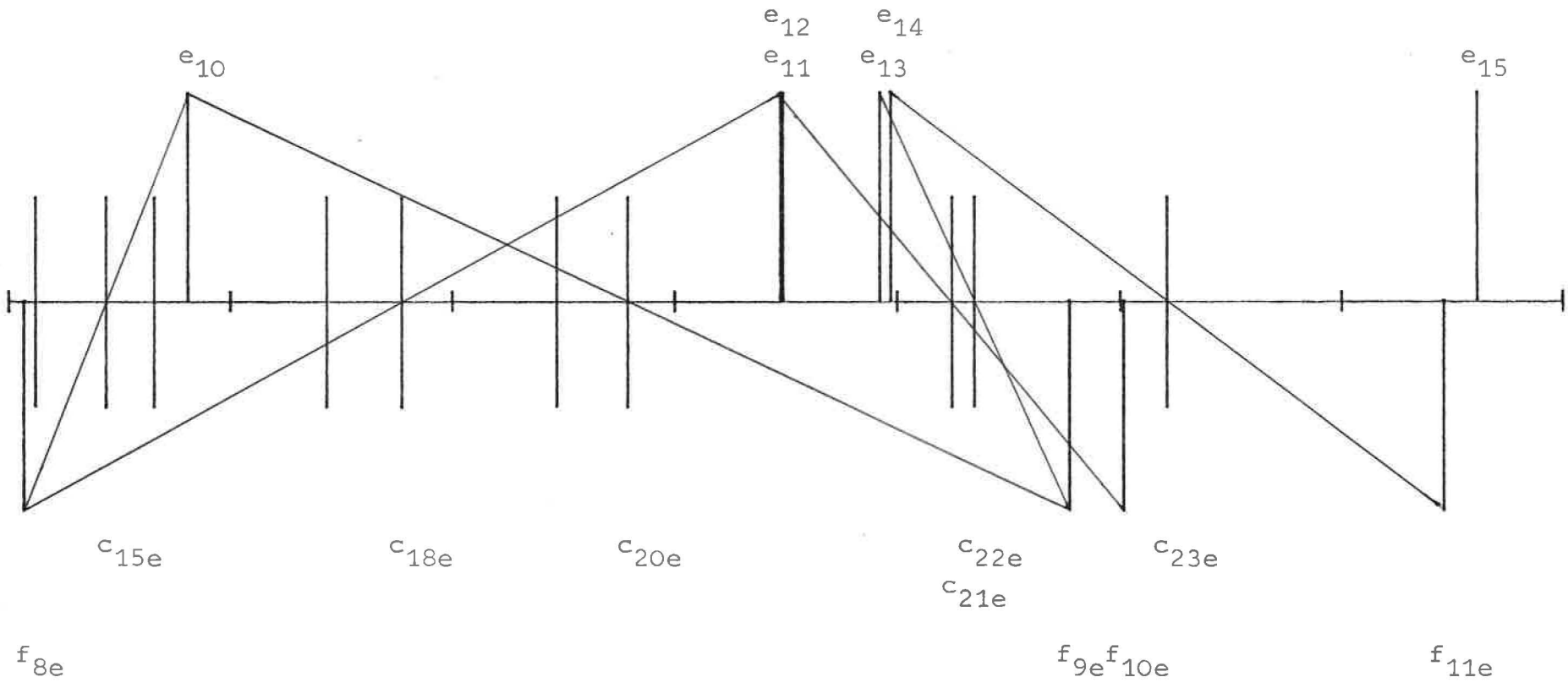

Fig.51: $^{127}I_2$; λ= 633 nm

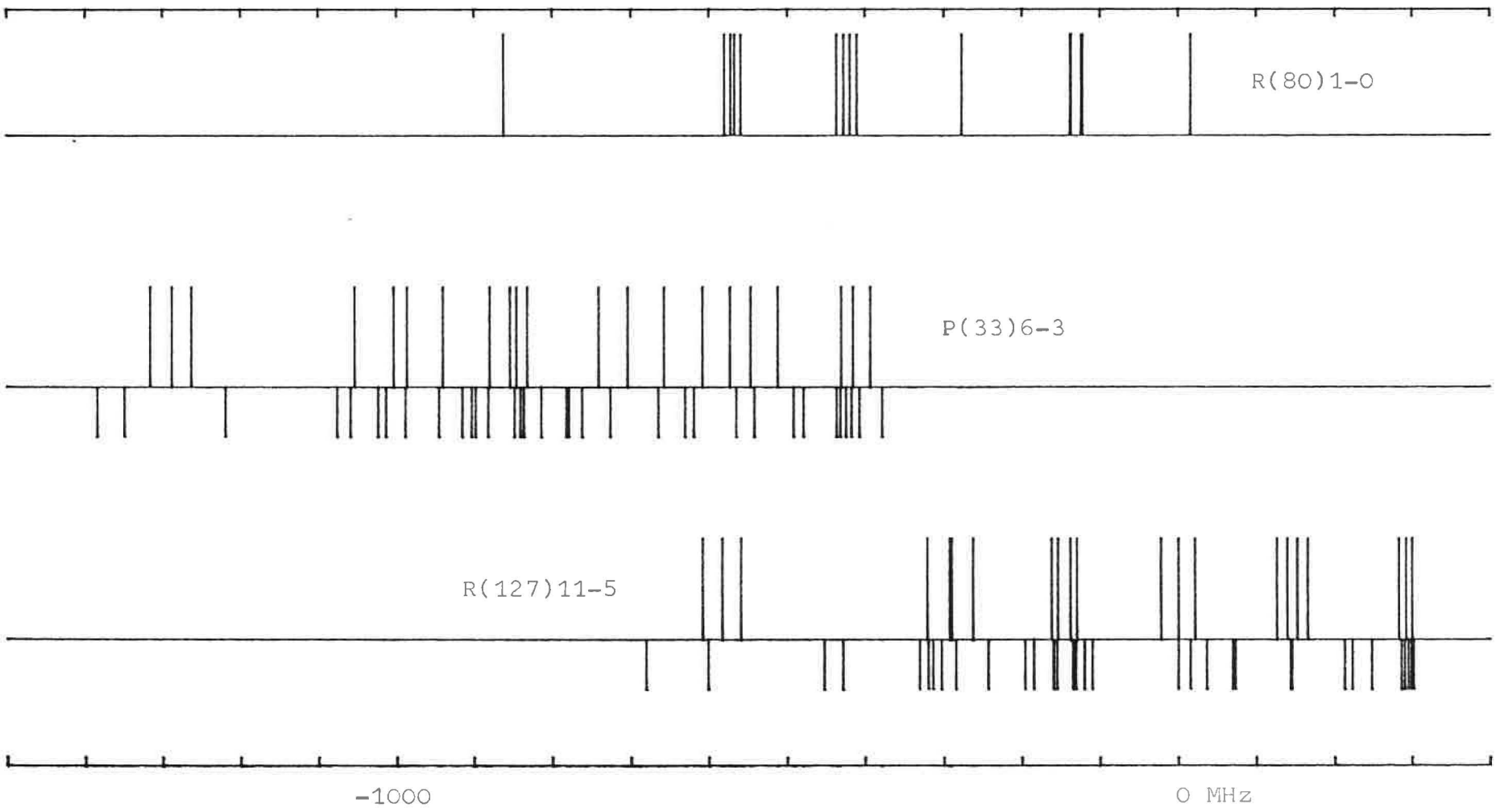

Fig.52: $^{127}I_2$; $^{129}I_2$; ^{127}I-^{129}I; λ= 633 nm

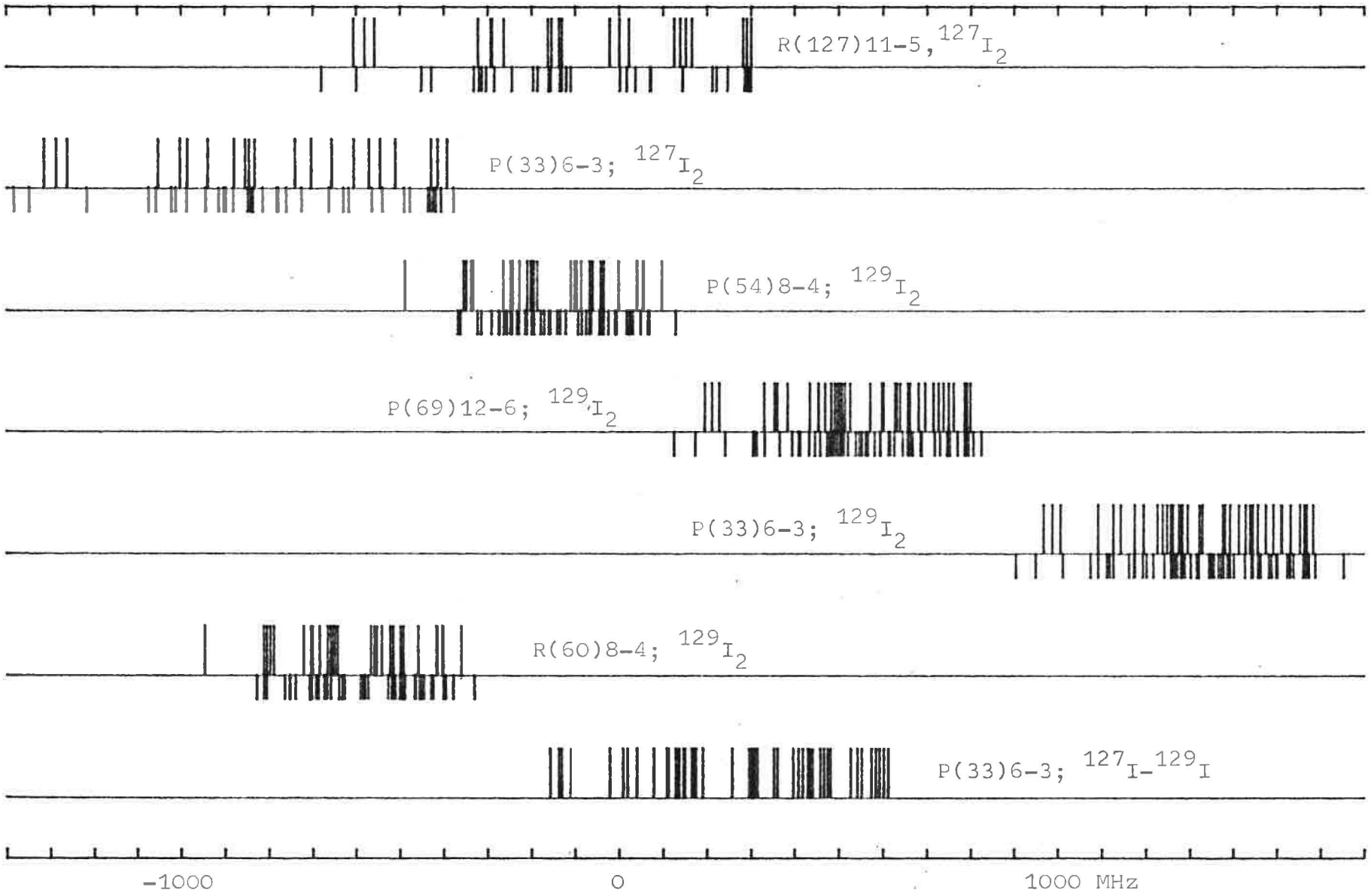

Fig.53: $^{127}I_2$; $^{129}I_2$; ^{127}I-^{129}I; λ= 633 nm

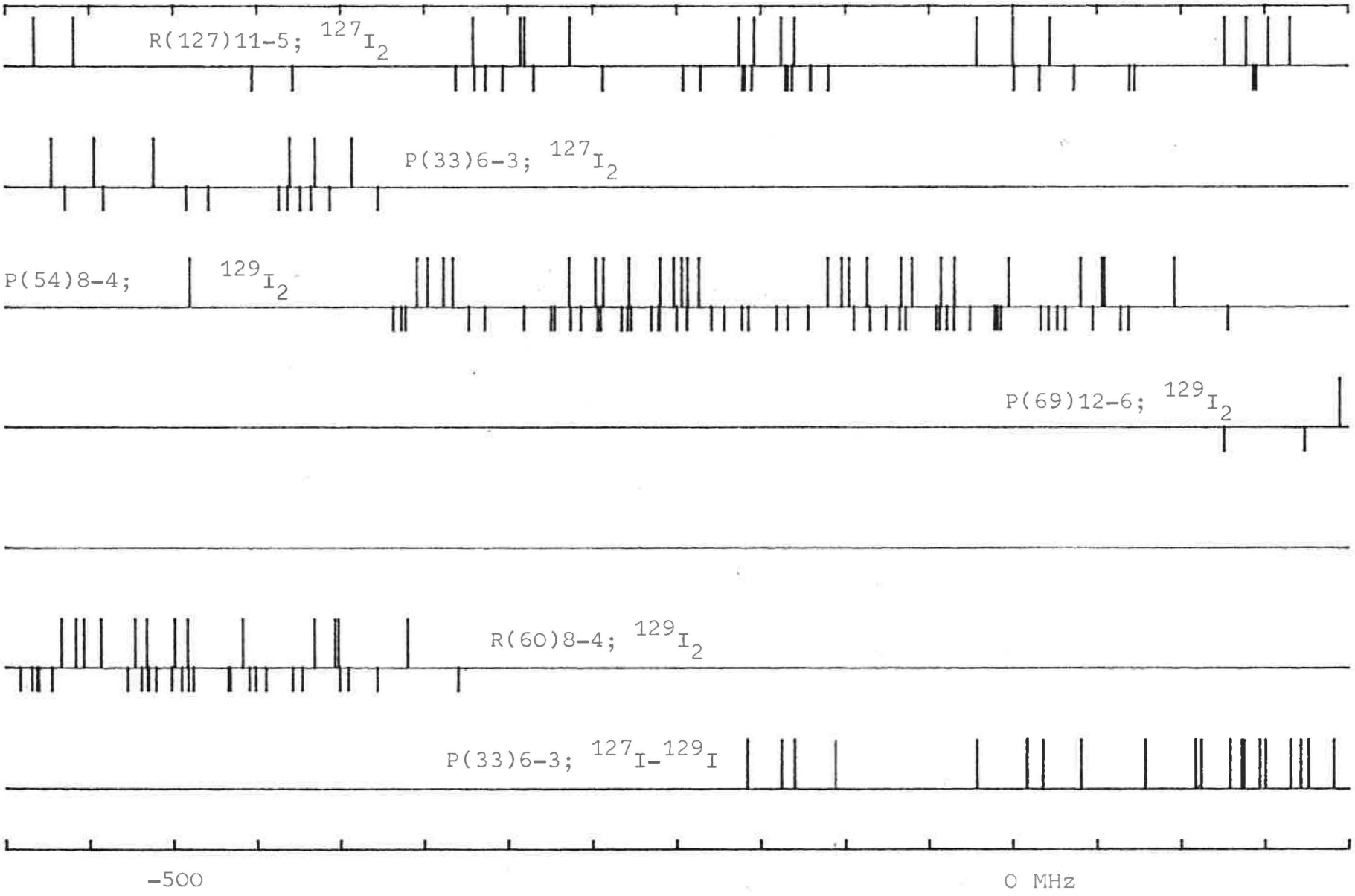

Fig.54: $^{127}I_2$; $^{129}I_2$; ^{127}I-^{129}I; λ= 633 nm

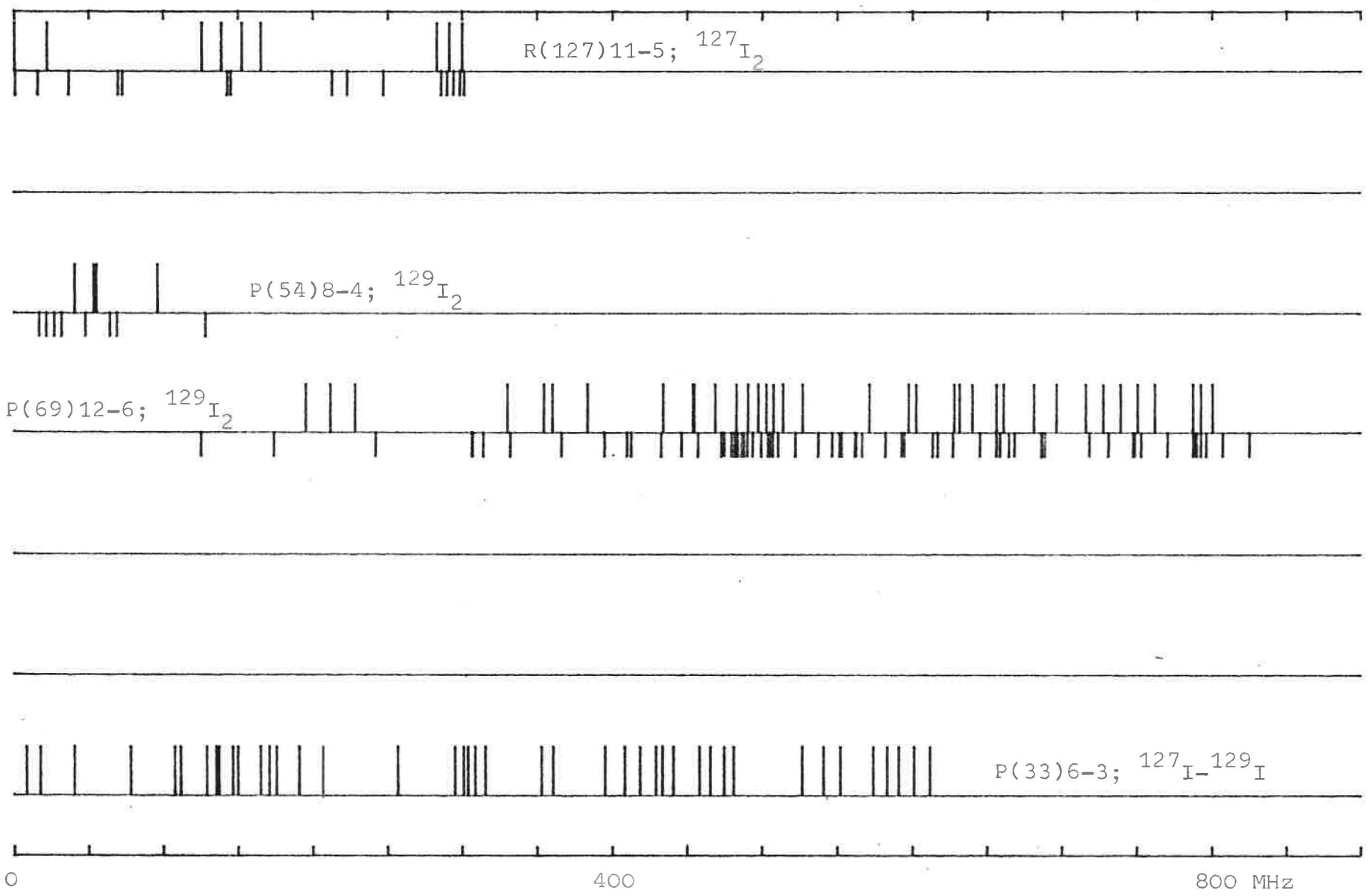

Fig.55: $^{127}I_2$; λ= 612 nm

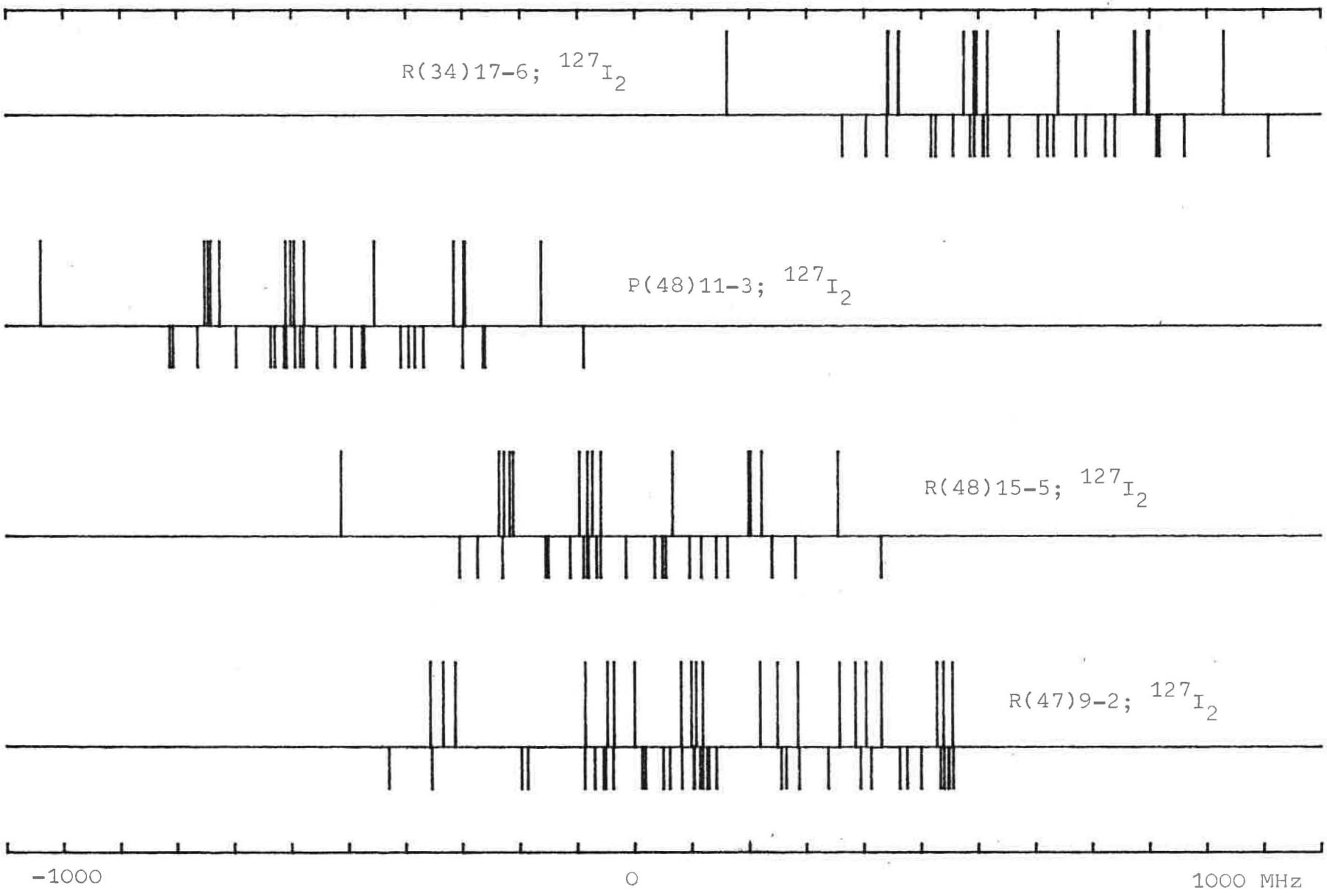

Fig.56: $^{127}I_2$; $^{129}I_2$; λ = 612 nm

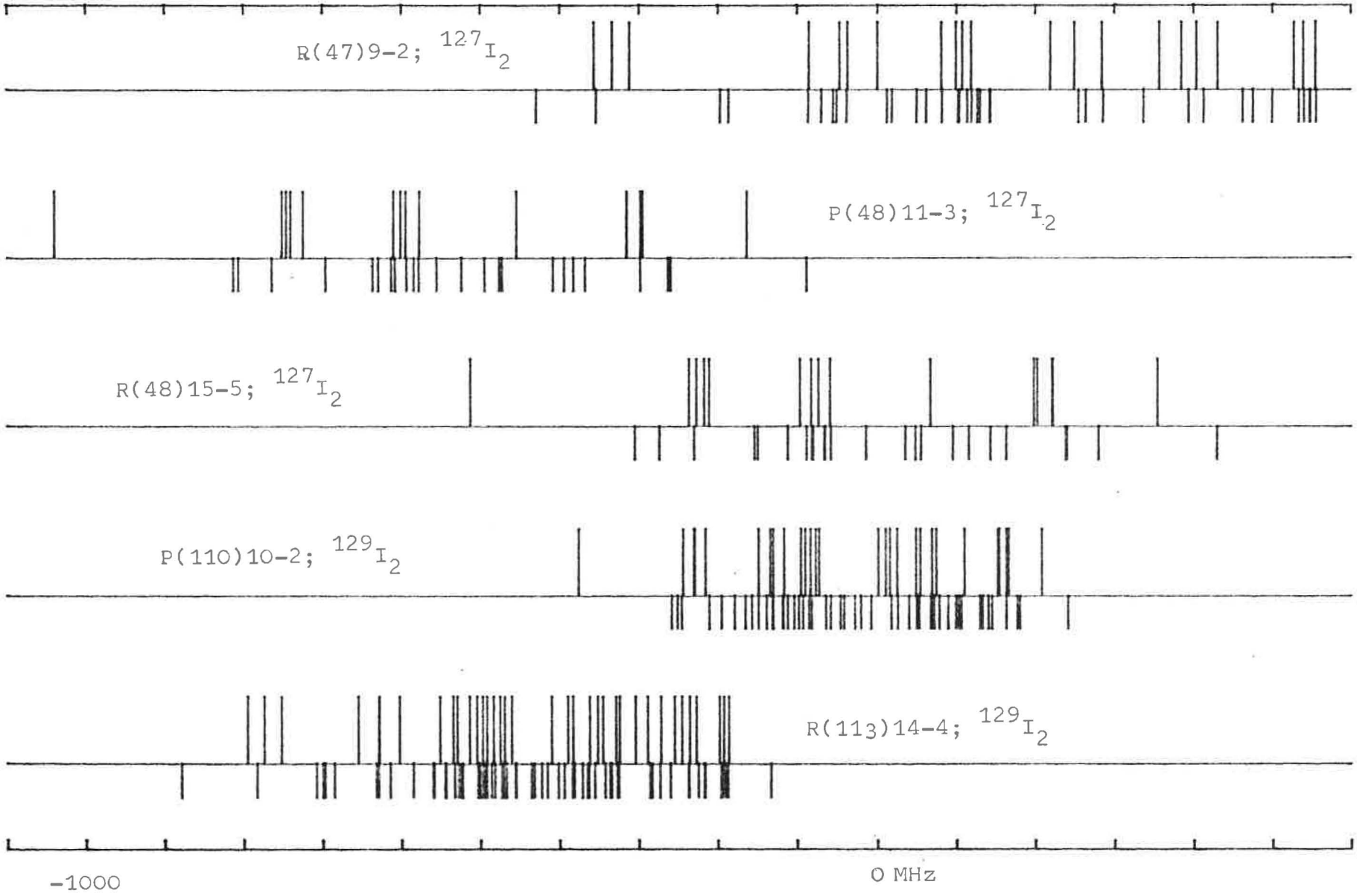

Fig.57: $^{127}I_2$; $^{129}I_2$; λ= 612 nm